ESTIMATION OF FREQUENCY RESPONSE FUNCTION FOR EXPERIMENTAL MODAL ANALYSIS

A Thesis Submitted
to the Graduate School of Engineering and Science of
İzmir Institute of Technology
in Partial Fulfillment of the Requirements for the Degree of

MASTER OF SCIENCE

in Civil Engineering

by
Eyyüb KARAKAN

July 2008
İZMİR

We approve the thesis of **Eyyüb KARAKAN**

Assist. Prof. Dr. Cemalettin DÖNMEZ
Supervisor

Assist. Prof. Dr. Mustafa ALTINKAYA
Committee Member

Assist. Prof. Dr. O.Özgür EĞİLMEZ
Committee Member

15 July 2008

Date

Assist. Prof. Dr. Şebnem ELÇİ
Head of the Civil Engineering Department

Prof. Dr. Hasan BÖKE
Dean of the Graduate School of Engineering and Sciences

ACKNOWLEDGEMENTS

I am very much indebted to my supervisor Assist. Prof. Dr. Cemalettin Dönmez for his supervision and his constant encouragement and attention, for his patience and efforts to broaden the horizon of this study and for providing a suitable atmosphere throughout the study. I thank the members of the thesis defense committee, Assist. Prof. Dr Mustafa Altınkaya of the Department of Electrical& Electronics Engineering at IYTE, Assist. Prof. Dr. O.Özgür Eğilmez for inspiring discussion and comments. I am equally grateful to Assist. Prof. Dr. Gürsoy Turan, Prof. for special assistance in the every stages of this thesis during the three years. I also would like to thank to research assistant Deniz Alkan for his support for experimental studies.Thanks to research assistants Nisa Yılmaz and Can Ali Güven of Civil Engineering Department at İYTE, who has always been there with support and solutions. Thanks to research assistant Yusuf Yıldız of Architecture Department at İYTE, who has always been there with solutions.

Finally, I would like to express my gratitude to my parents Taha and Emine Karakan and my sisters Jülide Karakan and Şule Karakan and my brother S.Emre Karakan for their encouragement, help, immense patience and trust throughout my education and in every moment of my life.

ABSTRACT

ESTIMATION OF FREQUENCY RESPONSE FUNCTION FOR EXPERIMENTAL MODAL ANALYSIS

Every structural system has unique dynamic parameters based on the mass, stiffness and the damping characteristics. If a system is linear and time invariant, dynamic parameters could be shown to be measured and formulated by the Frequency Response Function (FRF). The study of defining the dynamic parameters of a system thru well designed experiments and analysis is called experiment modal analysis. Experimental modal analysis has two major study areas which are modal testing and modal parameter estimation. FRFs are calculated based on the measured data in modal experiment and it is the main input to the modal parameter estimation. Based on the measured/synthesized FRF dynamic parameters of the structures considered could be obtained. In this study basics of the experimental modal analysis is studied. The primary objective is to see the effects of various testing and analysis parameters on the synthesis of FRF. This goal is achieved by testing and discussion of several simple structural systems.

In the thesis general information about experimental modal analysis is presented. The experiment and the modal analysis results of the studied systems, which are simple beam, H-frame, square plate and 2D frame is presented. Selected parameters that are effective on the FRF synthesis is discussed. These parameters are the attachment type of the accelerometers, the tip hardness of the impact hammer and the digital signal processing errors such as leakage, windowing, filtering and averaging. The hammer and accelerometers calibrations will be discussed briefly as well. The results are discussed in order to provide some guidance for understanding the effects of the selected parameters on the FRFs.

ÖZET

DENEYSEL MODAL ANALİZ İÇİN FREKANS TEPKİ FONKSİYONUNUN KESTİRİMİ

Bu tez kapsamında deneysel modal analiz üzerine çalışılmıştır. Ölçüm ve analizlerin tekniğine uygun olarak tasarlanıp uygulanması durumunda bu teknik ile yapısal bir sistemin dinamik özellikleri (frekanslar, sönüm oranları ve modal şekilleri) kestirilebilmektedir. Bu dinamik parametreler her sistem için tektir. Bu tezin temel amacı, bir grup yapısal basit sistem kullanarak deneysel ve analitik parametrelerin Frekans Yanıt Fonksiyonu (FYF) üzerine etkisini incelemektir.

Bu tez çalışması kapsamında ilk olarak deneysel modal analiz ile ilgili genel bilgiler verilmiştir. Basit kiriş, kare plaka, H-çerçeve ve 2 boyutlu çerçeve elemanları ile deneysel modal analiz testleri yapılmış ve her bir sistemin dinamik özellikleri olan frekanslar, sönüm oranları ve modal şekilleri bulunmuştur. Yapısal sistemlerin dinamik parametreleri sonlu elemanlar modelleri ile karşılaştırılmıştır ve çıkan sonuçlar irdelenmiştir. Ayrıca, deney sırasında kullanılan farklı sertlikteki çekiç uçlarının, ivmeölçer ile sistemi tutturmakta kullanılan sıcak tutkal, yapıştırıcı, çimento ve alçı malzemelerini kullanarak yapılan ölçümlerin FYF'na etkileri incelenmiştir. Ek olarak, FYF'larının kalitesinin parazit ve sistematik hatalar gibi faktörlerle olumsuz yönde nasıl etkilendiği araştırılmıştır. Deneysel modal analizde kullanılan örtüşme önler filtrenin, dörtgen ve üstel pencereleme yöntemlerinin ve ortalama alma işlemlerinin FYF'u üzerinde nasıl değişim gösterdiği araştırılmıştır. Deneysel modal analizde sisteme giren dürtü yanıtlarını kestirmede kullanılan H_1, H_2 algoritmalarının FYF'u üzerindeki etkileri gösterilmiştir.

TABLE OF CONTENTS

LIST OF FIGURES

Figure **Page**

LIST OF TABLES

Table **Page**

CHAPTER 1

INTRODUCTION

1.1. Introduction

Civil engineering structures are exposed to vibrations such as explosion, traffic, wind and earthquake. During this vibration, if the frequency of the structure is collided with the main structure frequency, the resonance occurs. As a result of this, damaging and collapsing would be unevitable for the structure.

While making theoretical analysis of structure lots of hypothesis is done from material properties to boundary conditions. Besides, while constructing the building, many mistakes could be done. Therefore, the structure analyzed theoretically should be compared with the other one which was built already to determine whether they have the same dynamic characteristic or not (Reynolds, et al. 2002). Especially, if the complex structures are considered while forming finite element model, theoretical analysis might be deficient and the structures can't be presented (Miglietta 1995, Tealghani and Pappa 1996). It is necessary to decide the dynamic characteristics of historical buildings as well. The difficulties in defining the proper values of historical building material properties makes difficult to determine theoretically dynamic characteristic of historical buildings of material properties (Armstrong, et al. 1995). But, it is necessary to determine the damaging and physical life of the structure such as railway bridges which were constructed in the past and are in use still now (Aksel 1993). Moreover, it is necessary to define dynamic characteristic of existing steel and reinforced concrete structures (Çakar 2003).

The understanding of the physical nature of vibration phenomena has always been important for researchers and engineers. As the structures are becoming lighter and more flexible due to increased material strength, efficiency and safety needs demand more information about the dynamic characteristics of the structures (Ewins 2000). Vibration of structures could cause major problems and operating limitations such as discomfort, malfunction, reduced performance or fatigue (Wicks 1991). Two approaches may be

considered to resolve the vibration problem: Either prevention with proper design or with modification of the structure. In any case, a through understanding of the vibration of structure is essential. For simple structures, such as beams, analytical predictions using closed form solutions can be easily found. Unfortunately closed form solutions are not available for complex structures. Alternative analytical and experimental tools are needed. The most widely used analytical tool is the Finite Element Method (FEM), while the experimental counterparts are largely based on modal testing and analysis. The primary objective of this thesis is to see the effects of various testing and analysis parameters on the synthesis of frequency response function (FRF).

The discussion will start with a brief literature survey on the modal testing and experimental modal analysis. Afterwards the modal experimental and analysis parameters that are effecting the FRF are discussed. In order to get the experimental data for the variation of the parameters considered, several simple structural systems are designed and manufactured. These systems are a simple beam, an H-frame and a square plate. Effect of the selected parameters on FRF is discussed. Based on the experience gathered the difficulties of modal testing and the remedies to overcome these problems is discussed as well.

1.2. Modal Analysis

Modal analysis is the process of determining the inherent dynamic characteristics of a system in forms of natural frequencies, damping factors and mode shapes (Jimin and Zhi-Fang 2001, Avitable 1998). The values obtained are called the dynamic parameters of the system considered. Depending on the mass, stiffness, damping and its distributions, every system has a unique set of dynamic parameters. As a result these parameters could be used to identify the systems. The identified parameters could be used to formulate a mathematical model of the considered system. The formulated mathematical model is referred as the modal model of the system and the information for the characteristics is known as its modal data. Modal analysis embraces both theoretical and experimental techniques. The theoretical modal analysis anchors on physical model of a dynamic system comprising its mass, stiffness and damping properties. These properties may be given in

forms of partial differential equations. The solution of the equation provides the natural frequencies and mode shapes of the system. Experimental modal analysis is the process of determining the modal parameters of a linear, time invariant system from properly designed experiments. Quick development of data acquisition over the last two decades has given rise to major advances in the experimental analysis, which has become known as modal testing.

1.3. Experimental Modal Analysis

Experimental modal analysis is an experimental technique used to derive the modal model of a linear time-invariant vibratory system (Allemang 1999). There are three basic assumptions of the experimental modal analysis of which the structure going to be tested must obey. The first assumption is that the structure is assumed to be linear system. The second assumption is that the structure during the test can be considered as time invariant. The third assumption is that the structure is observable. The last assumption that is often made the structure obeys Maxwell's reciprocity theorem (Allemang 1999). The theoretical basis of the technique is secured upon establishing the relationship between the vibration response at one location and excitation at the same or another location as a function of excitation frequency. This relationship, which is often a complex mathematical function, is known as FRF. The practice of modal testing involves measuring the FRFs or impulse responses of a structure. A practical consideration of modal testing is the amount of FRF data needed to be acquired in order to adequately derive the modal model of the tested object. With sufficient data, numerical analysis will derive modal parameters by using curve fitting techniques (Ewins 2000).Figure 1.1 shows that the three steps of modal testing. In summary, experimental modal analysis involves three constituent phases:

1) Preparations for the test,
2) Frequency response measurements
3) Modal parameter identification.

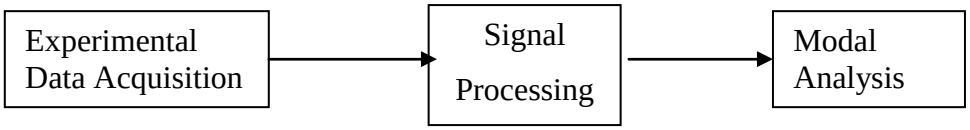

Figure 1.1. Three Stages of Modal Testing

Modal model is based on the vibration measurements that are taken from the physical structure. Compared to the finite element models, this is the main advantage of the modal models. However, due to a number of limitations and errors, the model created from the measured data may not represent the actual behavior of the structure as closely as desired (Schwarz and Richardson 1999). In general, limitations and errors of modal testing are:

- Random errors due to noise.
- Possible loose attachment of transducers to the structure.
- Attachment of the mechanical devices of the structure
- Poor modal analysis of experimental data (user experience).
- Limited number of measured degrees of freedom.
- Stationary mode due to the excitation at the node of the mode.
- Difficulty in measuring rotational degrees of freedom.

The theoretical background of modal testing and practical aspects of vibration measurement techniques could be find in Ewins (2000).

1.4. Application Areas of Modal Models

Typically more confidence can be placed in experimental data since measurements are taken from the real structure. Therefore, the mathematical models, which have been created as a result of modal testing, can be used in various ways to avoid or to cure some of

the problems encountered in structural dynamics. In this section, the applications of modal testing methods for improving the structural dynamics will be considered (Ewins 2000).

1.4.1. Updating of the Analytical Models (Calibration)

The modal test results could be used to update/calibrate the analytical models which are formed by other means. Typically, analytical models are formed by using the finite element method. The errors of the analytical models mainly resulted from the many assumptions made. For example, material properties, geometry and the boundary conditions of the system defined in the model may not be in accordance with the physical system (Ewins 2000). Modal models depend on the in-situ measurements taken at the site. As a result all the real properties of the physical system are considered. It is accepted that modal models are more realistic. So, analytical models could be updated using the modal model results. Model updating can be applied as the adjustment of the dynamic parameters of an existing analytical model with the dynamic parameters obtained as a result of the modal test/analysis. Therefore, updated FE model more accurately reflects the dynamic behavior of the system considered. Model updating can be divided into two steps:

1. Comparison of FE model and modal testing results.

2. Modifying FE model in order to correlate FEM and modal testing results.

If the difference between analytical and experimental data is within some preset tolerances, the analytical model can be judged to be adequate and no updating is necessary.

Most difficulties are encountered during modifying FEM in order to correlate FEM and modal testing results (Avitabile 2002). The difficulties in locating the errors in a theoretical model are mostly due to measurement process and can be summarized as:

1) Insufficient experimental modes: If the measured modes are not sufficient to represent the necessary dynamic characteristics of the system considered, one of the causes could be insufficient experimental modes. The most common cause of this condition is the poorly selected reference locations. If the selected reference locations are at the node of a mode, that mode could not be observed from the measured data. Performing Multiple Input Multiple Output tests minimize this problem (Jimin and Zhi-Fang 2001). Number of

measurement locations and the frequency band controls the number of modes considered in a test.

2) Insufficient experimental coordinates: The upper limit of the number of modes that could be observed in a modal test is the number of experimental coordinates. Typically this number is limited by the sensor and hardware available. In order have a maximum efficiency from the hardware available the selection of reference locations should be made properly. Such a selection needs pre-information about the dynamics of the system. A finite element model, if available, could be a great tool to assist in the selection of proper references (Avitabile 2000). Another tool available is the pre-testing the system using limited hardware and time.

3) Mesh incompatibility of the FE models: The selection of the mesh is directly related to the number of modes. Basically, in the finite element model, it is needed to put enough mesh to find a sufficient number of mode shapes (Avitabile 2000).

4) Experimental random and systematic errors: Experimental errors are associated with the variance on the measurement and reduction of the data; systematic errors are associated with the process whereby you collect data (Avitabile 2007).

1.5. Sources of Error in Modal Testing

The accurate measurement of frequency response function depends on minimizing the errors involved the digital signal processing. In order to take full advantage of experimental data, the errors in measurement must be reduced to acceptable levels. However, engineering in some applications experiments demand high quality test data. These applications consist of not only mechanical and aeronautical engineering but also building structures, space structures, nuclear plants. In these cases, the results are useless for the objectives of the study, if test data with poor quality are used. In recent years there has been a strong demand for high quality modal testing date suitable for advanced applications such as structural modification and model updating (Ewins 2000, Avitable 2001, Wicks 1991)

In this section, sources of error in modal testing are studied more systematically. The sources of the errors in modal testing procedure can be categorized in three groups:

(i) Experimental data acquisition errors

(ii) Signal processing errors

(iii) Modal analysis errors,

It is well known that the quality of measured Frequency Response Functions (FRFs) is adversely affected by many factors, most significant sources being noise and systematic errors. It is also known that the accuracy and the reliability of various analyses using the measured FRFs depend strongly on the quality of measured data. For this reason, the factors effecting FRF are shown below respectively.

1) Boundary Conditions of the structure

- Free-free
- Fixed

2) Measurement noise

- Equipment Problem (power supply noise)
- Cabling Problems
- Rattles, cable motion

3) Nonlinearity

4) Digital Signal Processing Errors and Solutions

- Aliasing,
- Leakage
- Windowing
- Filtering
- Zooming
- Averaging

5) Calibration (operator error)

- Complete system calibration
- Transducer Calibration

6) Transducers and Amplifiers

- Accelerometers sensitivity:
- Attachment and Location of Transducers

1. Attachment
2. Location

7) Hammer Tip:

- Hard Tip
- Medium Tip
- Soft Tip
- Super Soft Tip

1.6. Objectives and Scope of This Thesis

The primary objective of this thesis is to see the effects of various testing and analysis parameters on the synthesis of FRF. Based on the measured FRF's, dynamic parameters of the structures considered could be obtained. These parameters are the natural frequencies, mode shapes and damping ratios of the system. These parameters are unique to every system. By using the several simple structure systems, the experimental and analytical parameters that are effecting of FRF are discussed.

This thesis consists of six chapters. In the first chapter, firstly general information about modal analysis and experimental modal analysis and literature survey are presented. After that the application areas of this method, the source of error in modal testing are explained. In the second chapter, the theory from the vibration point of view involves more thorough understanding of how the structural parameters of mass, damping and stiffness relate to the impulse response function (time domain), the frequency response function (frequency domain), and transfer function (Laplace domain) for single and multiple degree of freedom systems. In the third chapter, modal data acquisition that will be used in the estimation of modal model involves many important technical things. Modal data acquisition also includes the typical signal processing errors that are random and bias errors. In addition to this, averaging methods are presented. Categorizing different methods of experimental modal analysis is explained. A number of different frequency response function testing configurations single input/single output (SISO), single input/multiple output (SIMO), multiple input/single output (MISO), multiple input/multiple output

(MIMO) are explained. In the fourth and fifth chapters, the frequency response function differences and variations of simple systems that are studied in experimental modal analysis like, simple beam, H-frame, square plate are compared with different accelerometer bonding like hot glue, plaster, cement, glue will be described. Besides, the effect of impact hammer with different materials in the same simple system to FRF will be described. In addition to this, by using the simple beam data, the effects of the digital signal processing errors on the frequency response function such as aliasing, leakage, windowing, filtering and averaging are answered. Also the hammer and accelerometers calibrations are explained how to do. In the last chapter, contain the evaluation and discussion of test data recorded during the experimental modal analysis. The results and discussion are made to understand the effects of different testing conditions which are related to the aliasing, averaging, filtering, hammer tips and the other ones, on the frequency response functions.

CHAPTER 2

THEORY OF VIBRATION

2.1. Introduction

Modal testing/analysis based on the theory of vibration. The following sections briefly explain the theory of vibration necessary for modal analysis of linear systems. Discussion starts with the single degree of freedom (SDOF) systems and continues with multi degree of freedom (MDOF) systems (Allemang 1999, Chopra 2001, Ewins 2000).

2.2. Single Degree of Freedom System

The number of the degrees of freedom is defined as the minimum number of independent coordinates required to determine the motion all of the parts of the system. It is essential to know the number of degrees of freedom of a dynamic system to study its vibration characteristics. The simplest vibratory system can be described by a SDOF system which consists of a single particle. Based on the linearity assumption, MDOF systems can be viewed as a linear combination of SDOF systems (Chopra 2001). In its most basic form SDOF system is represented in Figure 2.1.

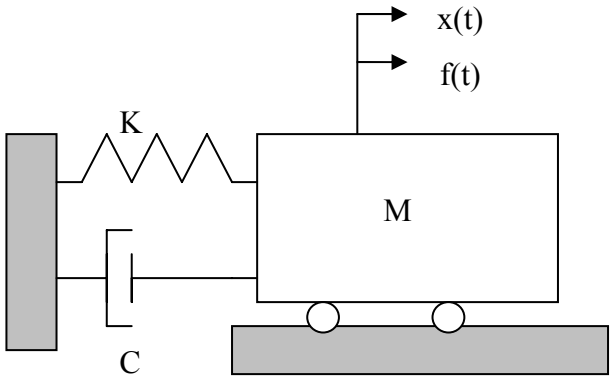

Figure 2.1. Single Degree of Freedom System

The free body diagram of the SDOF system given in Figure 2.1 contains four force vectors effecting the system in the x-direction as shown in Figure 2.2:

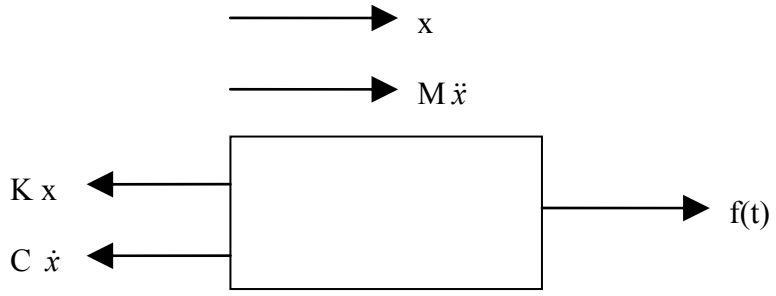

Figure 2.2. Free Body Diagram of SDOF System

The general mathematical representation of a single degree of freedom system is obtained from Newton's law of motion and expressed in Equation (2.1), where the external force applied should be equal to resisting forces that are resulted from the motion of the mass.

$$M\ddot{x}(t) + C\dot{x}(t) + Kx(t) = f(t) \tag{2.1}$$

where;

M = Mass of the system

C = Damping of the system

K = Stiffness of the system

$f(t)$ = General force function

$x(t) = displacement$

$\dot{x}(t) = velocity$

$\ddot{x}(t) = acceleration$

Equation (2.1) is a linear, time invariant, second order differential equation. By setting f(t)= 0, the homogeneous form of Equation (2.1) can be solved.

$$M\ddot{x}(t) + C\dot{x}(t) + Kx(t) = 0 \tag{2.2}$$

From differential equation theory solution to this equation is $x(t) = Xe^{st}$, where s is a complex valued number to be determined. Taking appropriate derivatives and substituting into Equation (2.2) yields:

$$(Ms^2 + Cs + K)Xe^{st} = 0 \tag{2.3}$$

Thus, for a non-trivial solution:

$$Ms^2 + Cs + K = 0 \tag{2.4}$$

where:

Equation (2.4) is the characteristic equation of the system, whose roots λ_1 and λ_2 are:

$$\lambda_{1,2} = -\frac{C}{2M} \pm \left\{ \left(\frac{C}{2M} \right)^2 - \left(\frac{K}{M} \right) \right\}^{1/2} \tag{2.5}$$

Thus the general solution of Equation (2.2) is

$$x(t) = Ae^{\lambda_1 t} + Be^{\lambda_2 t} \tag{2.6}$$

A and B are constants that should be determined from the initial conditions imposed on the system at time $t = 0$.

For most real structures, the damping ratio is rarely greater than ten percent. Therefore, all further discussion will be limited to under damped systems ($\zeta<1$). With reference to Equation (2.6), this means that the two roots, $\lambda_{1,2}$ are always complex conjugates. Also, the two coefficients (A and B) are complex conjugates of one another (A and A*). For an under-damped system, the roots of the characteristic equation can be written as:

$$\lambda_1 = \sigma_1 + j\omega_1 \tag{2.7}$$

$$\lambda_1^* = \sigma_1 - j\omega_1 \tag{2.8}$$

where;

σ_1 = Damping factor

ω_1 = Damped natural frequency

ζ = Damping ratio

The roots of characteristic Equation (2.4) can also be written as:

$$\lambda_1, \lambda_1^* = -\zeta_1 \Omega_1 \pm j\Omega_1 \sqrt{1-\zeta_1^2} \tag{2.9}$$

Ω_1 = Undamped natural frequency (rad/sec)

ζ_1 = Relative damping with respect to critical damping.

The damping factor,σ_1, is defined as the real part of a root of the characteristic equation. This parameter has the same units as the imaginary part of the root of the characteristic equation, radians per second. The damping factor describes the exponential decay or growth of the oscillation. In real structures energy is always dissipated through some mechanism of damping. Therefore, there is always decay in oscillation. In the foregoing discussion viscous damping is considered. For many purposes the actual damping in a SDF structure can be idealized satisfactorily by a linear viscous damper. The damping coefficient is selected so that the vibrational energy it dissipates is equivalent to the energy dissipated in all the damping mechanisms. This idealization is therefore called equivalent viscous damping (Chopra 2001).

Critical damping is defined as that value of (C_c), which makes the radical of the roots zero; that is;

$$\left(\frac{C_c}{2M}\right)^2 - \left(\frac{K}{M}\right) = 0 \rightarrow \frac{C_c}{2M} = \sqrt{\frac{K}{M}} = \Omega_1 \tag{2.10}$$

$$C_c = 2M\sqrt{\frac{K}{M}} = 2M\Omega_1 \tag{2.11}$$

The actual damping in a system can be specified in terms of (C_c), by introducing the damping ratio. The damping ratio, ζ_1, is the ratio of the actual system damping to the critical system damping. As a result, damping ratio is a dimensionless quantity.

$$\zeta_1 = \frac{C}{C_c} = -\frac{\sigma_1}{\Omega_1} \tag{2.12}$$

2.2.1. Time Domain: Impulse Response Function

The impulse response function of a SDOF system can be determined from Equation (2.6) assuming that the initial conditions are zero and the system excitation, *f(t)*, is a unit impulse. The response of the system, *x(t)*, to such a unit impulse is known as the impulse response function, *h(t)*, of the system.

Therefore:

$$h(t) = Ae^{\lambda_1 t} + A^* e^{\lambda_1^* t} \tag{2.13}$$

$$h(t) = e^{\sigma_1 t}\left[Ae^{(+j\omega_1 t)} + A^* e^{(-j\omega_1 t)}\right] \tag{2.14}$$

Thus, using Euler's formula for $e^{j\omega t}$ and $e^{-j\omega t}$, the coefficients (A and A^*) control the amplitude of the impulse response, the real part of the pole is the decay rate and the imaginary part of the pole is the frequency of oscillation. Figure 2.3 illustrates a typical impulse response function, for a SDOF system.

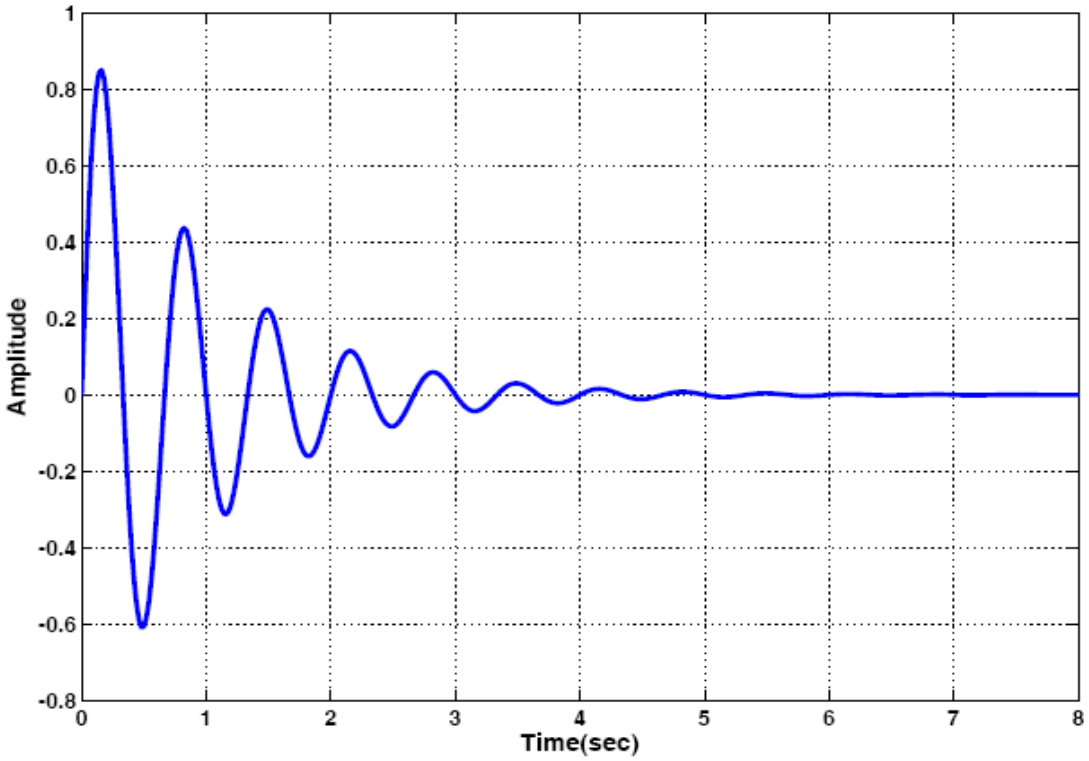

Figure 2.3. Time domain: Impulse Response Function

2.2.2. Laplace Domain: Transfer Function

Equation (2.1) is the time domain representation of the system in Figure 2.1. An equivalent equation of motion may be determined for the Laplace or s-domain. Laplace transform is defined from zero to positive infinity with initial conditions. Laplace formulation is a transformation from the time domain signal *f(t)* to the *s* domain. The Laplace representation advantage is the conversion of the differential equation to an algebraic equation. Theory behind Laplace transform could be found in classical texts concerning vibrations. The Laplace transforms begins by taking the Laplace transform of Equation (2.1). Thus, Equation (2.1) becomes:

$$\left[Ms^2 + Cs + K\right]X(s) = F(s) + \left[Ms + C\right]X(0) + M\dot{X}(0) \tag{2.15}$$

X(0) and $\dot{X}(0)$ are the initial displacements and velocities at time t=0.

If the initial conditions are zero, Equation (2.15) becomes

$$\left[Ms^2 + Cs + K\right]X(s) = F(s) \tag{2.16}$$

Then Equation (2.16) becomes

$$B(s)X(s) = F(s) \tag{2.17}$$

where;

$$B(s) = Ms^2 + Cs + K \tag{2.18}$$

Therefore, using the same logic as in the frequency domain case, the transfer function can be defined.

$$X(s) = H(s)F(s) \tag{2.19}$$

where;

$$H(s) = \frac{1}{Ms^2 + Cs + K} \tag{2.20}$$

The quantity *H(s)* is defined as the *.transfer function* of the system. In other words, a transfer function relates the Laplace transform of the system input to the Laplace transform of the system response. From Equation (2.19), the transfer function can be defined as:

$$H(s) = \frac{X(s)}{F(s)} \tag{2.21}$$

Going back to Equation (2.16), the transfer function can be written:

$$H(s) = \frac{1}{Ms^2 + Cs + K} = \frac{1/M}{s^2 + \left(\frac{C}{M}\right)s + \left(\frac{K}{M}\right)} \tag{2.22}$$

Note that Equation (2.22) is valid under the assumption that the initial conditions are zero. The denominator term is referred to as the *characteristic equation* of the system. The roots of the characteristic equation are given in Equation (2.5). The transfer function, H(s), can now be rewritten, just as in the frequency response function case, as:

$$H(s) = \frac{1/M}{(s-\lambda_1)(s-\lambda_1^*)} = \frac{A}{(s-\lambda_1)} + \frac{A^*}{(s-\lambda_1^*)} \tag{2.23}$$

The residues are defined in terms of the partial fraction expansion of the transfer function equation. Equation (2.23) can be expressed in terms of partial fractions as follows:

$$H(s) = \frac{1/M}{(s-\lambda_1)(s-\lambda_1^*)} = \frac{c_1}{(s-\lambda_1)} + \frac{c_2}{(s-\lambda_1^*)} \tag{2.24}$$

The residues of the transfer function are defined as being the constants c_1 and c_2. The terminology and development of residues comes from the evaluation of analytical functions in complex analysis. The residues of the transfer function are directly related to the amplitude of the impulse response function. The residues c_1 and c_2 can be found by multiplying both sides of Equation (2.24) and evaluating the result at $s = \lambda_1$. Thus:

$$\frac{1/M}{(s-\lambda_1^*)}\Big|_{s=\lambda_1} = c_1 + \left[\frac{c_2(s-\lambda_1)}{(s-\lambda_1^*)}\right]\Big|_{s=\lambda_1} \tag{2.25}$$

$$\frac{1/M}{(\lambda_1-\lambda_1^*)} = c_1 \tag{2.26}$$

Thus:

$$c_1 = \frac{1/M}{(\sigma_1 + j\omega_1)-(\sigma_1 - j\omega_1)} = \frac{1/M}{j2\omega_1} = A \tag{2.27}$$

Similarly;

$$c_2 = \frac{1/M}{(\sigma_1 - j\omega_1) - (\sigma_1 + j\omega_1)} = \frac{1/M}{-j2\omega_1} = A^* \tag{2.28}$$

In general, for MDOF system, the residue A can be a complex quantity. But, for SDOF system A^* is purely imaginary.

Therefore;

$$H(s) = \frac{1/M}{(s-\lambda_1)(s-\lambda_1^*)} = \frac{A}{(s-\lambda_1)} + \frac{A^*}{(s-\lambda_1^*)} \tag{2.29}$$

2.3. Multiple Degree of Freedom System

Structures are typically more complicated than the single mass, spring, and damper system. In this section, the general case for a MDOF system will be used to show how the frequency response functions of a structure are related to the modal vectors of that structure. The two-degree of freedom system, shown in Figure 2.4, is the basic example of a MDOF system. Figure 2.4 is a useful example for discussing modal analysis concepts since a theoretical solution can be formulated in terms of the mass, stiffness and damping matrices or in terms of the frequency response functions.

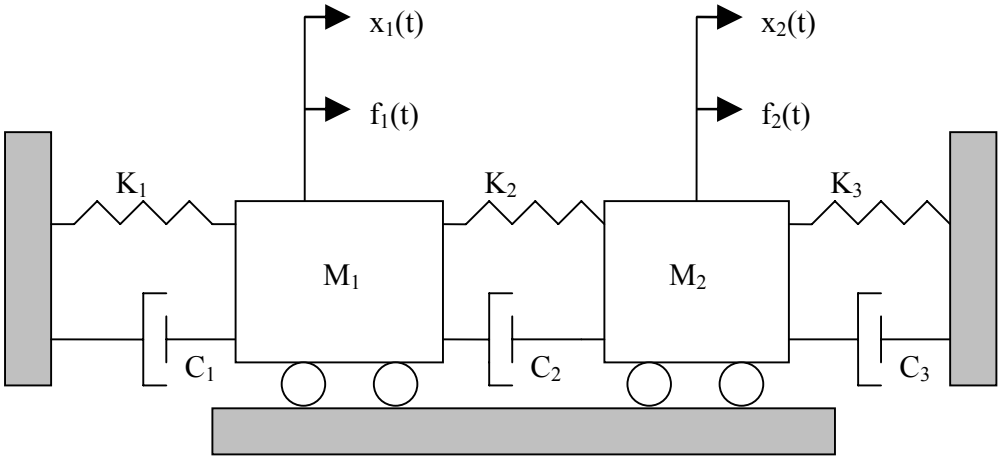

Figure 2.4. Multi Degree of Freedom System

The equations of motion for the system in Figure 2.4, using matrix notation, are as follows:

$$\begin{bmatrix} M_1 & 0 \\ 0 & M_2 \end{bmatrix}\begin{bmatrix} \ddot{x}_1 \\ \ddot{x}_2 \end{bmatrix}+\begin{bmatrix} (C_1+C_2) & -C_2 \\ -C_2 & (C_2+C_3) \end{bmatrix}\begin{bmatrix} \dot{x}_1 \\ \dot{x}_2 \end{bmatrix}+\begin{bmatrix} (K_1+K_{2)} & -K_2 \\ -K_2 & (K_2+K_3) \end{bmatrix}\begin{bmatrix} x_1 \\ x_2 \end{bmatrix}=\begin{bmatrix} f_1 \\ f_2 \end{bmatrix} \quad (2.30)$$

The solution of Equation (2.30) when the mass, damping, and stiffness matrices are known could be found in classical text concerning vibrations. Here solution will not be discussed.

The improvement of the frequency response function solution for the MDOF case is similar to the SDOF case, which relates the mass, damping, and stiffness matrices to a transfer function model involving multiple degrees of freedom. Similar to the analytical case, where the ultimate solution can be described in terms of SDOF systems, the

frequency response functions between any input and response degree of freedom can be represented as a linear superposition of the SDOF models derived.

Accordingly, for the MDOF system, the equations for the impulse response function, the frequency response function, and the transfer function are defined as follows:

Impulse Response Function (Time domain):

$$[h(t)] = \sum_{r=1}^{N} [A_r]\, e^{\lambda_r t} + [A_r^*]\, e^{\lambda_r^* t} = \sum_{r=1}^{2N} [A_r]\, e^{\lambda_r t} \tag{2.31}$$

Frequency Response Function (Frequency Domain):

$$[H(\omega)] = \sum_{r=1}^{N} \frac{[A_r]}{j\omega - \lambda_r} + \frac{[A_r^*]}{j\omega - \lambda_r^*} = \sum_{r=1}^{2N} \frac{[A_r]}{j\omega - \lambda_r} \tag{2.32}$$

Transfer Function (Laplace Domain):

$$[H(s)] = \frac{[A_r]}{s - \lambda_r} + \frac{[A_r^*]}{s - \lambda_r^*} = \sum_{r=1}^{2N} \frac{[A_r]}{s - \lambda_r} \tag{2.33}$$

where:

t = time variable

ω = Frequency variable

s = Laplace variable

The residual terms are calculated is relatively straightforward and involves an examination of FRF curve at either end of the frequency range of interest. The residual terms, necessary in the modal analysis process to take account of modes which do not analyze directly but which exist and have influence of FRF data.

$$A_{pqr} = Q_r \psi_{pr} \psi_{qr} \tag{2.34}$$

A_{pqr} = Residue

Q_r = Modal scaling factor

ψ_{pr} = Modal coefficient

λ_r = System pole

N = Number of positive modal frequencies

p = Measured degree of freedom (output)

q = Measured degree of freedom (input)

r = Modal vector number

It is important to note that the residue, A_r in Equation (2.31) through Equation (2.33) is the product of the modal deformations at the input q and response p degrees of freedom and a modal scaling factor for mode r. Therefore, the product of these three terms is unique but each of the three terms by themselves is not unique. This is consistent with the arbitrary normalization of the modal vectors. Modal scaling, Q_r, refers to the relationship between the normalized modal vectors and the absolute scaling of the mass matrix (analytical case) and/or the absolute scaling of the residue information (experimental case). Modal scaling is normally presented as modal mass or modal A.

The driving point residue, A_{qqr}, is particularly important in deriving the modal scaling.

$$A_{qqr} = Q_r \psi_{qr} \psi_{qr} = Q_r \psi_{qr}^2 \tag{2.35}$$

For undamped and proportionally damped systems, the r-th modal mass of a MDOF system can be defined as:

$$M_r = \frac{1}{2\, j\, Q_r\, \omega_r} = \frac{\psi_{pr}\ \psi_{qr}}{2\, j\, A_{pqr}\, \omega_r} \tag{2.36}$$

where;

M_r = Modal mass

Q_r = Modal scaling constant

ω_r = Damped natural frequency

If the largest scaled modal coefficient is equal to unity, Equation (2.36) will also compute a quantity of modal mass that has physical significance. The physical significance is that the quantity of modal mass computed under these conditions will be a number between zero and the total mass of the system.

The modal mass defined in Equation (2.36) is developed in terms of displacement over force units. If measurements, and residues, are developed in terms of any other units (velocity over force or acceleration over force), Equation (2.36) will have to be altered accordingly.

Once the modal mass is known, the modal damping and modal stiffness can be obtained through the following SDOF equations:

Modal Damping

$$C_r = 2\ \sigma_r\, M_r \tag{2.37}$$

Modal Stiffness

$$K_r = (\sigma_r^2 + \omega_r^2)\, M_r = \Omega_r^2\ M_r \tag{2.38}$$

2.4. Damping Mechanisms

Damping is an energy dissipation phenomenon. In order to evaluate MDOF systems that exist in the real world, the effect of damping on the complex frequencies and modal vectors must be considered. Many physical mechanisms are needed to describe all of the possible forms of damping that may be present in a particular structure or system. It is generally difficult to ascertain which type of damping is present in any particular structure. The initial proposal of proportional damping came long before the study of modal analysis. The simplest form of the damping model is the viscous damping that is proportional to the system mass or stiffness matrices of the system. Therefore:

$$[C] = \alpha [M] + \beta [K] \tag{2.39}$$

where α and β are real positive constant.

Proportional damping is a special type of damping which simplifies the system analysis. The damping matrix must be proportional to either or both of the mass and stiffness matrices. The advantage in using proportional damping is that the mode shapes for both the damped and undamped cases are the same and the modal resonance frequencies are also very similar. Under this assumption, proportional damping is the case where the equivalent damping matrix is equal to a linear combination of the mass and stiffness matrices. For this mathematical form of damping, the coordinate transformation that diagonalizes the system mass and stiffness matrices also diagonalizes the system damping

matrix. When a system with proportional damping exists, that system of coupled equations of motion can be transformed to a system of equations that represent an uncoupled system of SDOF systems that are easily solved.

The other form of the viscous damping is the non-proportional damping where damping matrix could not be formed as a linear combination of mass and stiffness matrices.

$$[M]\{\ddot{X}\}+[C]\{\dot{X}\}+[K]\{X\}=\{0\} \tag{2.40}$$

When the viscous damping of an 'n' DOF system is non-proportional, the solution of Equation (2.40) is in the form;

$$\{x(t)\}=\{X\}e^{st} \tag{2.41}$$

$$\{\dot{x}(t)\}=s\{X\}e^{st} \tag{2.42}$$

$$\{\ddot{x}(t)\}=s^2\{X\}e^{st} \tag{2.43}$$

Here, s is the Laplace operator and $\{X\}$a complex vector for displacement amplitudes.

Then Equation (2.40) becomes;

$$(s^2[M]+s[C]+[K])\{X\}=\{0\} \tag{2.44}$$

This is a complex and higher order eigenvalue problem. The solution to this problem relies on the state-space approach. This approach invents a new displacement vector defined as;

$$\{y\} = \begin{Bmatrix} x \\ \dot{x} \end{Bmatrix}_{2nx1} \tag{2.45}$$

With this new vector, Equation (2.40) transformed into:

$$\begin{bmatrix} C & M \\ M & 0 \end{bmatrix}_{2nx2n} \{\dot{y}\} + \begin{bmatrix} K & 0 \\ 0 & -M \end{bmatrix}_{2nx2n} \{y\} = \{0\} \tag{2.46}$$

or

$$[A]\{\dot{y}\} + [B]\{y\} = \{0\} \tag{2.47}$$

Equation (2.47) is a normal eigenvalue problem and its solution consists of 2n complex eigenvalues λ_r and 2n corresponding complex eigenvectors $\{\theta\}_r$.For the non-proportional damped system, there are phase differences between various parts of the system, resulting in complex mode shapes. This difference is manifested by the fact that, for undamped modes all points on the structure pass through their equilibrium positions simultaneously, and for complex modes this is not true. Thus, undamped modes have well-defined nodal points or lines while complex modes do not have stationary nodal lines.

2.5. Graphical display of a Frequency Response Function

Graphical display of FRF plays a vital role in modal analysis. Frequency response function can be seen in different forms. For simple supported beams, frequency response functions are shown real-imaginary, magnitude-phase, and log magnitude-phase graphs in Figure 2.5 through Figure 2.9.

The amplitude-phase plot consists of two parts: the magnitude of the FRF versus frequency and the phase versus frequency. The phase plot does not have much variety since the information of phase cannot be processed numerically in the same way magnitude data can. Therefore, the main focus will be on the magnitude plot of an FRF.

The real and imaginary plots consist of two parts: the real part of the FRF versus frequency and the imaginary part of the FRF versus frequency. Obviously the natural frequency occurs when the real part becomes zero. This observation is less useful than it appears to be since experimental FRF data may not have sufficient frequency resolution to pinpoint the location of the zero real part.

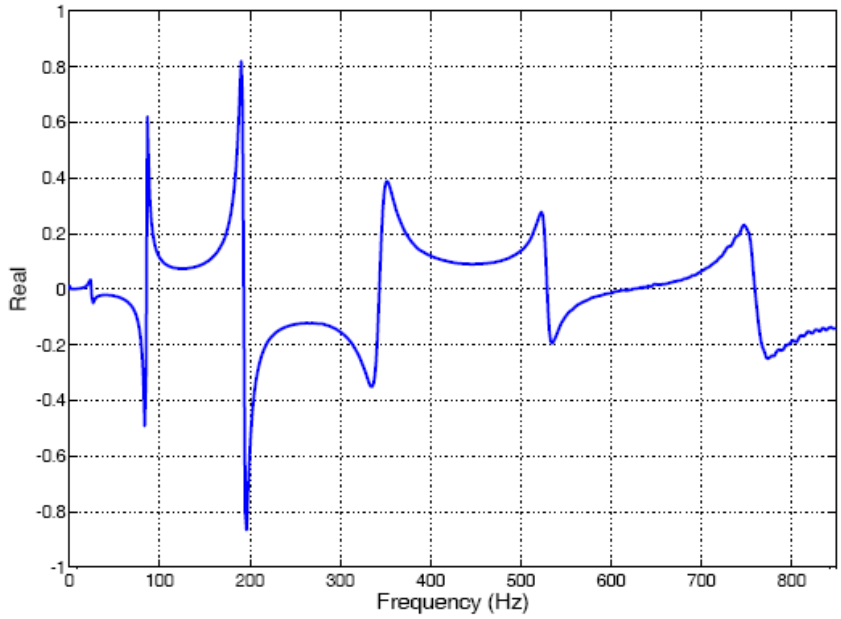

Figure 2.5. Frequency Response Function (Real format)

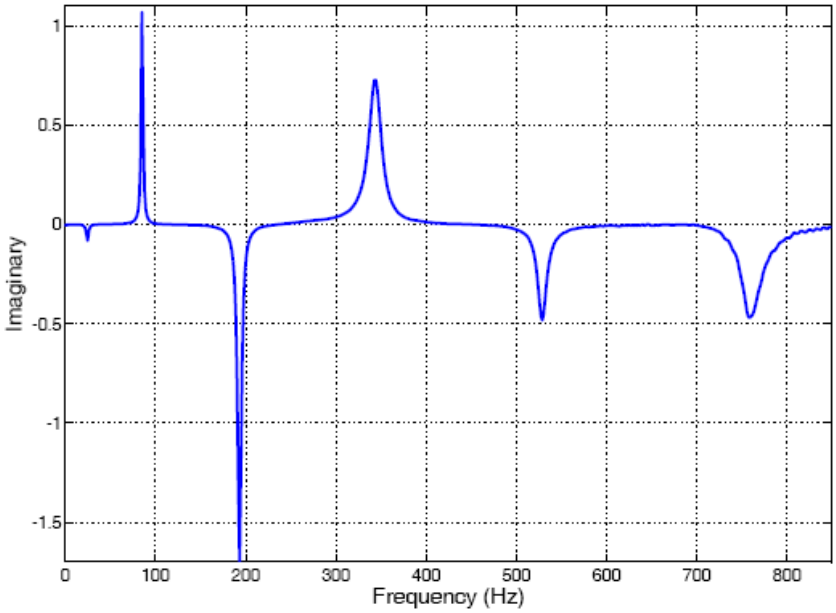

Figure 2.6. Frequency Response Function (Imaginary format)

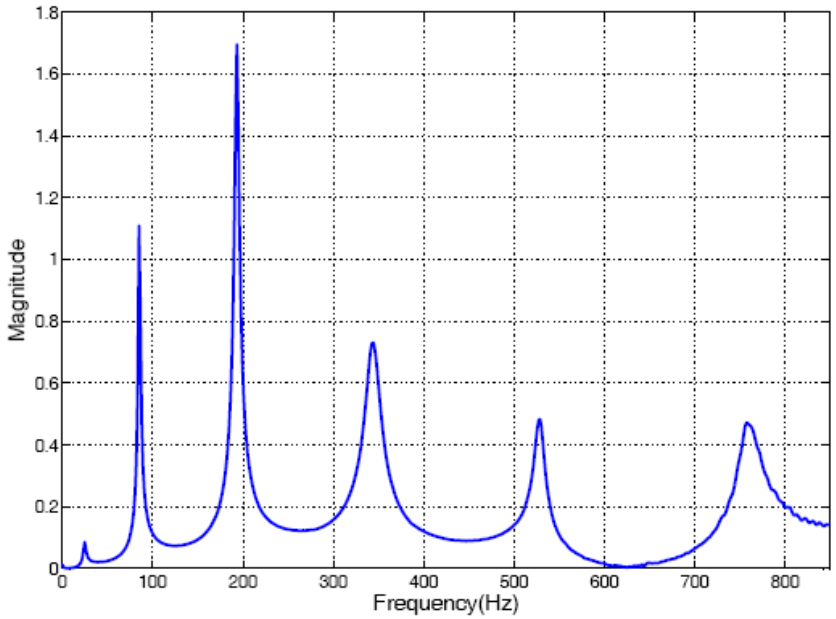

Figure 2.7. Frequency Response Function (Magnitude format)

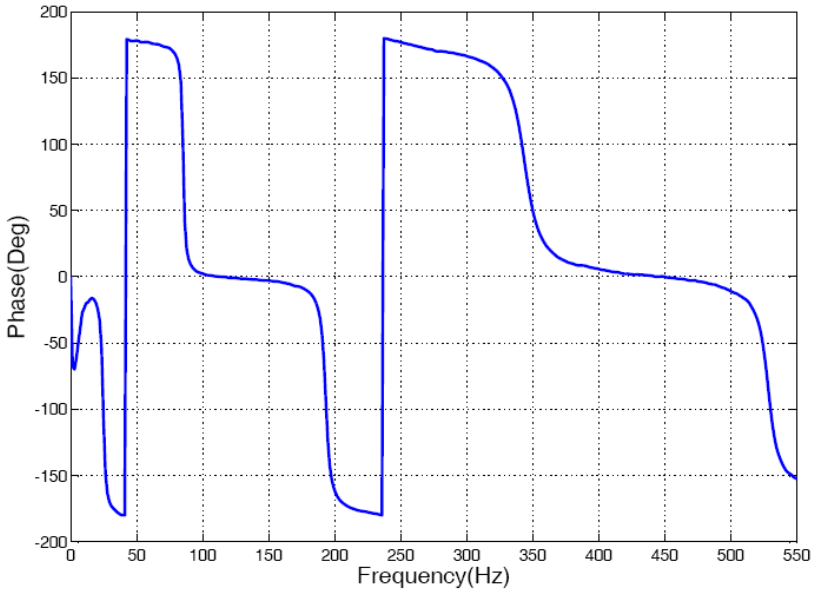

Figure 2.8. Frequency Response Function (Phase format)

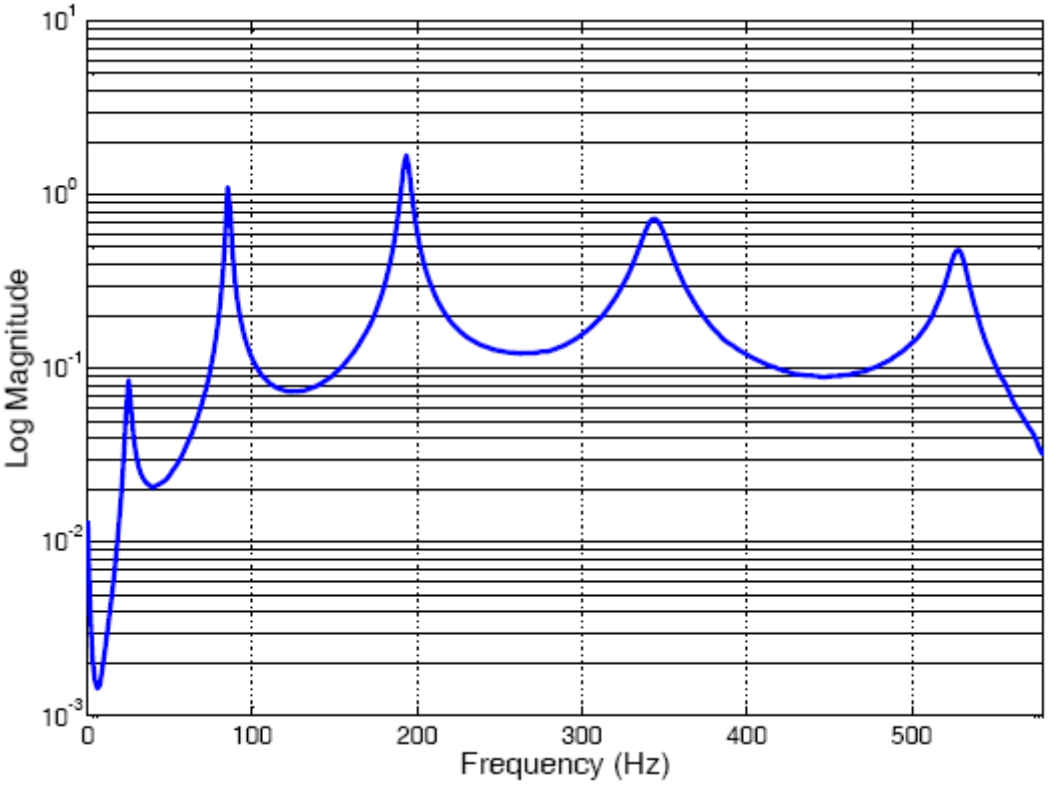

Figure 2.9. Frequency Response Function (Log Magnitude format)

CHAPTER 3

MODAL DATA ACQUISITION & EXPERIMENTAL MODAL ANALYSIS METHODS

3.1. Introduction

Modal data acquisition and related experimental modal analysis methods will be explained in this chapter. Modal data acquisition can be seen as the first step of experimental modal analysis. Acquisition of data, which will be used in the formulation of a modal model, involves many important concerns.

These concerns include successful acquisition of data, prevention of various reading and signal related errors, post processing of measured data, sampling theorems, modal analysis and domain transformations. These topics will be discussed in detail in the coming sections.

3.2. Modal Data Acquisition

In order to determine modal parameters, the measured input excitation and response data must be processed and put into a form that is compatible with the test and modal parameter estimation methods (Ewins 2000). Digital processing of the data is a very important step in modal data acquisition (Silva and Maia 1998). Signal processing is one of the technology areas where clear understandings of the Time-Frequency-Laplace domain relationships are important, (Avaitable 1998). The conversion of the data from the time domain into the frequency and Laplace domain is important both in the measurement and subsequently in the modal parameter estimation processes (Philips and Allemang 1998). The process of representing an analog signal as a series of digital values is a basic

requirement of modern digital signal processing analyzers. In practice, the goal of the analog to digital conversion (ADC) process is to obtain the conversion while maintaining sufficient accuracy in terms of frequency, magnitude, and phase information (Silva and Maima 1998). Considering the analog devices, these concerns were satisfied by the performance characteristics of each individual analog device. Typically analog devices are optimized during the fabrication and satisfying performance characteristics is a matter of selecting the right equipment for the purpose. Beyond the analog devices the characteristics of the analog to digital conversion is the primary concern. Process of analog to digital conversion involves two separate concepts: sampling and quantization. Each concept is related to the dynamic performance of a digital signal processing analyzer. Sampling is the part of the process related to the timing between individual digital pieces of the time history (Silva 2000). Quantization is the part of the process related to describing analog amplitude as a digital value. Primarily, sampling considerations alone affect the frequency accuracy while both sampling and quantization considerations affect magnitude and phase accuracy (Ewins 2000).

3.2.1. Sampling

Sampling is the process of converting a signal into a numeric sequence as a function of discrete time or space (Silva 2000). Analog signals should be converted to "digital" form in order to process in computers. While an analog signal is continuous in both time and amplitude, a digital signal is discrete in both time and amplitude. To convert a signal from continuous time to discrete time, a process called sampling is used. The value of the signal is measured at certain intervals in time. Each measurement is referred to as a sample (Application Note 243-3-HP).

If the signal contains high frequency components, it is needed to sample at a higher rate to avoid loosing high frequency information in the signal. If it is necessary to preserve the information up to a certain frequency in the signal, it is necessary to sample at twice the target frequency of the signal (Figliola and Beasley 1995). This is known as the Nyquist rate. The Sampling Theorem states that a signal can be exactly reproduced if it is sampled

at a frequency F, where F is greater than twice the maximum frequency in the signal (Allemang 1999).

Sampling Theory: If a time signal *x(t)* is sampled at equal steps of *ΔT*, no information regarding its frequency spectrum *X(f)* is obtained for frequencies higher than $f_c = 1/(2*\Delta T)$. This fact is known as Shannon's sampling theorem, and the limiting (cutoff) frequency is called the Nyquist frequency. In vibration signal analysis, a sufficiently small sample step *ΔT* should be chosen in order to reduce aliasing distortion in the frequency domain, depending on the highest frequency of interest in the analyzed signal (Allemang 1999, Figliola and Beasley 1995). This, however, increases the signal processing time and the computer storage requirements, which is undesirable particularly in real-time analysis. It also can result in stability problems in numerical computations. The Nyquist sampling criterion requires that the sampling rate *(1/ΔT)* for a signal should be at least twice the highest frequency of interest. Instead of making the sampling rate very high, a moderate value that satisfies the Nyquist sampling criterion is used in practice, together with an anti-aliasing filter to remove the distorted frequency components.

Shannon's Sampling Theorem states, the following in a very simple form:

$$F_{samp} = \frac{1}{\Delta t} = F_{Nyq}\ x\ 2.0 \tag{3.1}$$

$$F_{Nyq} \geq F_{\max} \tag{3.2}$$

In order to be certain that Equation (3.1), and Equation (3.2) are always satisfied, an analog, low pass filter (LPF) with a cutoff frequency below the Nyquist frequency must always be used when acquiring data. Generally, LPF is built into the digital signal analyzer (Allemang 1999, Figliola and Beasley 1995).

3.2.2. Quantization

Quantization error is the difference between the actual analog signal and the measured digitized value. Note that, when measuring transient events that cannot be averaged, this error limits the achievable magnitude accuracy (Allemang 1999, Figliola and Beasley 1995, Montalvao 1999).

3.2.3. ADC Errors

Most modern data acquisition systems minimize errors associated with the analog to digital conversion of data to the extent that the average user does not need to be concerned with the ADC errors (Jimin and Zhi-Fang 2001). The primary ADC errors are aliasing and quantization errors.

3.2.3.1. Aliasing

An aliased signal provides a poor representation of the analog signal. Aliasing causes a false lower frequency component to appear in the sampled data of a signal. The Figure 3.1 shows an adequately sampled signal and Figure 3.2 shows an undersampled signal.

In the Figure 3.2, the undersampled signal appears to have a lower frequency than the actual signal—two cycles instead of ten cycles.

Increasing the sampling frequency increases the number of data points acquired in a given time period. Often, a fast sampling frequency provides a better representation of the original signal than a slower sampling frequency.

For a given sampling frequency, the maximum frequency can accurately represent without aliasing is the Nyquist frequency. The Nyquist frequency equals one-half the sampling frequency, as shown by the following equation.

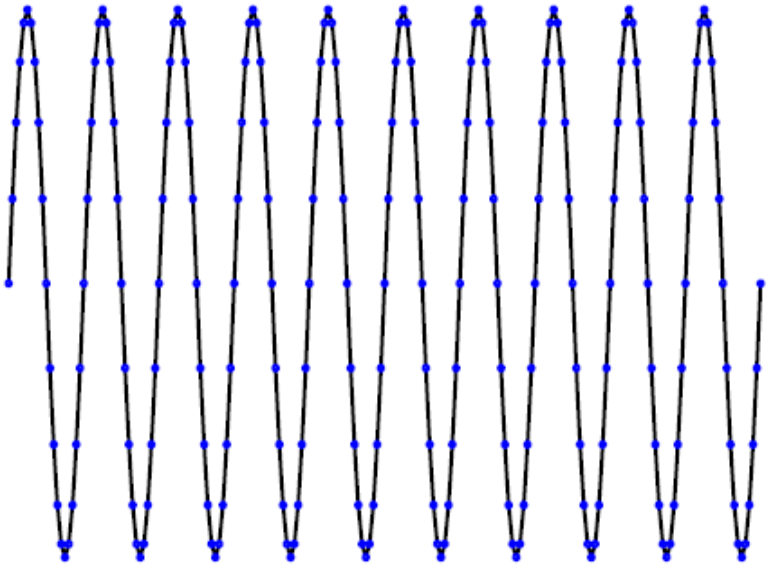

Figure 3.1. Adequately Sampled Signal

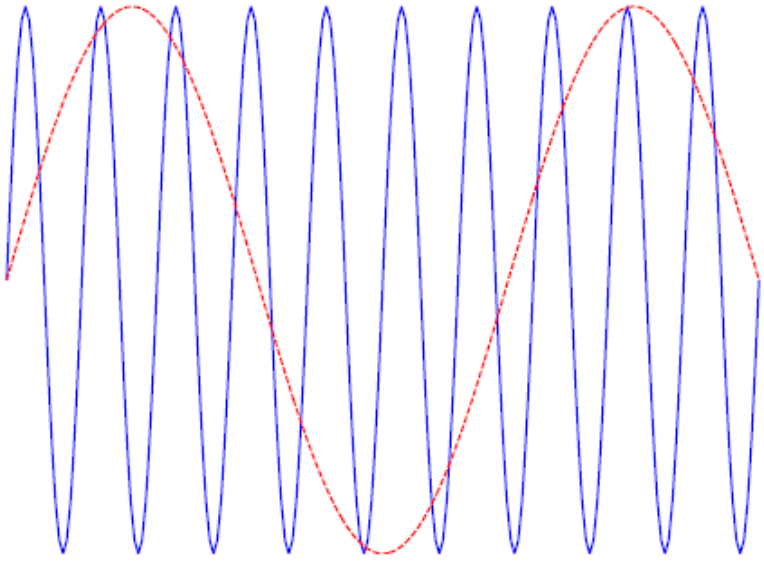

Figure 3.2. Aliased Signal Due to Undersampling

$$f_N = (f_s / 2) \tag{3.3}$$

where f_N is the Nyquist frequency and f_s is the sampling frequency.

Signals with frequency components above the Nyquist frequency appear aliased between DC and the Nyquist frequency. In an aliased signal, frequency components actually above the Nyquist frequency appear as frequency components below the Nyquist frequency. For example, a component at frequency $f_N < f_0 < f_s$ appears as the frequency $f_s - f_0$.

The next two figures illustrate the aliasing phenomenon. The Figure 3.3 shows the frequencies contained in an input signal acquired at a sampling frequency, f_s, of 100 Hz.

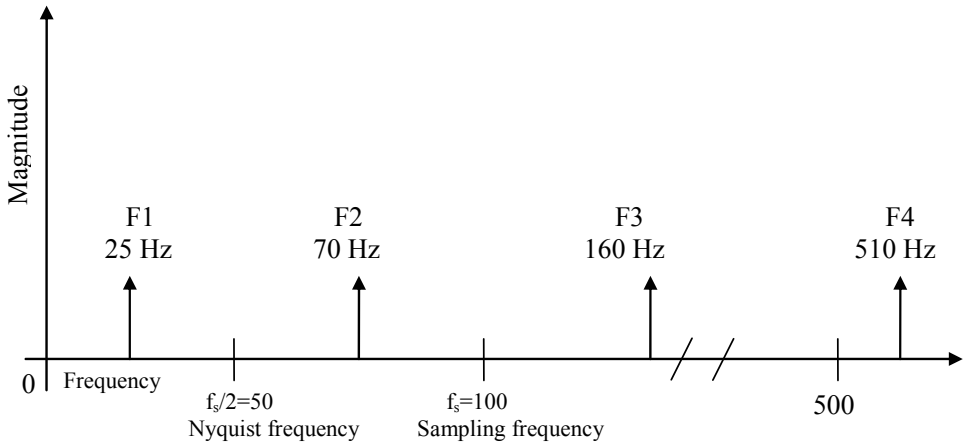

Figure 3.3. Input Signal Acquired

The Figure 3.4 shows the frequency components and the aliases for the input signal from the Figure 3.3

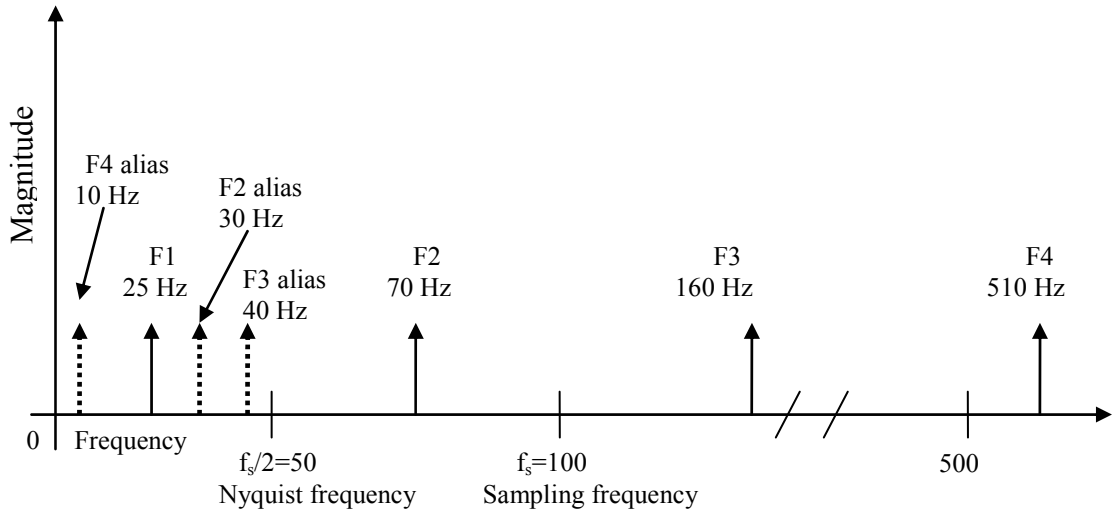

Figure 3.4. Aliases for the Input Signal

In the Figure 3.4, frequencies below the Nyquist frequency of $f_s/2$ = 50 Hz are sampled correctly. For example, F1 appears at the correct frequency. Frequencies above the Nyquist frequency appear as aliases. For example, aliases for F2, F3, and F4 appear at 30 Hz, 40 Hz, and 10 Hz, respectively.

The alias frequency equals the absolute value of the difference between the closest integer multiple of the sampling frequency (CIMSF) and the input frequency (IF), as shown in the following equation:

$$AF = |CIMSF - IF| \tag{3.4}$$

where AF is the alias frequency, CIMSF is the closest integer multiple of the sampling frequency, and IF is the input frequency. For example, you can compute the alias frequencies for F2, F3, and F4 from the figure above with the following equations:

Alias F2 = |100 – 70| = 30 Hz

Alias F3 = |(2)100 – 160| = 40 Hz

Alias F4 = |(5)100 – 510| = 10 Hz

Anti-Aliasing Filters: Use an anti-aliasing analog lowpass filter before the A/D converter to remove alias frequencies higher than the Nyquist frequency. A lowpass filter allows low frequencies to pass but attenuates high frequencies. By attenuating the frequencies higher than the Nyquist frequency, the anti-aliasing analog lowpass filter prevents the sampling of aliasing components.

The Figure 3.5 shows both an ideal anti-alias filter and a practical anti-alias filter. The following information applies to the Figure 3.5:

- f_1 is the maximum input frequency.
- Frequencies less than f_1 are desired frequencies.
- Frequencies greater than f_1 are undesired frequencies.

An ideal anti-alias filter, shown in part of the Figure 3.5, passes all the desired input frequencies and cuts off all the undesired frequencies. However, an ideal anti-alias filter is not physically realizable.

Part b of the Figure 3.5 illustrates actual anti-alias filter behavior. Practical anti-alias filters pass all frequencies less than f_1 and cut off all frequencies greater than f_2. The region between f_1 and f_2 is the transition band, which contains a gradual attenuation of the input frequencies. It is wanted to pass only signals with frequencies less than f_1, the signals in the transition band might cause aliasing. Therefore, in practice, use a sampling frequency greater than two times the highest frequency in the transition band. Using a sampling frequency greater than two times the highest frequency in the transition band means f_s might be greater than $2f_2$ (Ewins 1995, Labview 2005).

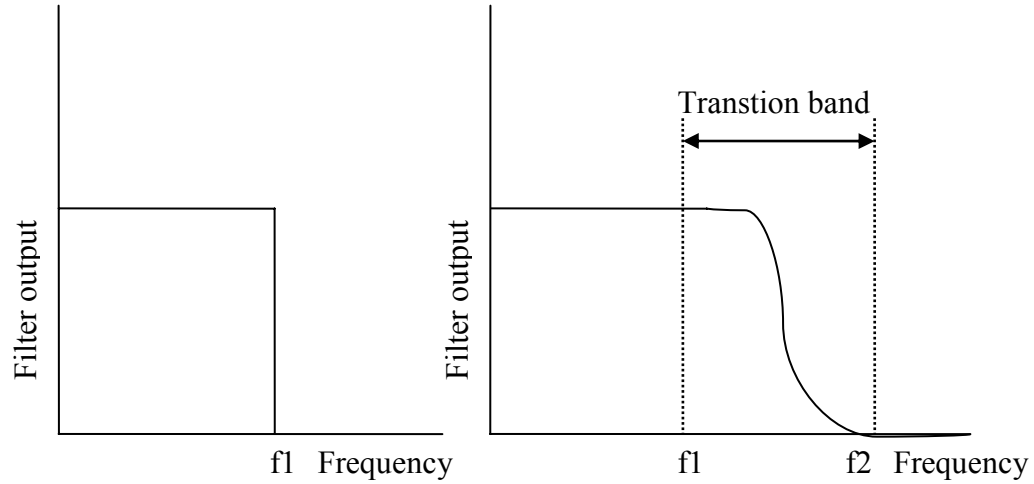

Figure 3.5. Anti-Alias Filter

3.2.4. Discrete Fourier Transform

The algorithm used to transform samples of the data from the time domain into the frequency domain is the discrete Fourier transform (DFT). The DFT establishes the relationship between the samples of a signal in the time domain and their representation in the frequency domain. The DFT is widely used in the fields of spectral analysis, applied mechanics, acoustics, medical imaging, numerical analysis, instrumentation, and telecommunications.

3.2.4.1. Discrete Fourier Transform Errors

The primary digital signal processing error involved with making measurements is an error associated with the discrete Fourier transform which is used to transform the digital time data to digital frequency data. This error is a bias error that is known as leakage or truncation error. Actually, it is not really an error but is a limitation of discrete Fourier

transform. The discrete Fourier transform is expected to give the same answer as the integral Fourier transform, which is true when only certain conditions are met concerning the time domain data (Allemang 1999).

3.2.4.2. Leakage Error

Leakage error is basically due to a violation of an assumption of the Discrete Fourier transform algorithm. Leakage is probably the most common and, therefore, the most serious digital signal processing error (Ewins 2000, Silva 2000). Unlike aliasing and many other errors, the effects of leakage can only be reduced, not completely eliminated.

Leakage is a serious problem in many applications of digital signal processing, including FRF measurement, and ways of avoiding or minimizing its effects. There are various possibilities, which include:

- Changing the duration of the measurement sample length to match any underlying periodicity in the signal so as to capture an exact number of cycles of the signal.
- Increasing the duration of the measurement period, T, so that the separation between the spectral lines is finer.
- Adding zeroes to the end of the measure sample.
- By modifying the signal sample obtained in such a way as to reduce the severity of the leakage effect.

3.2.4.3. Windowing

In many situations, the most practical solution to the leakage problem involves the use of windowing and there are a range of different windows for different classes problem (Ewins 2000).

The type of window to use depends on the type of signal acquired and on the application. Choosing the correct window requires some knowledge of the signal that to be analyzed.

3.2.4.4. Averaging

Generally, averaging is utilized primarily as a method to reduce the error in the estimate of the frequency response functions. This error can be broadly considered as noise on either the input and/or the output. This error can be considered to the sum of random and bias components (Phillips and Allemang 2003). Random errors can be effectively minimized through the common approach to averaging, RMS spectral averaging. However, bias errors cannot generally be effectively minimized through this form of averaging alone.

3.2.5. Transducer Considerations

Although there are various types of transducers, the piezoelectric type is the most widely used for modal testing. It has wide frequency and dynamic ranges, good linearity and is relatively durable. The piezoelectric transducer is an electromechanical sensor that generates an electrical output when subjected to vibration. This is accomplished with a crystal element that creates an electrical charge when mechanically strained (Application Note 243-3).

The mechanism of the response transducer, called an accelerometer, functions in a similar manner. When the accelerometer vibrates, an internal mass in the assembly applies a force to the crystal element which is proportional to the acceleration. This relationship is simply Newton's Law: force equals mass times acceleration.

Although the resonant frequency of the accelerometer is a function of its mass and stiffness characteristics, the actual natural frequency is generally dictated by the stiffness of the mounting method used. The different various mounting methods are effects different frequency ranges.

Another important consideration is the effect of mass loading from the accelerometer (Cakar 2005). This occurs as a result of the mass of the accelerometer being

a significant fraction of the effective mass of a particular mode. A simple procedure to determine if this loading is significant can be done as follows:

- Measure a typical frequency response function of the test object using the desired accelerometer.
- Mount another accelerometer (in addition to the first) with the same mass at the same point and repeat the measurement.
- Compare the two measurements and look for frequency shifts and amplitude changes.

If the two measurements differ significantly, then mass loading is a problem and an accelerometer with less mass should be used. On very small structures, it may be necessary to measure the response with a non-contacting transducer, such as an acoustical or optical sensor, in order to eliminate any mass loading (Şanlıtürk and Çakar 2005).

3.2.6. Noise/Error Minimization

Three algorithms, referred to as the H_1, H_2, and H_v algorithms, are commonly available for estimating FRFs. Table 3.1 summarizes this characteristic for the three methods that are widely used.

Table 3. 1. Summary of FRF Estimation Models

Frequency Response Function Models		
Technique	Assumed Location of Noise	
	Force Inputs	Response
H_1	No Noise	Noise
H_2	Noise	No Noise
H_v	Noise	Noise

3.3. Experimental Modal Analysis Methods

Categorizing different methods of experimental modal analysis is helpful when reviewing the literature in the area of experimental modal analysis. These methods are grouped according to:

1. Type of measured data that is acquired
a. Sinusoidal Input-Output Model
b. Frequency Response Function Model
c. Damped Complex Exponential Response Model
d . General Input-Output Model
2. Type of model used in modal parameter estimation stage
a. Parametric Model
i. Modal Model
ii. [M], [K], [C] Model
b. Non-Parametric Model
3. According to the domain of the modal parameter estimation model
a. Time Domain
b. Frequency Domain
c. Spatial Domain

In this section, experimental modal analysis method of frequency response function is explained in detail only. Frequency response function is a commonly used method in experimental modal analysis. (Richardson 1986, Shye et al. 1987).

3.3.1. Frequency Response Function Model

The frequency response function method of experimental modal analysis is the most commonly used approach to the estimation of modal parameters. This method originated as a testing technique as a result of the use of frequency response functions to determine

natural frequencies for effective number of degrees of freedom. In this method, frequency response functions are measured using excitation at single or multiple points. The relationships between the input $F(\omega)$ and the response $X(\omega)$ for both single and multiple inputs are shown in Equation (3.5) through Equation (3.7). In the following sections frequency response function model and frequency response function method are explained.

Single input relationship;

$$X_p = H_{pq} F_q \tag{3.5}$$

$$\begin{bmatrix} X_1 \\ X_2 \\ . \\ . \\ X_p \end{bmatrix} = \begin{bmatrix} H_{1q} \\ H_{2q} \\ . \\ . \\ H_{pq} \end{bmatrix} F_q \tag{3.6}$$

where; X_p is the spectrum of the p^{th} response, F_q is the spectrum of the q^{th} input, and H_{pq} is the frequency response function for output location p, input location q.

Multiple input relationship;

$$\begin{bmatrix} X_1 \\ X_2 \\ . \\ . \\ X_p \end{bmatrix}_{N_o x 1} = \begin{bmatrix} H_{11} & . & . & . & H_{1q} \\ H_{21} & . & . & . & H_{2q} \\ . & . & . & . & . \\ . & . & . & . & . \\ H_{p1} & . & . & . & H_{pq} \end{bmatrix}_{N_0 x N_i} \begin{bmatrix} F_1 \\ F_2 \\ . \\ . \\ F_q \end{bmatrix}_{N_i x 1} \tag{3.7}$$

The frequency response functions are used as input data to modal parameter estimation algorithms that estimate modal parameters using a frequency domain model and

spatial domain model. Through the use of the fast Fourier transform, the Fourier transform of the frequency response function and the impulse response function can be calculated for use in modal parameter estimation algorithms involving time domain models.

3.3.2. Frequency Response Function Testing Method

For current approaches to experimental modal analysis, the frequency response function is the most important measurement to be made. When estimating frequency response functions, a measurement model is needed that will allow the frequency response function to be estimated from measured input and output data in the presence of noise and errors. Some of the errors are:

- Leakage (FFT error)
- Aliasing (FFT error)
- Noise
    1. Equipment problem (Power supply noise)
    2. Cabling problems (Shield problem)
    3. Rattles, cable motion
- Calibration (Operator error)
    1. Complete system calibration
    2. Transducer calibration

Several important points to be remembered before attempting to estimate frequency response functions are:

1. The system (with the boundary conditions for that test) determines the frequency response functions for the given input/output locations.
2. It is important to eliminate or at least minimize all errors (aliasing, leakage, noise, calibration, etc.) when collecting data.
3. Since modal parameters are computed from estimated frequency response functions, the modal parameters are only as accurate as the estimated frequency response function.

There are number of different frequency response function testing configurations (Avaitable 2002). These different testing configurations are function of acquisition channels or excitation sources. These testing configurations are (Allemang 1999):

1. Single input single output (SISO)
    - Only option with two channel data acquisition system
    - Longest testing time.
    - Time invariance problem between measurements.
2. Single input multiple output (SIMO)
    - Multiple channel system (3 or more).One ADC channel for each response signal to be measured plus one ADC channel for an input signal.
    - Shorter testing time than SISO. Transducers not necessarily moved.
    - Consistent frequency and damping for data acquired simultaneously.
    - Time invariance problems between measurements from different inputs.
3. Multiple input single output (MISO)
    - Multiple channel system required (3 or more). One ADC channel for each input signal to be measured plus one ADC channel for a response signal.
    - Long testing time. Roving response transducer.
    - More than one input location per measurement cycle.
    - Detects repeated roots. Maxwell reciprocity checks.
    - Time invariance problems between measurements from different responses.
4. Multiple input multiple output (MIMO)
    - Multiple channel system (up to 512 channels). Increased set-up time.
    - Large amount of data to be stored and organized.
    - Shortest testing time.
    - Consistent frequency and damping for all data acquired simultaneously.
    - Detects repeated roots. Maxwell reciprocity checks.
    - Best overall testing scheme.

3.3.3. Excitation

Excitation is any form of input that is used to create a response in a structural system (Allemang 1999). The choice of excitation can make the difference between a good measurement and a poor one. Excitation selection should be approached from both the type of function desired and the type of excitation system available because they are interrelated. The excitation function is the mathematical signal used for the input. The excitation system is the physical mechanism used to prove the signal. In general, choosing a hammer for the excitation system dictates an impulsive type excitation function.

The primary assumption concerning the excitation of a linear structure is that the excitation is observable. Whenever the excitation is measured, this assumption simply implies that the measured characteristic properly describes the actual input characteristics.

3.3.3.1. Classification of Excitation

Inputs which can be used to excite a system in order to determine frequency response functions belong to one of the two classifications (Allemang 1999).

a) Random signals,

b) Deterministic signals.

Random signals are defined by their statistical properties over some time period and no mathematical relationship can be formulated to describe the signal whereas deterministic signals can be represented in an explicit mathematical relationship (Silva 1995). Deterministic signals are further divided into “periodic” and “non-periodic” classifications. The most common inputs in the periodic deterministic signal designation are sinusoidal while the most common inputs in the non-periodic deterministic designation are transient in form.

Excitation mechanisms fall into four categories: shaker, impactor, step relaxation and self-operating (Allemang 1999, Ewins 2000). Step relaxation involves preloading the structure with a measured force through a cable then releasing the cable and measuring the transients. Self-operating involves exciting the structure through an actual operating load.

This input cannot be measured in many cases, thus limiting its usefulness. Impactors are the most common and are discussed in more detail in the following sections. Another method of excitation mechanism classification is to divide them into attached and nonattached devices. A shaker is an attached device, while an impactor is not.

3.3.3.2. Impact Excitation

With the ability to compute FRF measurements in an FFT analyzer, impact testing was developed during the late 1970's (Schwarz and Richardson 1999) and has become most popular modal testing method used today. One of the common excitation mechanisms in modal testing is an impact device. Although it is a relatively simple technique to implement, it's difficult to obtain consistent results. The convenience of this technique is attractive because it requires very little hardware and provides shorter measurement times. It is convenient to use and very portable for field and laboratory tests. As shown in Figure 3.6, a typical impact tests needs a hammer, an accelerometer, data acquisition system and a system to be tested.

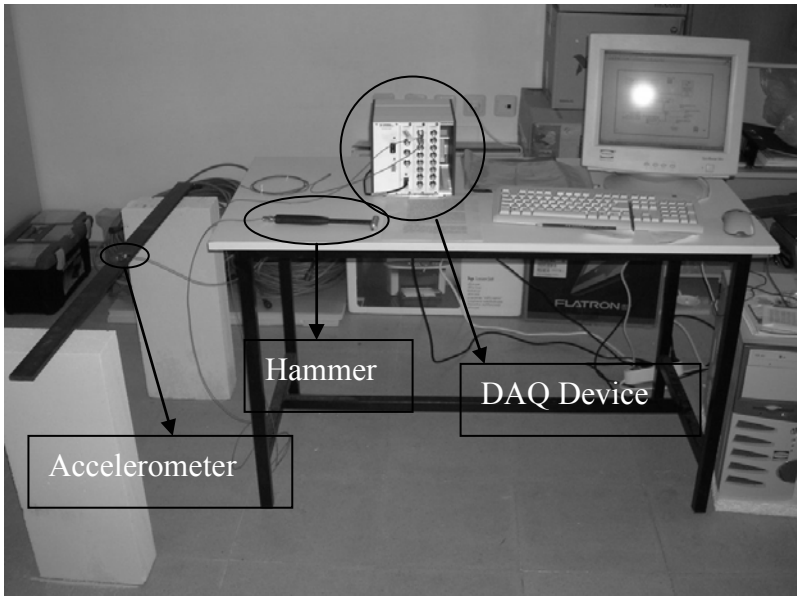

Figure 3.6. Impact Testing

Since the force is an impulse, the amplitude level of the energy applied to the structure is a function of the mass and the velocity of the hammer. This is due to the concept of linear momentum, which is defined as mass times velocity. The linear impulse is equal to the incremental change in the linear momentum. It is difficult though to control the velocity of the hammer, so the force level is usually controlled by varying the mass. Impact hammers are available in weights varying from tens of grams to several kilograms. Also, mass can be added to or removed from most hammers, making them useful for testing objects of varying sizes and weights.

When impact testing is used, windows are generally required on both the force and response data in order to minimize different errors. In many impact testing situations the use of an exponential window is necessary to minimize the effects of leakage. Normally, for lightly damped systems, a window that attenuates to 1-5 percent at the end of the response is appropriate.

CHAPTER 4

EXPERIMENTAL STUDY

4.1. Introduction

The success of the modal analysis is based on a carefully designed and performed modal experiment. The reason for this dependency is the sensitivity of the measured system data to measurement errors, electronic noise, calibration and the signal processing. In this study modal experiments of simple systems have been planned and performed in order to get the first hand experience about the parameters of the design and application of modal experiments. The design, implementation and the results of the selected simple system experiments will be presented in this chapter.

There are three parameter groups and two verifications in design of modal experiments. The parameters are the selection of test equipments, data acquisition variables and location and number of inputs and outputs to the system (acceleration reading and excitation locations in our test designs). The verifications are the sensor calibrations and the validity of the basic assumptions of the modal analysis for the system at hand. These topics will be discussed in detail in the following sections.

In order to start the design of a modal experiment, some characteristics of the system, should be obtained at the beginning. For this purpose some preliminary measurements from the system should be made. The linearity and time invariance of the system should be controlled as a first action to verify the suitability of the system to the basic assumptions of the modal analysis. Next, the decisions about triggering, number of averages, duration of the record, frequency resolutions and intervals should be taken. And finally location and number of measurement points should be decided. Measurements performed at a few points on the system are typically sufficient for these decisions.

The chapter is organized to discuss the issues in experimental design first and than continue with the presentation of modal experiments and analysis of the simple systems considered.

4.2. Modal Experiment Design

4.2.1. Sensors

The targeted physical quantities of the systems are measured thru the sensors. Typically the sensors used in this study transform the physical quantities into electrical signals. These analog signals are digitized and stored in computer environment for further study. Two types of physical quantities are measured in the experiments considered: acceleration and force. The sensors used for this purpose should be suitable to the measured system. The most important characteristics of the sensors for modal experiments are sensitivity, mass and frequency interval supported by the sensor. Since the considered systems typically have low and medium system frequencies, accelerometers with a general purpose piezoelectric crystal have been used. Three types of accelerometers were in reach. These are PCB-333B42, PCB-356A16 and PCB-393B04 accelerometers. These devices permit measurements in 0.05Hz-5000Hz frequency interval with 100mV/g-1000mV/g sensitivity. B42 and A16 have a weight of 7.5 gr and B04 is 50 grams. Comparing with the mass of the systems considered these sensors are relatively light and they do not cause significant changes in measurement system (Çakar and Şanlıtürk 2005).

Excitation to the system is given by an impact hammer. A PCB-086C04 impact hammer was available for this purpose. It has a normal mass of 160gr. If required, an additional 75gr mass could be attached. It can perform measurements at 1.1mV/N of sensitivity for the frequencies up to 8 kHz. It is designed for structural behavior testing and incorporates an Integrated Circuit Piezoelectric (ICP) quartz force sensor that is mounted on the striking end of the hammer head. It provides a nearly constant force over a broad frequency range. The striking end of the hammer has a threaded hole that permits the user to install a variety of impact tips. Tips of different stiffness permit the user to vary the pulse width and frequency content of the applied force. The hammer velocity at impact also

affects the frequency content in addition to the signal energy level. The available tips of the hammer are color coded according to their stiffness using the following convention:

- Super soft => Red
- Soft => Black
- Medium => Blue
- Hard = >Steel

In general, a softer tip supplies a greater pulse duration and low frequency content than a harder tip. However, a harder tip will provide an impulse of larger amplitude and high frequency content to the excitation than a softer tip.

4.2.2. Data Acquisition

NI-SCXI data acquisition modules that are compatible with the sensors have been used in the study. There are two modules which are acting as analog to digital converter and the accelerometer signal conditioner. These are SCXI-1600 and SCXI-1531 respectively. SCXI-1600 is a high-performance plug-and-play USB device used for direct connection between USB-compatible computers and SCXI systems. It has a 16-bit ADC resolution and 200kS/s sampling rate. It can also control digital input, digital output, and analog output to other SCXI modules. SCXI-1531 is an eight channel ICP accelerometer conditioning module with programmable current gain and filter setting on each channel. It also has simultaneous sample and hold circuitry. Each channel has programmable gain settings of 1, 10, or 100 and programmable four-pole Bessel filter settings of 2.5, 5, 10 or 20 kHz. Each channel also has programmable floating 4 mA, 24 V compliant current sources. SCXI-1531 provides eight BNC connectors to interface with accelerometers. This module supports both multiplexed and parallel output modes. The fundamental task of all measurement systems is the measurement, processing and storage of the physical signals. In this project LabVIEW is used for these purposes. The raw data acquired from the experiments are transformed to frequency response functions thru Matlab (Mathworks, 2004). The modal analysis is performed thru the use of X-Modal software (UC-SDRL, X-

Modal II). It is experimental modal analysis software which is capable of identifying the dynamic parameters from the frequency response functions provided. There are several application modules available under X-Modal II among which are; Data Manager, Universal File Editor, Modal Parameter Estimation, Advanced Mode Indicator Function, Computed Order Tracking, and Impedance Modeling. Data Manager is the starting module. It handles loading and storing of data and results, as well as the start of the various other application modules. For this project Modal Parameter Estimation and Advanced Mode Indicator Function modules are used.

Modal parameter estimation is a special case of system identification where a priori model of the system is known to be in the form of modal parameters. Therefore, regardless of the form of measured input-output data, the form of the model used to represent the experimental data can be stated in a modal model using temporal (time or frequency) and spatial (input DOF and output DOF) information (Avaitable 1999). Advanced Mode Indication Function (AMIF) is an algorithm based on singular value decomposition (Avaitable 2001) method that is applied to multiple or single reference FRF measurements. AMIF was first developed in order to identify the proper number of modal frequencies, particularly when there are closely spaced or repeated modal frequencies (Shih, et al. 1989). AMIF is capable to indicate the existence of real normal or complex modes and the relative magnitudes of each mode.

4.2.3. Deciding on the number and location of the measurement points

The development of any theoretical concept in the area of vibrations, including modal analysis, depends on an understanding of the concept of the number of degrees of freedom (DOF) of a system. This concept is extremely important to the area of modal analysis since theoretically the number of modes of vibration of a mechanical system is equal to the number of DOF (Silva 2000). From a practical point of view, the relationship between this definition of the number of DOF (N_o) and the number of measurement DOF (Ni) is often confusing. The number of DOF for a mechanical system is equal to the number of independent coordinates (or minimum number of coordinates) that is required to locate and orient each mass in the mechanical system at any instant in time (Allemang

1999). As this definition is extended to any general deformable body, it should be obvious that the number of DOF should be considered as infinite. While this is theoretically true, it is quite common to view the general deformable body in terms of a large number of physical points of interest with six DOF for each of the physical points. In this way, the infinite number of DOF can be reduced to a large but finite number.

For a general deformable body, initially the number of DOF can be considered to be infinite or equal to some large finite number if a limited set of physical points of interest is considered. Considering that the frequencies of DOF are spanned in an interval from zero to infinity, if the interested frequency interval is defined, the number of DOF should be limited from infinity to a certain number. This is the first limitation that could be applied to the number of DOF. As this limitation is considered, the measurement of the system includes only the systems modes in the frequency interval measured. This frequency interval can be defined in two different ways. If the preliminary measurements are made in a sufficiently wide frequency interval, the selected number of peaks in the frequency response function could be used to define the number of modes (read as DOF) and the frequency interval for the modal experiment. Or, if a finite element analysis of the system is available, approximate frequency range and the measurement DOF of the system could be determined based on this analysis.

The next measurement limitation that needs to be considered involves the physical limitation of the measurement system in terms of amplitude. A common limitation of transducers, signal conditioning and data acquisition systems results in a dynamic range of 90 db in the measurement (He 2001). As a result DOF which are outside this range could not me measured by the hardware available.

Locations of the measurements are another limitation on the DOF of the system. The node point is a location of zero response. Obviously if the measurement is made at a nodal point, no data can be obtained for that specific mode. In order to avoid these condition reference locations (excitation and reading locations) must not be located at the node of a target mode. Specifically, if the excitation location is at the proximity of a nodal point, signals of that specific mode could become very weak. Using multiple references could minimize this limitation. Due to this reason selection of reference locations is not an

easy task. A finite element model, if available, is a great tool to assist in the selection of references.

4.2.4. Sensors Calibration

The accelerometers and hammer should be calibrated before any testing is performed. Otherwise the sensor readings become misleading. The objective of this experiment is to determine the calibration of force (load) and response (accelerometer) sensors using calibration methods. Gravimetric comparison calibration of accelerometers and force measuring impact hammers are accomplished by evaluating the transfer function of a rigid body mass. A reference sensor (measuring force when calibrating a hammer) is attached to one end of the mass with the test sensor on the other end. By exciting the instrumented mass and measuring the transfer function (A/F) the result should yield a flat line equal to 1/M over the valid frequency range. Any deviation in magnitude or phase from the expected flat line transfer behavior represents the characteristics for the test sensor under calibration. For hammer calibration, input is accomplished by striking a pendulous mass. Figure 4.1 shows that the calibration procedure for accelerometers.

The calibration procedure makes use of the following equations that are derived from Newton's second law of motion and the assumption that the sensitivity of the load cell on the instrumented hammer is equal to its satisfactory calibration value:

$$F = MA \tag{4.1}$$

$$F = \frac{V_f}{S_f} \tag{4.2}$$

$$A = \frac{V_a}{S_a} \tag{4.3}$$

where;

S_a = Sensitivity of accelerometer (mV/g)

S_f = Sensitivity of hammer (mV/N)

F = Force of impact (N)

A = Acceleration due to impact (g's)

M = Total mass (calibration body + accelerometer) (kg)

V_a = Signal from accelerometer (volts)

V_f = Signal from hammer (volts)

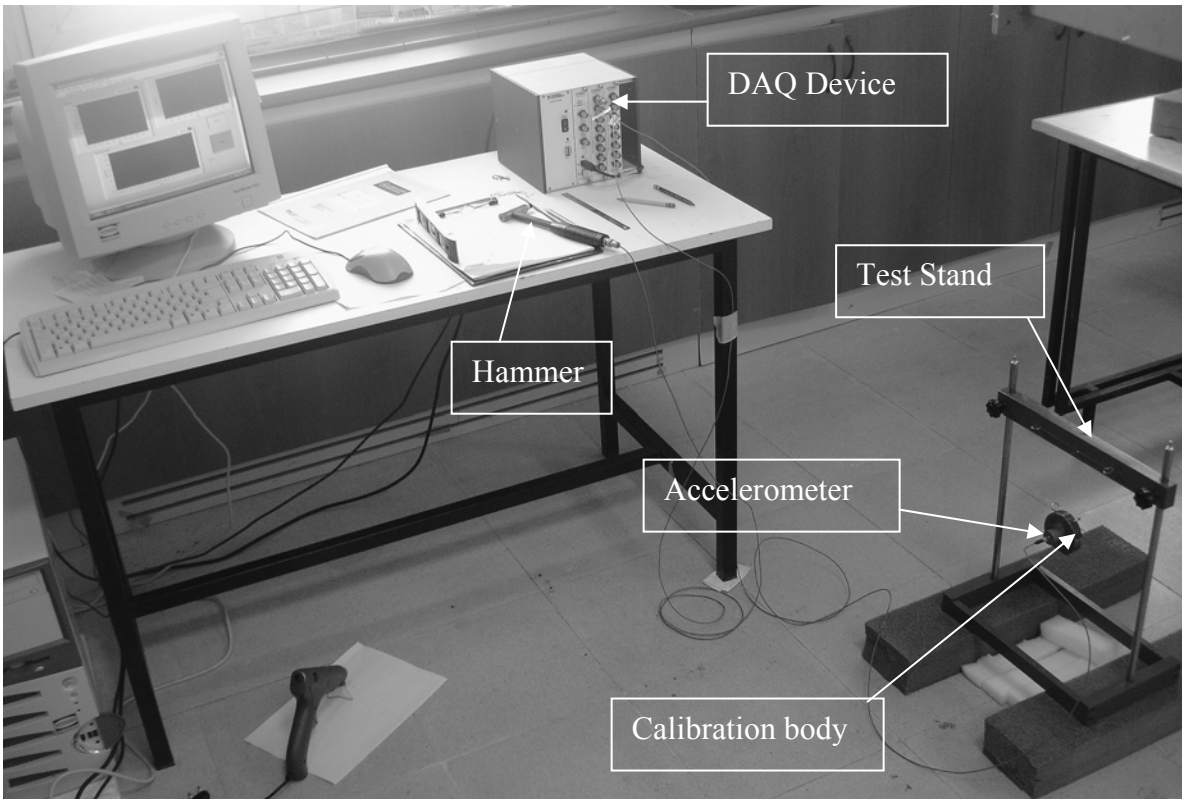

Figure 4.1. Testing Setup for Calibration Mechanism

Substituting Equation (4.1) and Equation (4.3) into Equation (4.1) yields;

$$\frac{V_f}{S_f} = Mx\frac{V_a}{S_a} \tag{4.4}$$

Solving Equation (4.4) for S_a gives;

$$S_a = Mx\frac{V_a}{V_f}xS_f \tag{4.5}$$

Equation (4.5) gives the calibrated sensitivity for each accelerometer. This value is multiplied by the nominal sensitivity of 1mV/g that is input for each accelerometer during the calibration process.

The accelerometer sensitivity values used for testing were the averages of five calibration results for each accelerometer. Five calibration values of standard deviation, average and standard deviation/average, are shown in Table 4.1 for each accelerometer and hammer. The final accelerometer sensitivity values are summarized in Table 4.2.

Table 4.1. Stdeva, Average, Stdeva/Average

Accelerometer	Stdeva	Average (mV/g)	Stdeva/Average
Hammer	0.01	1.30	0.01
Acc 30310	6.00	512.77	0.01
Acc 30314	3.56	512.77	0.01
Acc 30311	5.46	497.44	0.01
Acc 30313	2.01	513.63	0.00
Acc 17878	5.87	1007.43	0.01
3 Acc X direction	1.38	100.98	0.01
3 Acc Y direction	3.12	107.97	0.03
3 Acc Z direction	1.43	107.09	0.01

Table 4.2. Sensitivity Values

	Factory Calibration (mV/g)	Experimental Calibration (mV/g)	Difference (%)
Hammer	1.28	1.30	1.86
Acc 30310	504	505.76	0.35
Acc 30314	512	512.77	0.15
Acc 30311	496	494.67	0.27
Acc 30313	513	513.51	0.10
Acc 17878	1007	1007.43	0.04
3 Acc X direction	99.1	100.98	1.86
3 Acc Y direction	104.9	107.97	2.84
3 Acc Z direction	105.7	107	1.21

4.2.5. Control of the basic assumptions of modal analysis

There are two basic assumptions of the modal analysis that should be verified. The first assumption is time invariance. This is mainly to ensure that the structure's dynamic behavior and the whole measurement set-up system are time invariant. In general, a system which is not time invariant will have components whose mass, stiffness, or damping depend on factors that are not measured or are not included in the model. For example, some components may be temperature dependent. In this case the temperature of the component is viewed as a time varying signal, and, hence, the component has time varying characteristics. Therefore, the modal parameters that would be determined by any measurement and estimation process would depend on the time (by this temperature dependence) that any measurements were made. If the structure that is tested changes with time, then measurements made at the end of the test period would determine a different set of modal parameters than measurements made at the beginning of the test period (Silva and Nuno 1998). Thus, the measurements made at the two different times will be inconsistent, violating the assumption of time invariance.

The second assumption of the modal analysis is linearity. Without this assumption, modal analysis could not be performed. It simply states that response of the system could be formulated as a combination of certain modes. One way of checking the linearity is to ensure that the FRF data are independent of excitation amplitudes. This can be achieved either qualitatively or quantitatively (Wicks 1991). For the former, FRF data from the same locations can be measured repeatedly with different but uncontrolled changes of excitation amplitudes. The measured FRF data can be overlaid to verify the uniformity of the curves.

Another way of checking the linearity is thru checking the reciprocity. A linear and time-invariant structure honors Maxwell's reciprocity property. It states that a force applied at degree-of-freedom p causes a response at degree-of-freedom q that is the same as the response at degree-of-freedom p caused by the same force applied at degree-of-freedom q. With respect to FRF measurements, the FRF between points p and q determined by exciting at p and measuring the response at q should be same as the one obtained by exciting at q

and measuring the response at p ($H_{pq} = H_{qp}$). As shown in Eq. (4.6) the Maxwell's reciprocity theorem is

$$H_{pq} = \frac{X_p}{F_q} = H_{qp} = \frac{X_q}{F_p} \tag{4.6}$$

where;

X_p =Deflection at point p

X_q = Deflection at point q

F_p = Unit load at point p

F_q = Unit load at point p

4.3. Experimental Study of Simple Structures

In order to excel and get experience on modal analysis, several simple structural systems are designed and manufactured. These systems are a simple beam, an H-frame, a square plate and a four story 2-D frame. Using these simple systems some parameters that are considered to be important for FRF is studied. . Based on the experience gathered the difficulties of modal testing and the remedies to overcome these problems will be discussed in Chapter 5.

X-Modal software is used to perform the modal analysis on the FRF functions calculated based on the recorded data. The tests are conducted in the Modal Analysis and Testing Laboratory of Civil Engineering Department.

4.3.1. Simple Beam

As presented in Figure 4.2 and Figure 4.3, simple beam is a simply supported steel beam that has a uniform cross section. There are no additional mass on the beam other than its own mass. It can be assumed that steel is a linear material for load levels considered.

Natural frequencies and modal shapes of a simply supported beam that has a uniform section and linear material properties could be defined as explained in the coming paragraphs (Clough 1993). The dimensions of the model are given in Figure 4.2. Figure 4.3 show the beam with three accelerometers.

The solution presented in the coming sentences is limited to beams that have uniform sections and linear material properties. The significant physical properties of this beam are its flexural stiffness, $EI(x)$, and the mass per unit length, $m(x)$, both of which are constant along the span, L.

. The first three modes for the pilot test were identified from modal testing results. The analytical and modal testing results were compared. Modal shapes and frequencies calculated by the method above are valid only as validity of used variables and boundary conditions. Since there could be variations in the physical system, related to production and material, measured and calculated results are not expected to be same but should be in the same proximity.

Pilot test related to simple beam had been performed and measurement results with three degrees of freedom for simple beam and modal analysis and analytic investigations had been completed. In this part simple beam will be re-considered and finite elements model and modal experiment results taken from ten reading points will be compared. Reading and impulse point's distribution of simple beam is presented in Figure 4.4. Since no coupling is observed between directions in measurements, perpendicular, to longer side, component of beam cross section of accelerometer had been used in the analysis. Modal analysis had been done by using single input single output (SISO) data as if they were single input multi output (SIMO), using the reciprocity principle. For this purpose impact hammer and a three-axis accelerometer had been used. The accelerometer used was PCB-356A16 model, and has 100 mV/g sensitivity, 1-5000Hz frequency interval and 7.4gr of weight. The impulse had been given to the system with impact hammer. In order to excite the target frequency interval, hard hammer tip had been used. The frequency range, which is excited with this tip, is shown in Figure 4.5.

The data acquisition parameters selected for the modal test of the beam was determined based on the results of the preliminary tests and the preliminary finite element model of the beam and to some extent by trial and error. These parameters, defined in

LABVIEW software, and Matlab set the way in which the data is sampled during the test. The parameters are summarized below.

- Sampling frequency: 6000 Hz
- Number of Sample: 18010
- Length of time record: 3 seconds
- Trigger on input channel (hammer) at 10% of maximum voltage
- Trigger delay samples: 10
- Pre-trigger delay time: 0.5 seconds
- Maximum input range (hammer): +/- 250 N?
- Maximum sensor range (driving point reference): +/- 10 g
- Number of samples (N): 4096
- Windows: rectangular and exponential on input, exponential on response
- Exponential window decay rate: 0.1%
- Number of averages (hits per impact location): 5
- Noise reduction method: H1

The test is performed using ten impact locations, Figure 4.6. Five readings from each location is taken. Based on the measured data, there are four frequencies measured below 350Hz. These four frequencies had been chosen for measurement purposes. Data acquisition system had been arranged to collect 3 seconds of records and 6000 data/sec sampling frequency. A 2.5 kHz of analog low pass filter had been selected for measurement purposes. Recorded data is later passed thru 1000Hz Butterworth digital low pass filter, in order to eliminate higher frequencies.

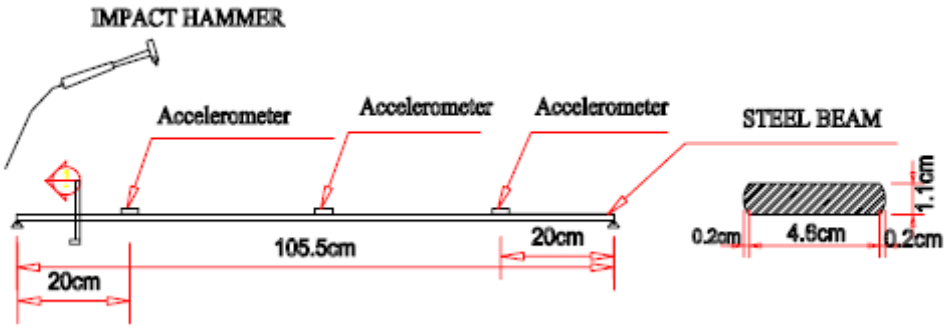

Figure 4.2. Geometric Properties of the Simple Beam

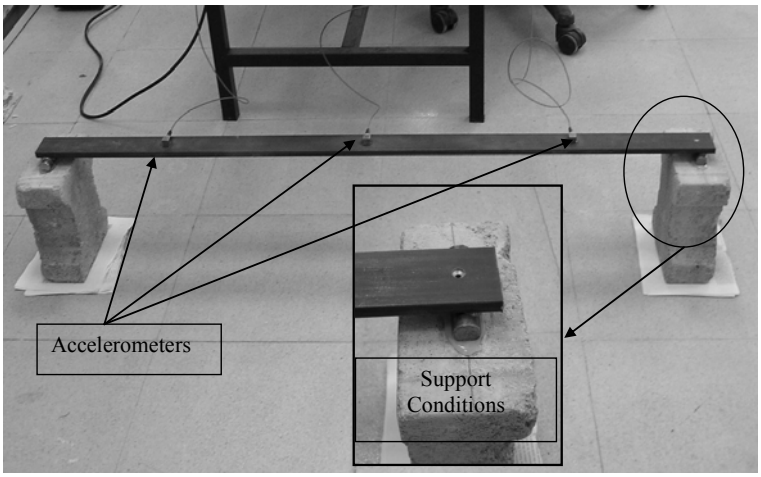

Figure 4.3. Simple Beam with Three Accelerometers

Acceleration records showed that in the first three seconds the wave had not been completely damped. An exponential window is applied to data to prevent aliasing error. A rectangular window is also applied to hammer data to eliminate the effect of noise outside the region of impact time. For every FRF, average values are taken by using five records to reduce the random errors. In many cases, more than five hits at each driving point location were required before acceptable data was obtained. FRF's calculated based on measured data is presented in Figure 4.5. Every reference location has a different FRF.

Figure 4.4. Sensor and Impact Locations of Test Structure

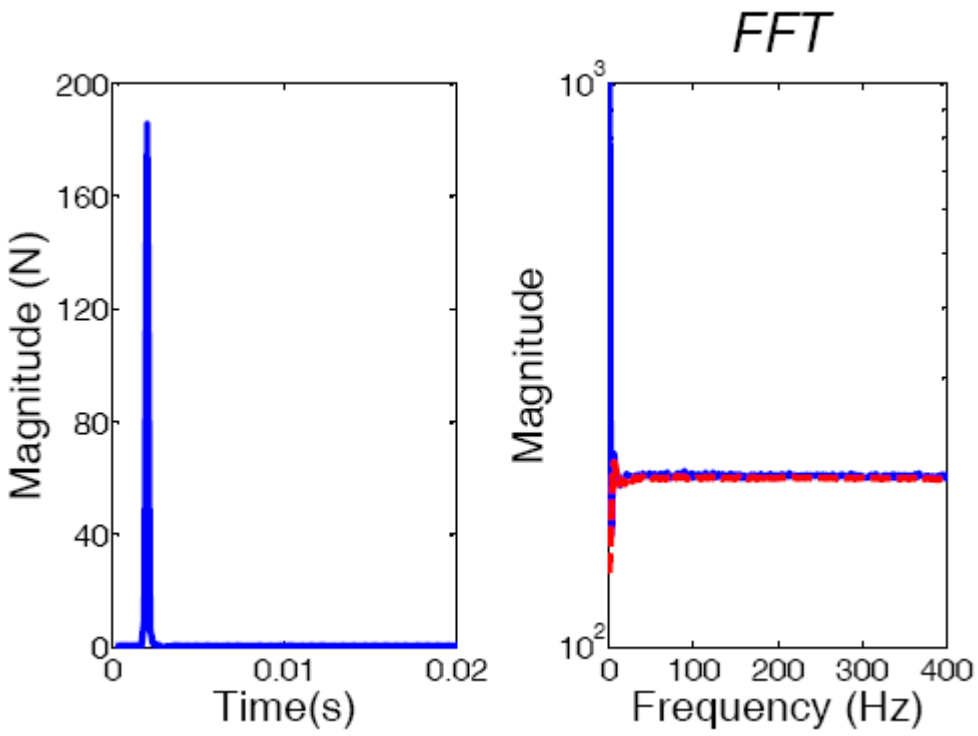

Figure 4.5. Typical Activity of Impulse to the System on Given Frequencies for Simple Beam

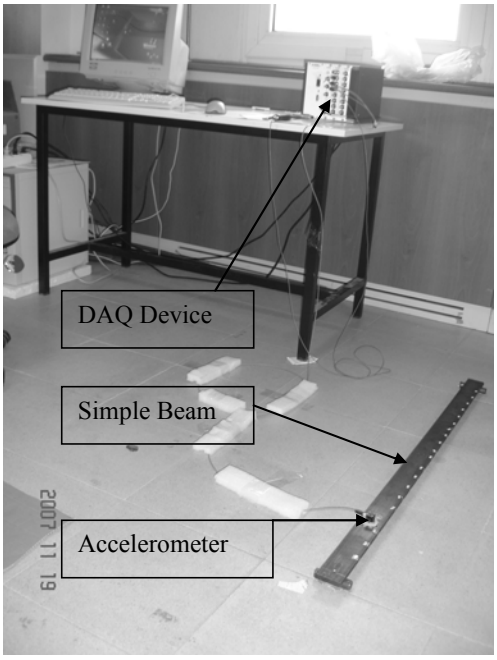

Figure 4.6. Detailed Test Set Up for Simple Beam

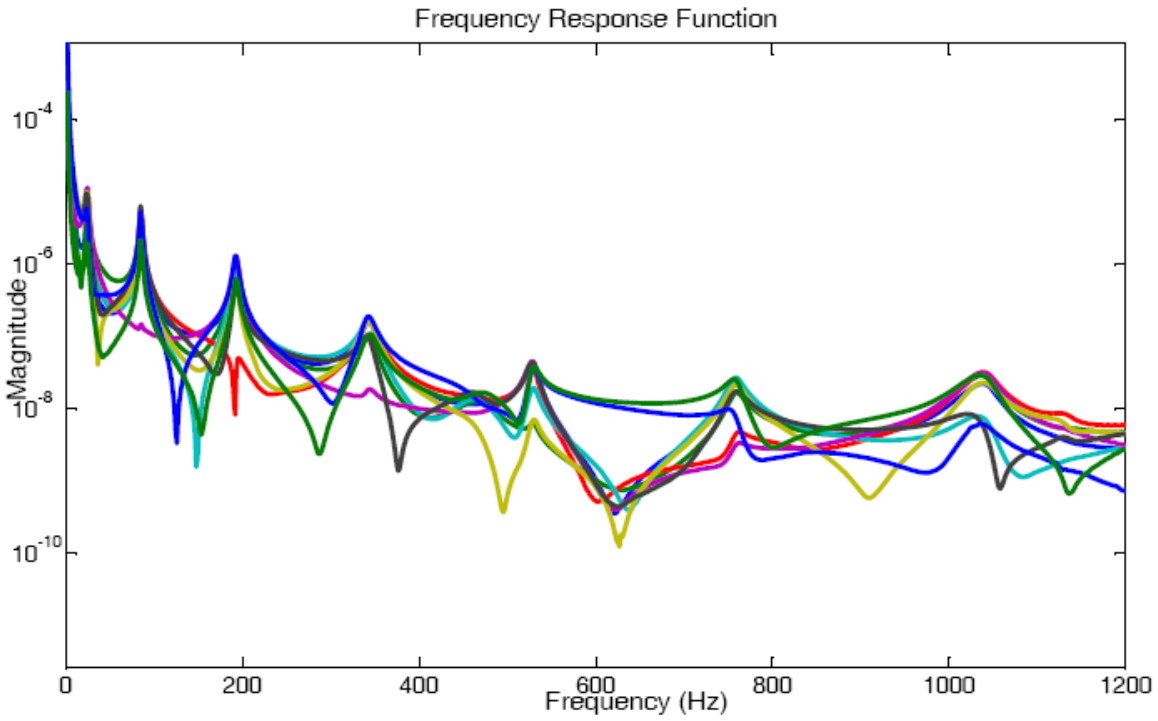

Figure 4.7. FRFs That Correspond to Considered 10 Points

To verify the fundamental assumptions of the modal analysis, linearity and reciprocity controls are made. Two different comparisons had been done to check the linearity. In the first comparison, two FRF's for 48N and 125N impact magnitudes had been compared Figure 4.8 a and Figure 4.9. The comparisons of FRF's show a good match. Considering the log scale of the vertical axis deviations are relatively small and limited to frequencies beyond 400 Hz. The reason of the deviation is explained by the comparison of FRFs of 85N and 140N impulses Figure 4.8 b and Figure 4.10. These FRFs showed that high energy stimulations prevent deviations by completely exciting the upper modes of the system. The problem in the first reading was the insufficient energy of 48N impulse for the frequencies above 400Hz. Therefore higher energy impulses are needed in order to perform modal analysis for the system properties above 400Hz. Reciprocity control is performed by interchanging the excitation and reading locations, Figure 4.11. The FRF data for this purpose are obtained by averaging 5 reading, Figure 4.7 The results show that the system obeys the Maxwell reciprocity principle.

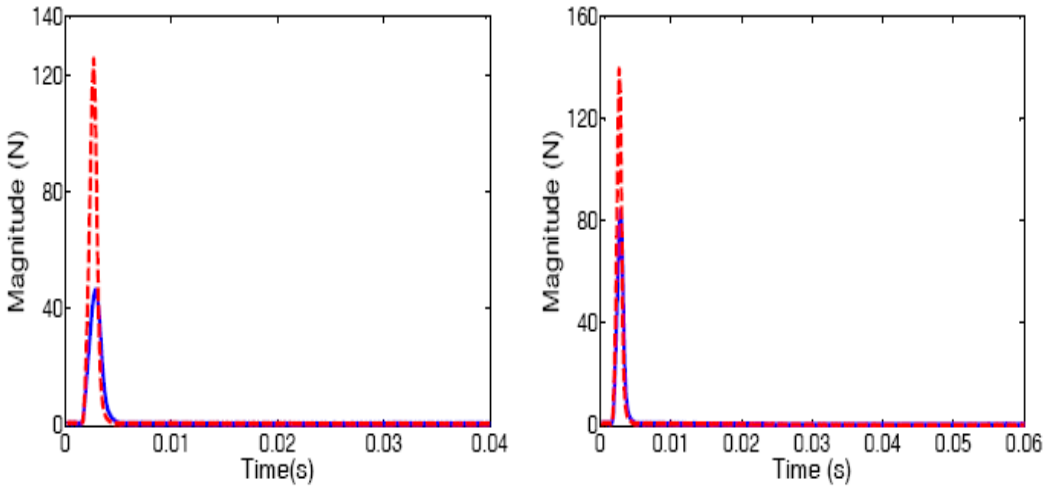

F=48N and F=125N

F=85 N and F=140N

Figure 4.8. Excitation Amplitudes of the Linearity Check

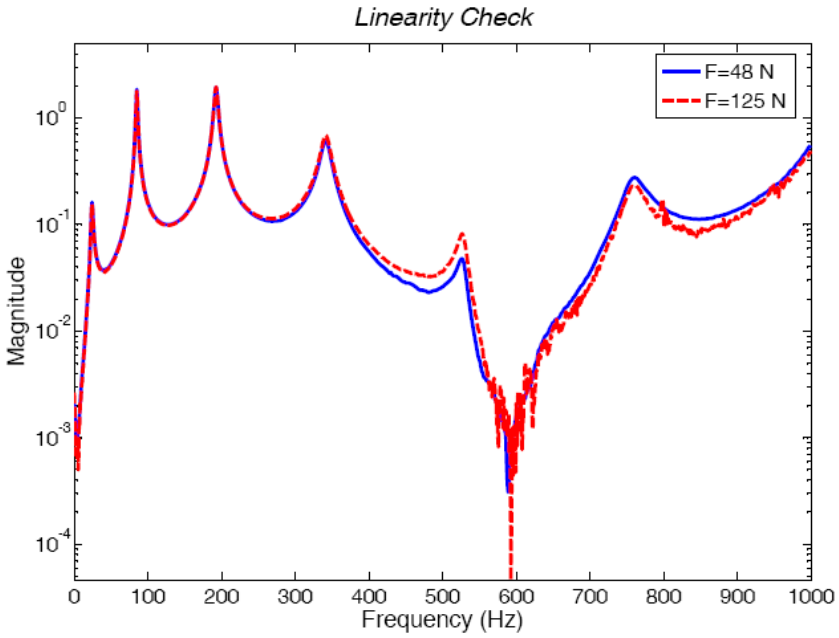

Figure 4.9. FRF for Two Different Excitation Amplitudes

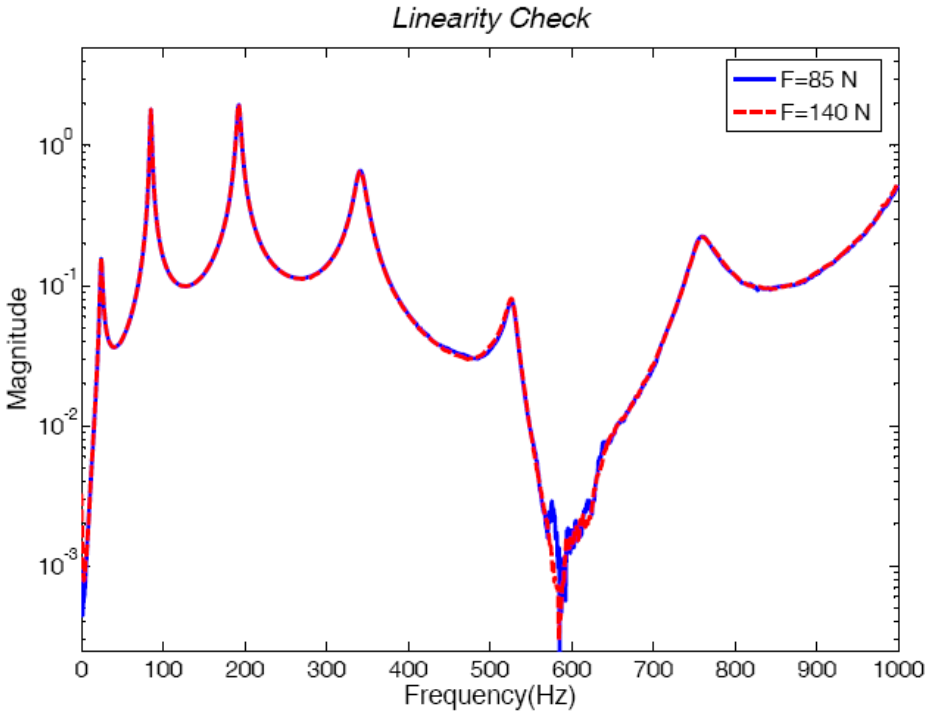

Figure 4.10. FRF for Two Different Excitation Amplitudes

Calculated discrete FRF data is used as an input to the X-modal analysis program to perform the modal analysis of the system. Natural frequencies, damping rates and modal shapes, shown in Figure 4.12 and listed in Table 4.3, had been obtained by using Complex Mode Indicator Function of the program. Damping rates had been corrected so that the effect of the exponential function had been eliminated (Fladung and Rost 1997). Simple beam had also been analyzed with SAP2000 (Computers and Structures 2004), program by using frame elements that has four degrees of freedom and modal parameters are calculated.

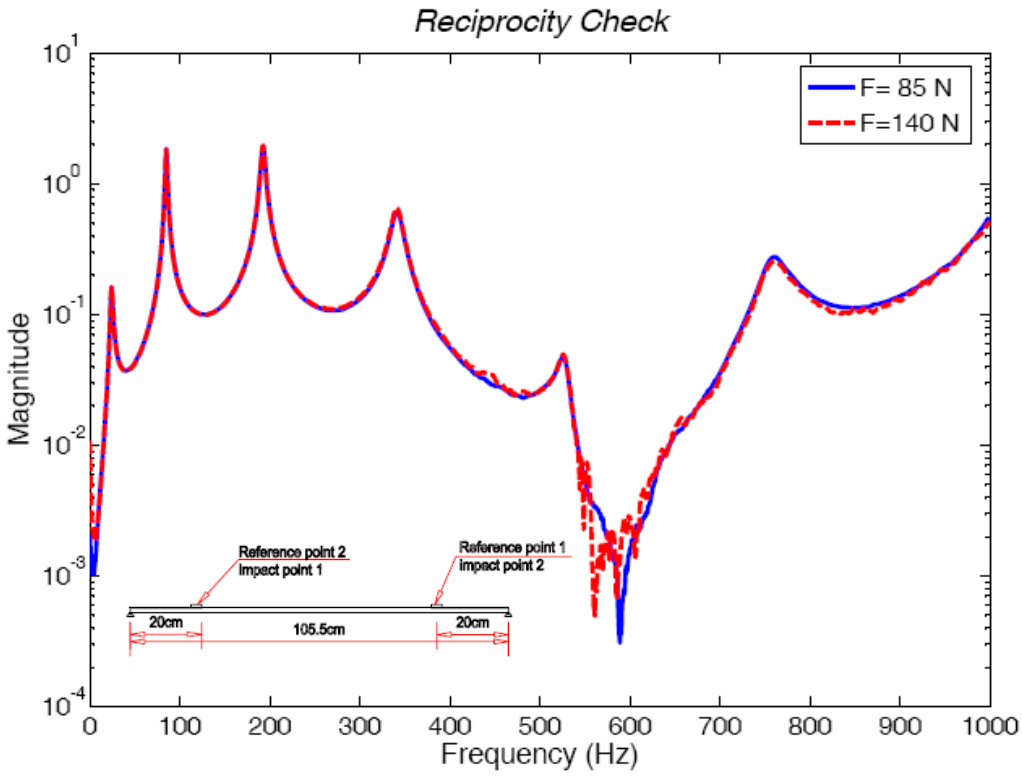

Figure 4.11. Reciprocity Control to FRF for Two Different Impact Locations

Table 4.3. The Results of Frequency and Damping Values Obtained from Modal and FEM Analysis

Mode #	Modal Analysis Frequency (Hz)	Sap Model Frequency (Hz)	Frequency Difference (%)	Modal Analysis Damping Constants (%)
1	24.0	23.5	2.1	3.2
2	85.1	87.7	3.0	0.7
3	192.3	194.5	0.7	1.1
4	341.7	343.7	0.6	1.8

When the results of modal and nominal structural analysis compared, modal analysis results show a rather rigid system. Considering that there are assumptions made for structural analysis and the material characteristics, it is possible to make some limited adjustments to make the results closer to each other. For this purpose, instead of accepting that the pin supports of the beam are perfect frictionless pins, a 50 kgf.m/rad rotational stiffness is provided at the supports of the beam. In reality due to imperfections in the geometry, the beam and the bearing rods of the supports are hot glued to each other and to the base. Based on this fact, modification made for the support condition is credible. The addition of rotational stiffness make the first modes match with each other but other modes were not sufficiently matching. In attempt to provide a better match in the higher frequency modes, the flexural rigidity of the beam is increased by 7%. Again considering the uncertainty about the modulus of elasticity of the material such a modification is credible. After this modification final results presented in Table 4.3 and Figure 4.12 are obtained.

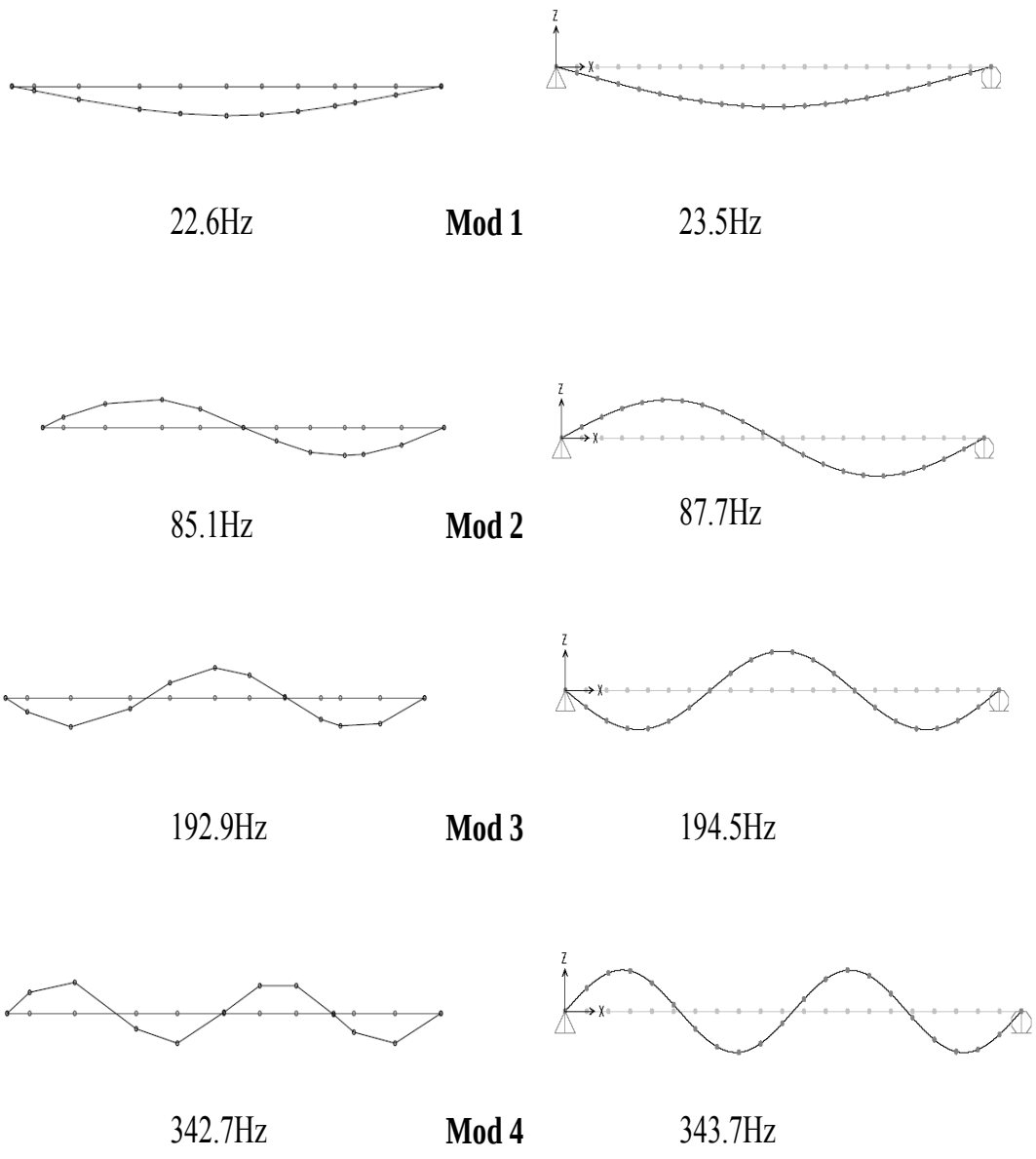

Figure 4.12. Mode Shapes and the Frequencies That are Obtained by Modal and Structural Analysis

4.3.2. H- Frame

The second simple system studied for this study is an H shaped steel frame. The frame is formed by adding heavy steel plates at the end of an H shape frame formed by box sections. The geometric detail of the system is provided in Figure 4.13. The system is supported to provide free-free boundary conditions. Since it is not possible to simulate an exact free-free boundary conditions in reality. The targeted condition is approximated by hanging the frame from the end points by elastic/rubber bands as shown in Figure 4.14 and Figure 4.15. Coupling is observed in the preliminary measurements. So in order to observe the motions in three perpendicular dimensions a triaxial accelerometer is decided to be used for detailed analysis. Modal analysis of the frame is performed by taking readings with a triaxial accelerometer at a single point and exciting the system from 46 points, Figure 4.15. The test is designed to obtain SISO data to use on multi input multi output (MIMO) data thru reciprocity principle. The accelerometer used was a PCB-356A16 model. It has 100 mV/g sensitivity, 1-5000Hz frequency interval and 7.4gr of weight.

The impulse is given to the system with the impact hammer. In order to excite the desired frequency interval medium hard hammer tip (blue tip) had been used. Excited frequencies, with this tip, had been presented in Figure 4.16.

Preliminary measurements show that the first nine frequencies of the frame are below 250Hz, this range is selected as the measurement range. Data acquisition system had been arranged to collect 3 seconds of records, as in simple beam, and 6KHz sampling frequency and 2.5KHz of analog low pass filter had been utilized. Since the target region is the 0-250Hz interval, the records is passed thru 350Hz Butterworth digital low pass filter. Similar to simple beam, it had been observed from the acceleration records that the motion did not stop in three seconds. As a result in order to prevent aliasing error, exponential window is used. A rectangular window is used for impact hammer data. Each FRFs is formed by the averages of five records to reduce the random errors. FRF's constructed from measured data is presented in Figure 4.17.

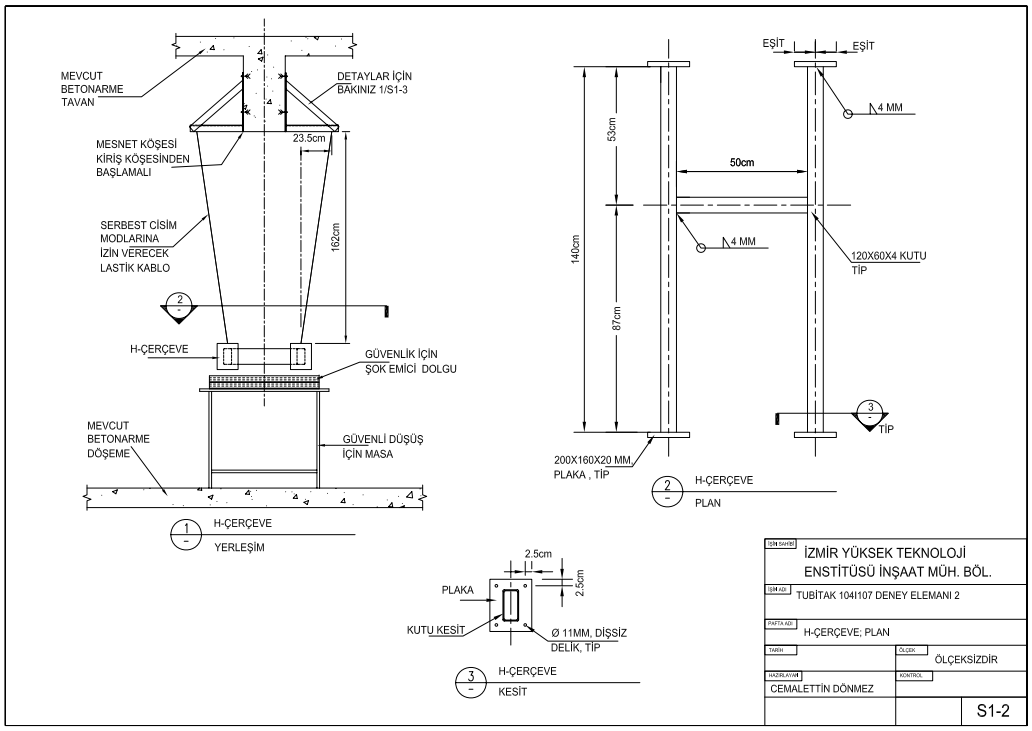

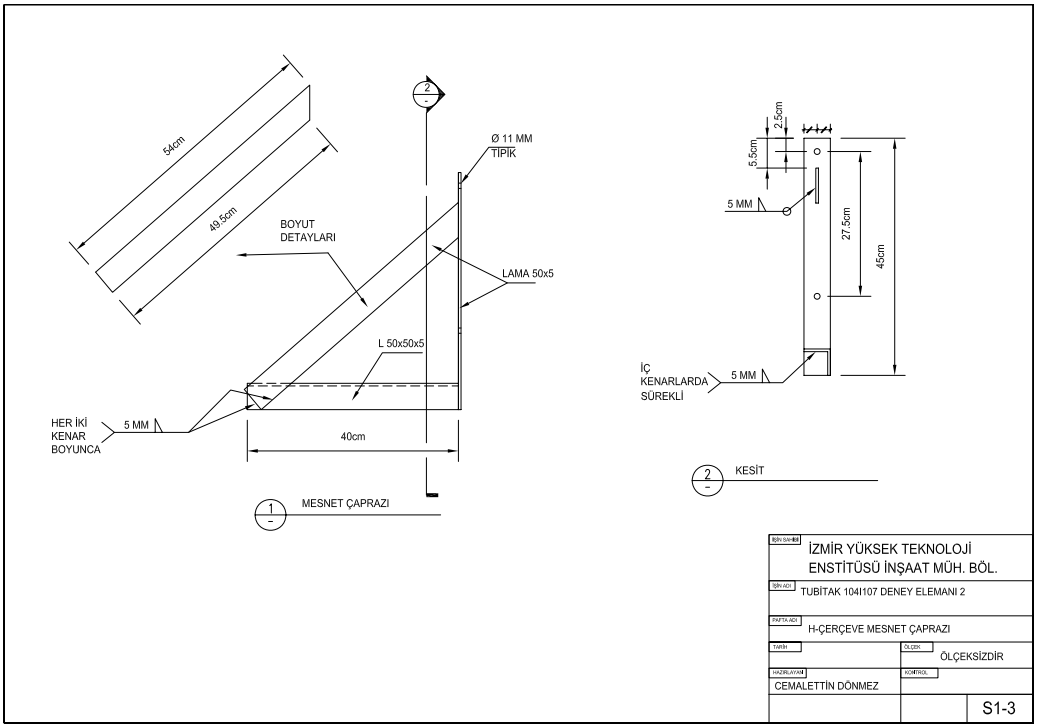

Figure 4.13. H –Frame Design and Support Details

Linearity and reciprocity controls of the frame are performed. The applied excitations and the resulted FRFs is presented in Figure 4.18. The figure shows that linearity applies in the frequency range considered. Reciprocity control is performed at the points mentioned in Figure 4.21 by averaging 5 different readings The FRFs presented in Figure 4.20 proves that reciprocity holds for the frame.

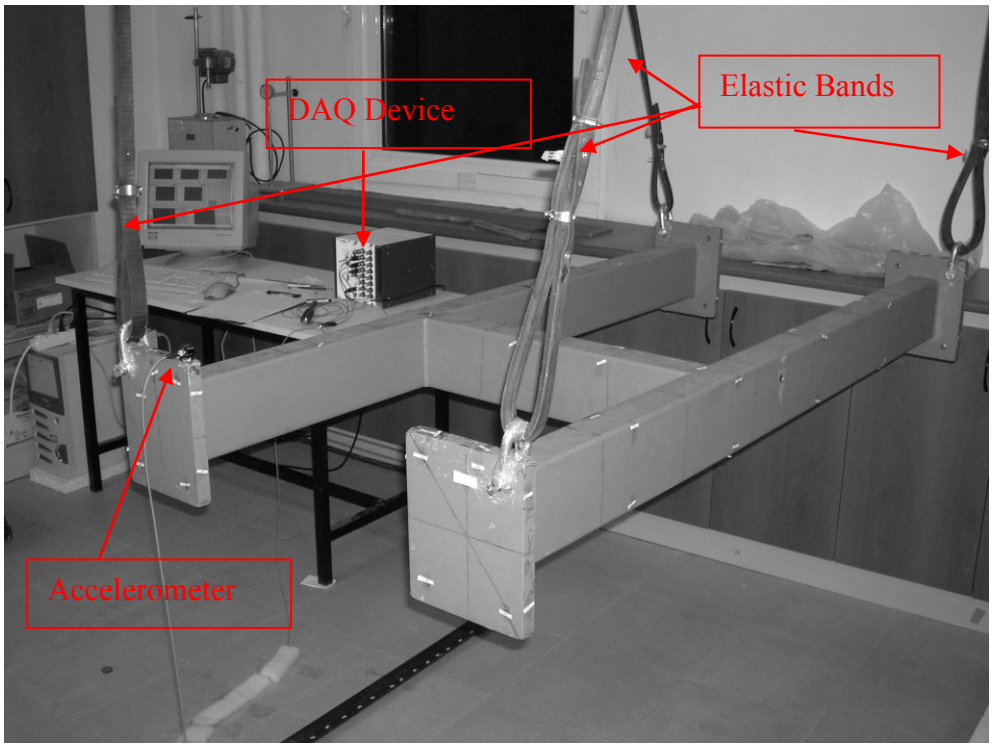

Figure 4.14. H-Frame and DAQ

The calculated and measured mode shapes and frequencies are compared in Figure 4.22, Figure 4.23 and Figure 4.24.

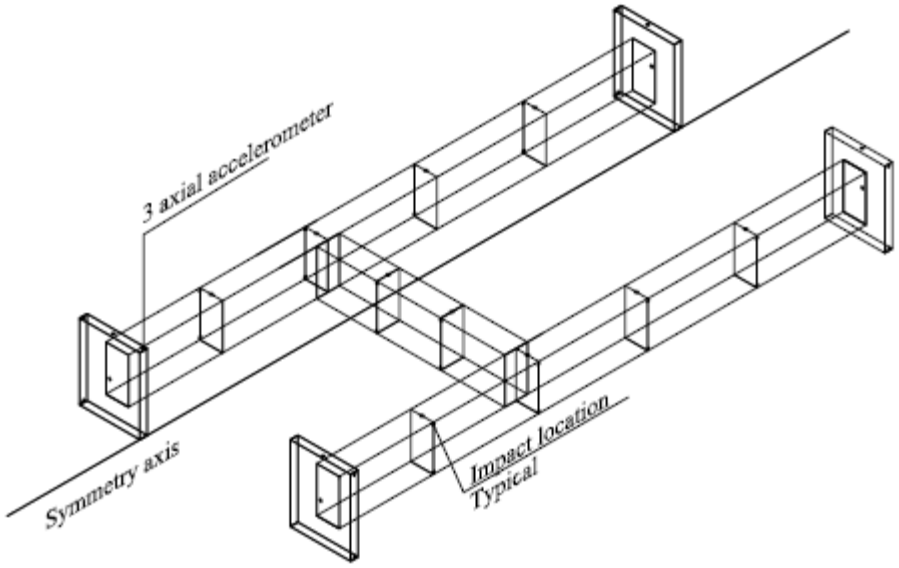

Figure 4.15. Impact Points and Accelerometer Location

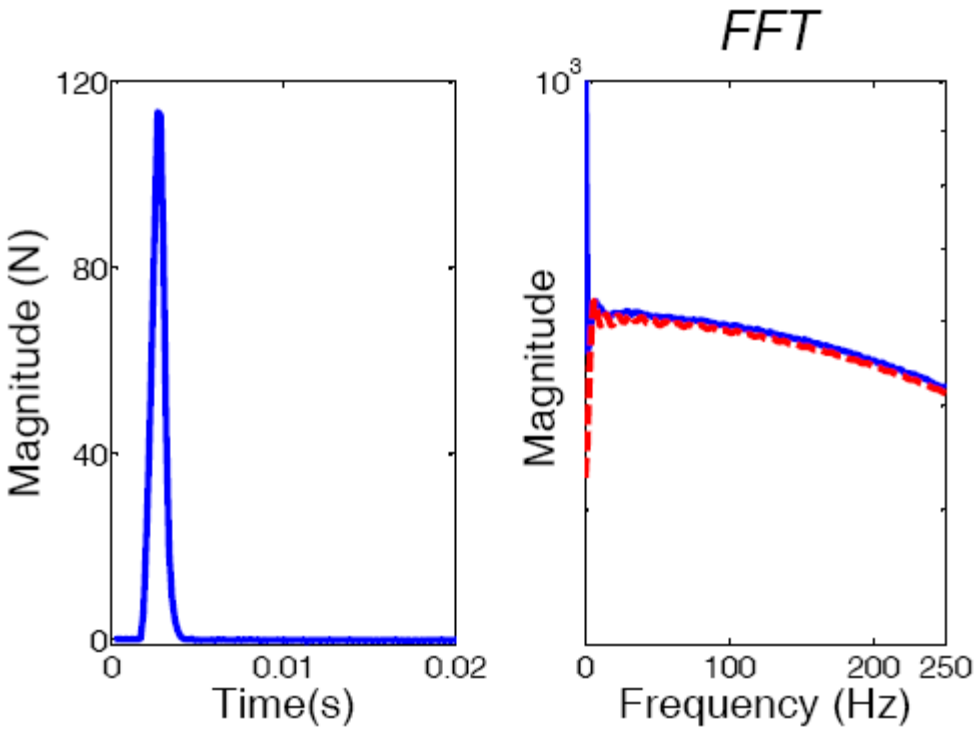

Figure 4.16. Typical Measurement Range for the H-Frame

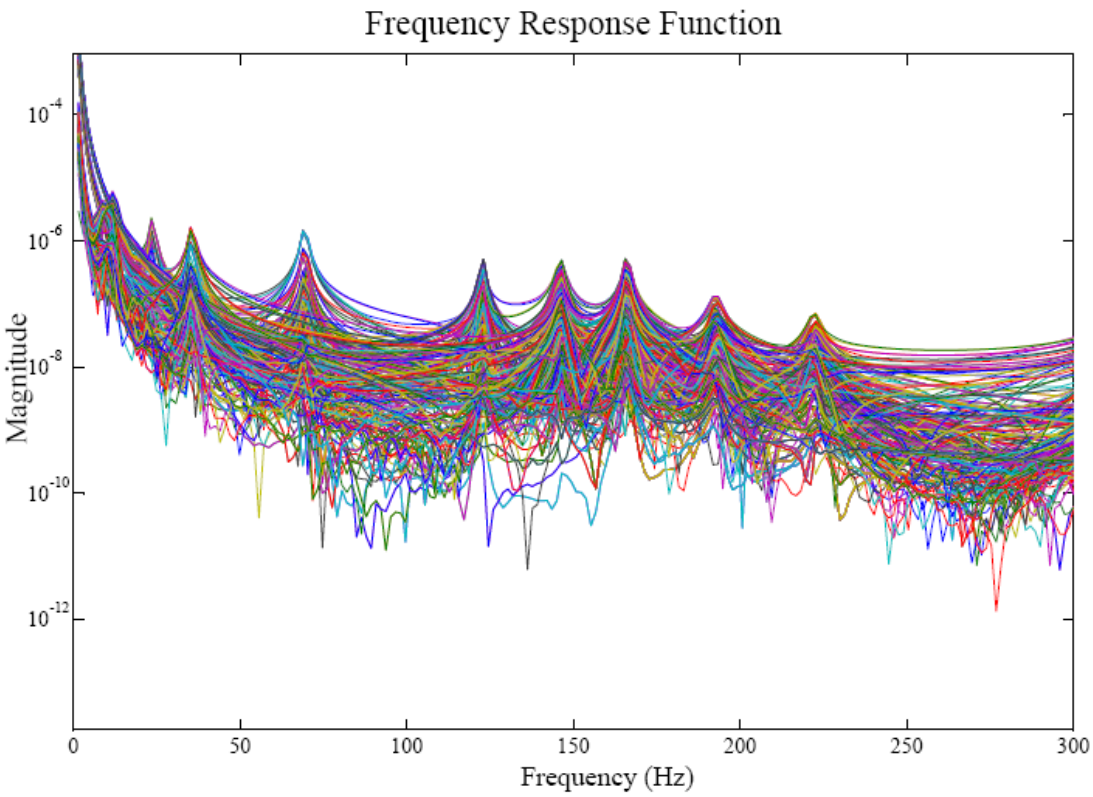

Figure 4.17. FRFs That Correspond to Considered 46 Points

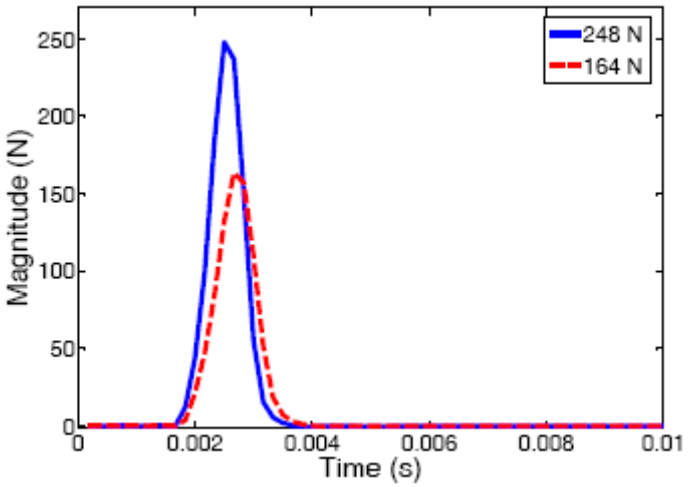

Figure 4.18. Amplitudes of the Excitations

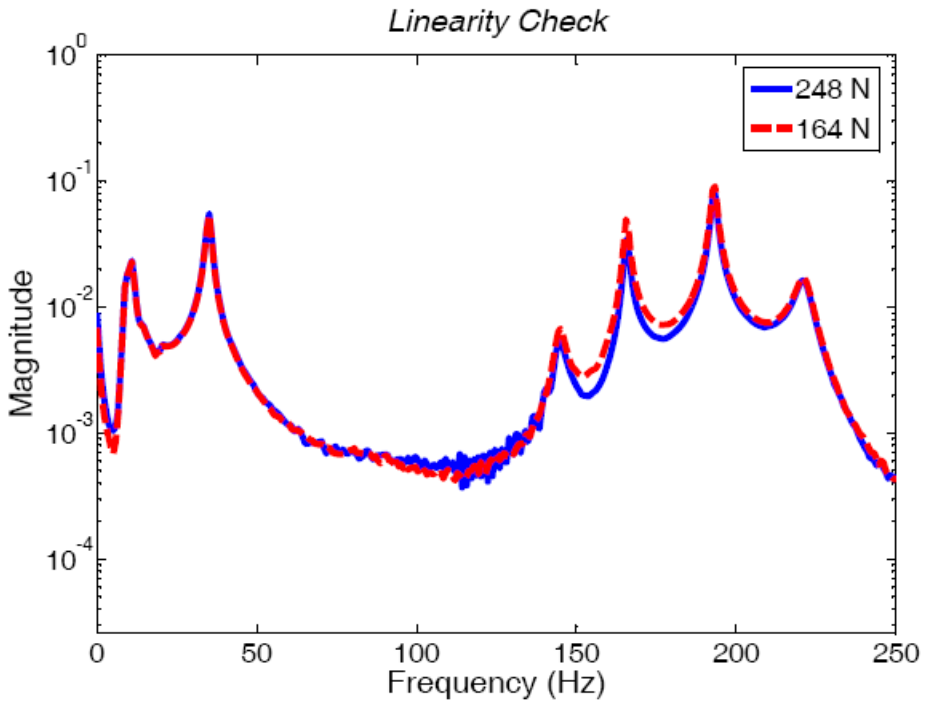

Figure 4.19. FRF of the H-Frame That are Constructed for Linearity Check

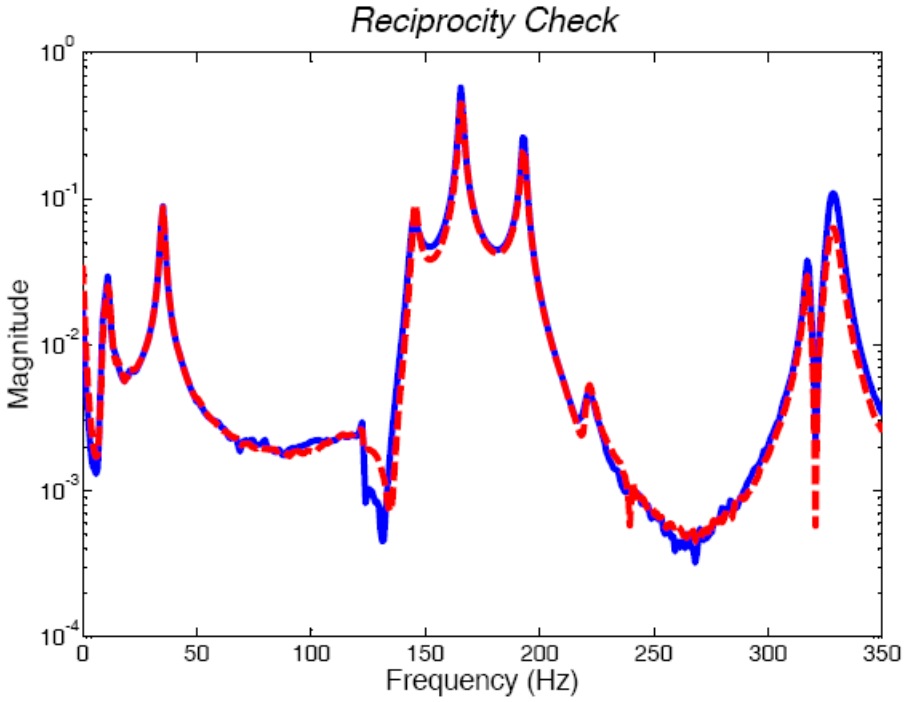

Figure 4.20. FRF of the H-Frame That are Constructed for Reciprocity Check

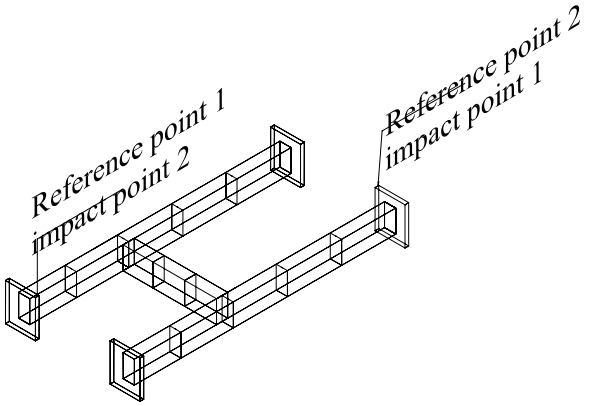

Figure 4.21. H-Frame Reciprocity Points

Table 4.4. The Results of Frequency and Damping Values Obtained from Modal and FEM Analysis

Mode #	Modal Analysis Frequency (Hz)	Sap Model Frequency (Hz)	Frequency Difference (%)	Modal Analysis Damping Constant (%)
1	23.6	24.3	3.0	1.1
2	35.4	33.0	6.8	1.0
3	69.3	70.7	2.0	0.4
4	69.9	71.2	1.8	0.2
5	122.8	125.8	2.4	0.2
6	146.1	134.2	8.1	0.4
7	166.0	157.6	5.1	0.2
8	192.5	194.5	1.0	0.7
9	222.2	220.1	1.0	0.6

Modal Analysis Results: **SAP Analysis Results:**

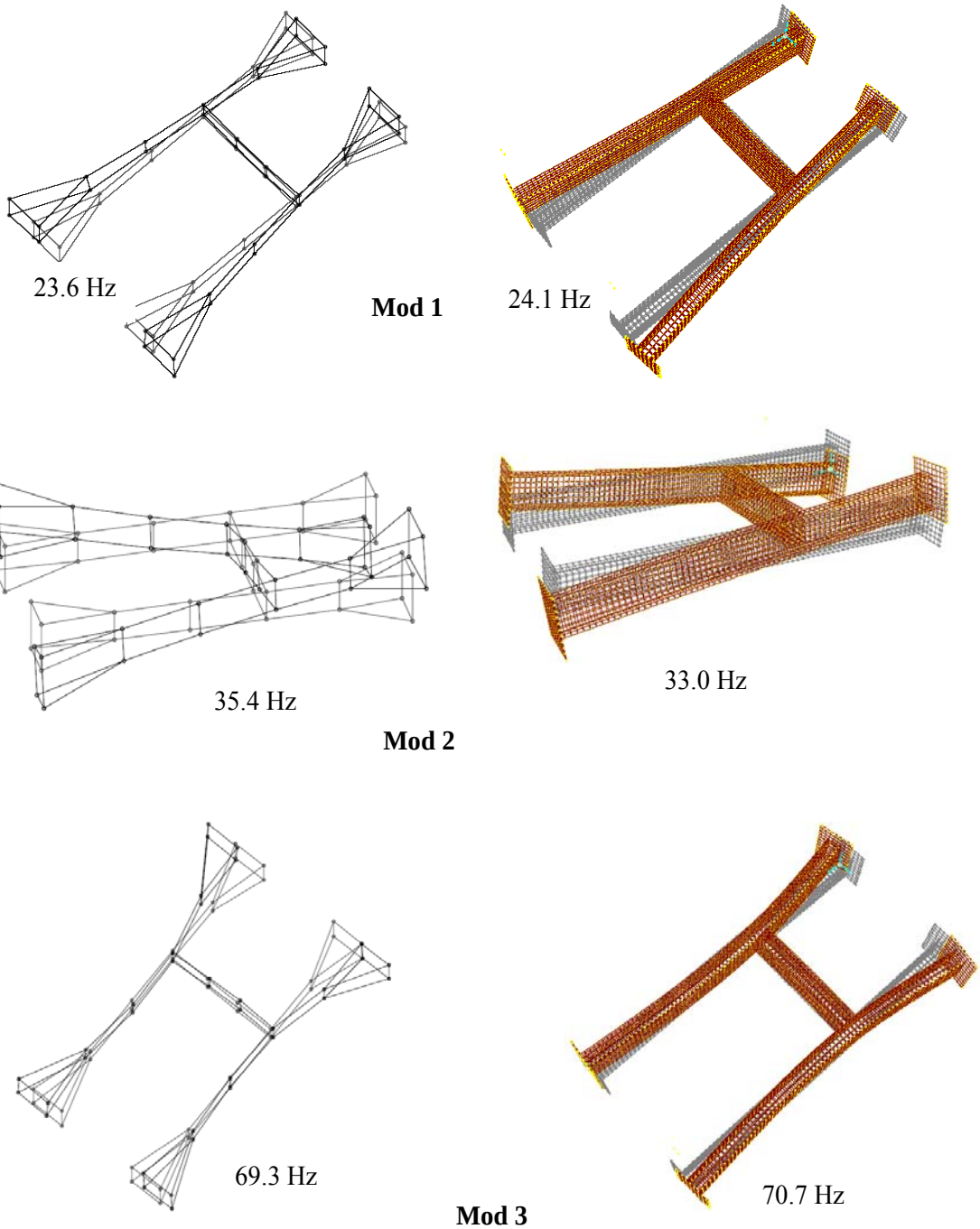

Figure 4.22. The Comparison of Modal Analysis and FEM Analysis Results Mod 1-3

Modal Analysis Results: **SAP Analysis Results:**

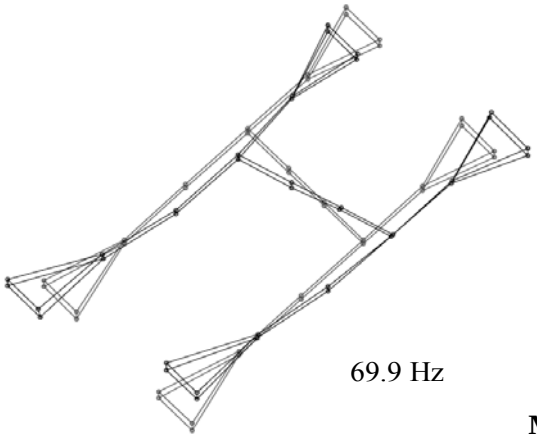

69.9 Hz

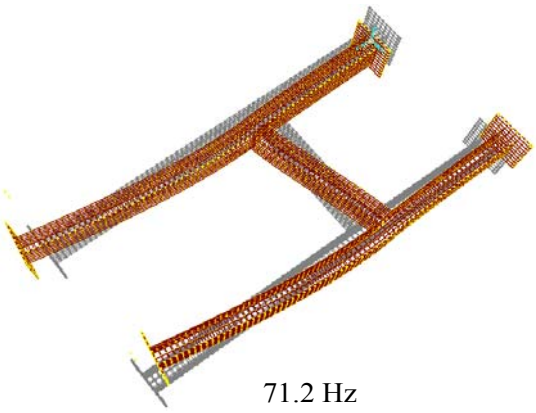

71.2 Hz

Mod 4

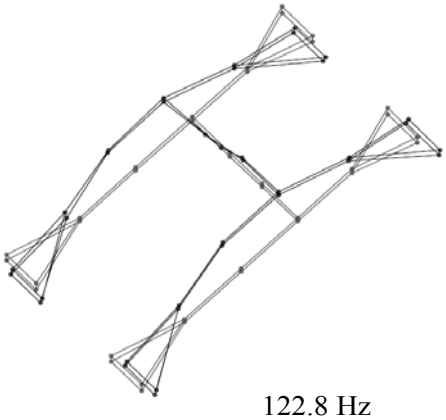

122.8 Hz

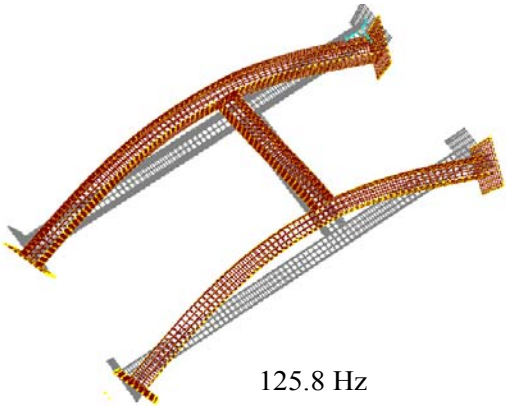

125.8 Hz

Mod 5

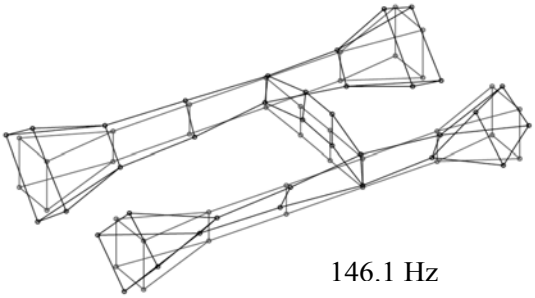

146.1 Hz

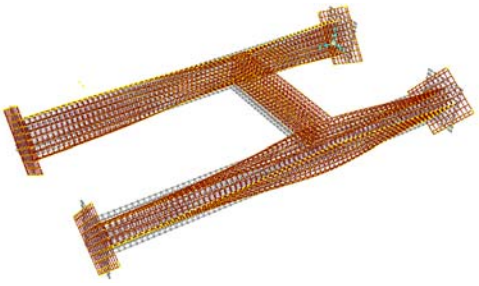

134.2 Hz

Mod 6

Figure 4.23. The Comparison of Modal Analysis and FEM Analysis Results Mod 4-6

Modal Analysis Results **SAP Analysis Results**

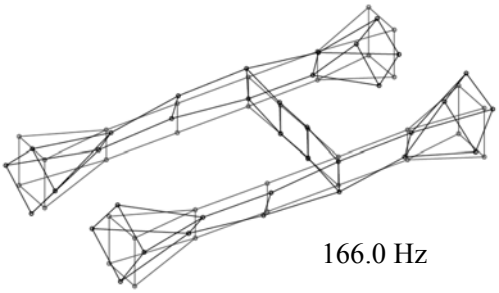

166.0 Hz

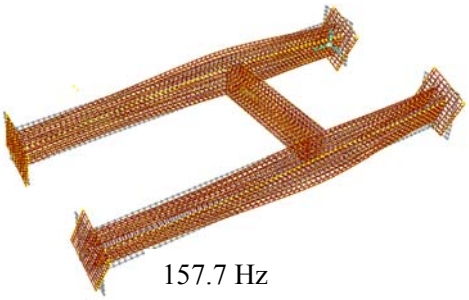

157.7 Hz

Mod 7

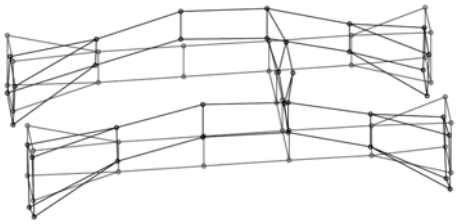

192.5 Hz

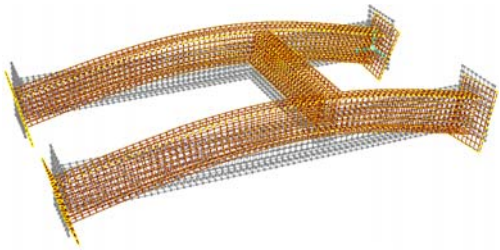

194.6 Hz

Mod 8

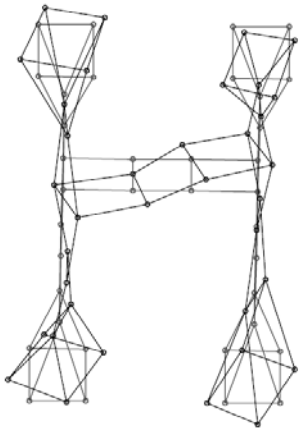

222.2 Hz

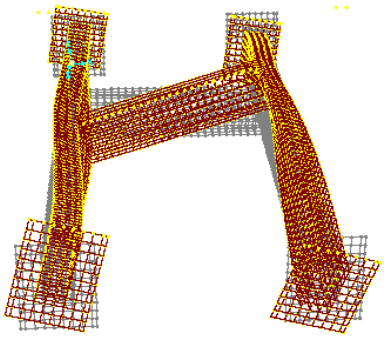

220.3 Hz

Mod 9

Figure 4.24. The Comparison of Modal Analysis and FEM Analysis Results Mod 7-9

As mentioned in the previous paragraphs to observe the coupling effect in the frame test set up is designed to obtain motion of the DOFs at three perpendicular directions for each measurement point. In order to decrease the amount of data needed to define the system dynamic parameters and not to loose any relevant data, the physical behavior information known about the system is put in the use. First simplification is accepting that movements of the parallel faces of the box section are same. This assumption permits the idealization of the box section like a steel plate. Second simplification is the assumption of axial rigidity of the frame along the axes of the box sections. It is known from mechanics that typically the motions that violate these assumptions have higher frequencies. Modals analysis results verify that assumptions are valid.

When the raw results of modal and digital analysis have been compared, it had been seen that modal analysis results show a rather rigid system. It is observed that the H-frame thickness is not 4mm. It is measured 2.4 mm. In order to make the results compatible %5 additional mass had been provided of the plate. Since the elasticity module was used by taking nominal values as base, this amount is within the acceptable limits with a small variation.

4.3.3. Square Plate

It is not uncommon that the frequencies of some modes could have the same value. This is called repeated root condition and creates difficulty in identifying the dynamic parameters of the systems. In order to create such a condition a square plate which potentially have repeated roots due to its symmetry is chosen Physical characteristics of the system is presented in Figure 4.25. The modal experiment is performed by exciting the system at 49 points with the impact hammer and taking readings with accelerometer from two selected points. These points are selected based on the preliminary readings and the finite element analysis of the system. It is observed that the sensor placed at the symmetry axis of the plate is at the node of some modes. And using a single sensor could not provide the sufficient information to identify the repeated roots. As a result it is decided to use two accelerometers. The impact points are selected to provide the sufficient precision to draw the mode shapes. The instrumented square plate is presented in Figure 4.26. Locations of

accelerometers and impact locations are presented in Figure 4.27. Since coupling is not observed in pre-measurements only out of plane DOFs of the plate is instrumented. Modal analysis had been performed by making use of single input single output (SIMO) data as it was multiple input multiple output (MIMO) thru reciprocity principle. The chosen accelerometers are PCB-333B42 model. They have 500mV/g sensitivity, 0.5-3000 Hz frequency interval and 7.5 gr of weight. Excitation to the system is given by medium hardness tip (blue tip) of the impact hammer. The typical frequency interval excited by this tip in the plate is presented in Figure 4.28.

In the pre-measurements taken from the plate, it is observed that the first eight frequencies are below 200Hz, 0-250 Hz frequency interval is defined as the measurement range. Data acquisition system is set to record 3 seconds of data, to 6KHz sampling rate and to 2.5KHz analog low pass filter. Since the target region is the 0-200Hz frequency interval, the records is passed thru 250Hz Butterworth digital low pass filter. The acceleration records of the plate show that in the first three seconds the wave is not completely die out. As a result in order to prevent aliasing error, the data is subjected to exponential window. Also similar to other tests the impact hammer data is subjected to rectangular windowing For every FRF average values are taken by using five records to reduce the random errors. The system FRF's constructed after this process is presented in Figure 4.29.

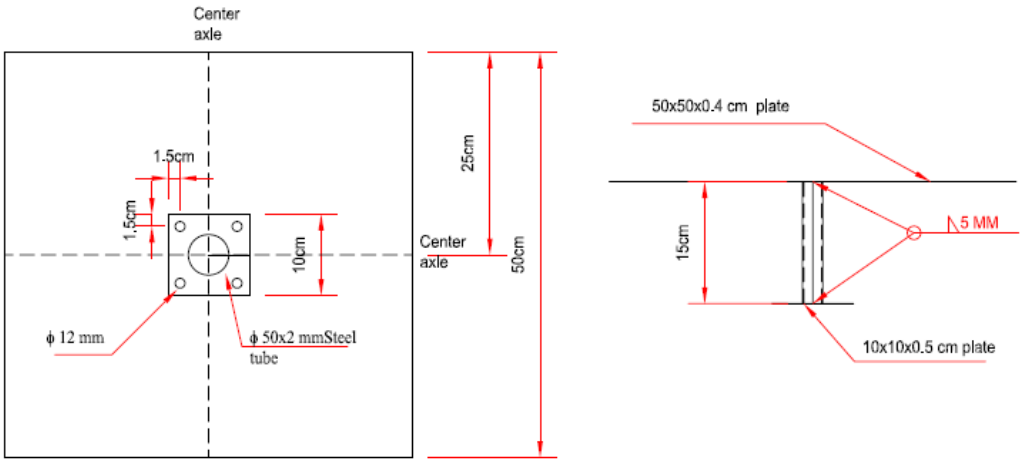

Figure 4.25. Details of the Square Plate

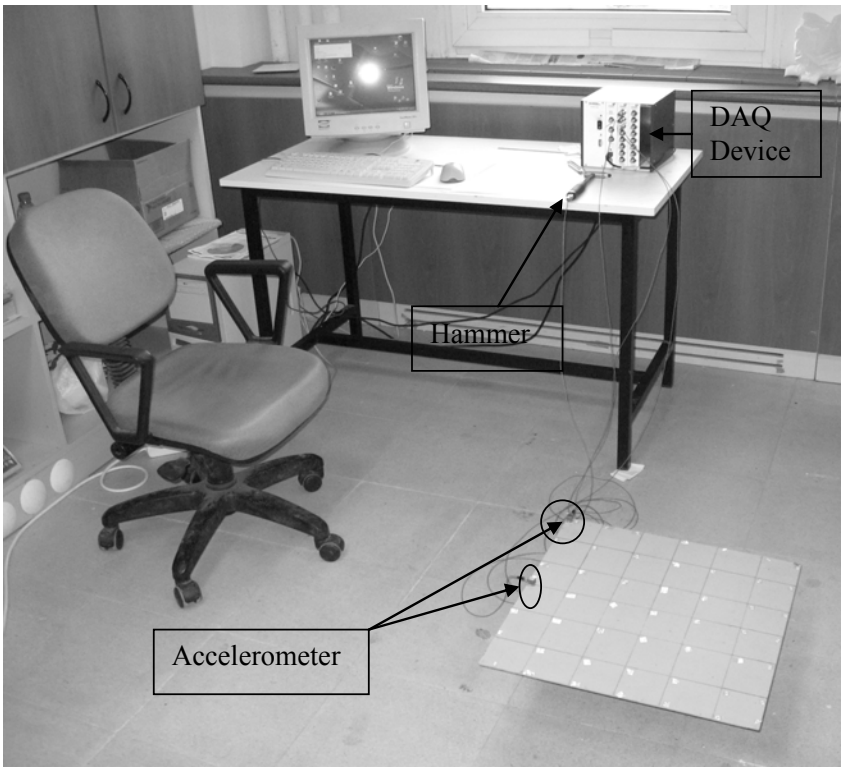

Figure 4.26. Instrumentation of the Square Plate

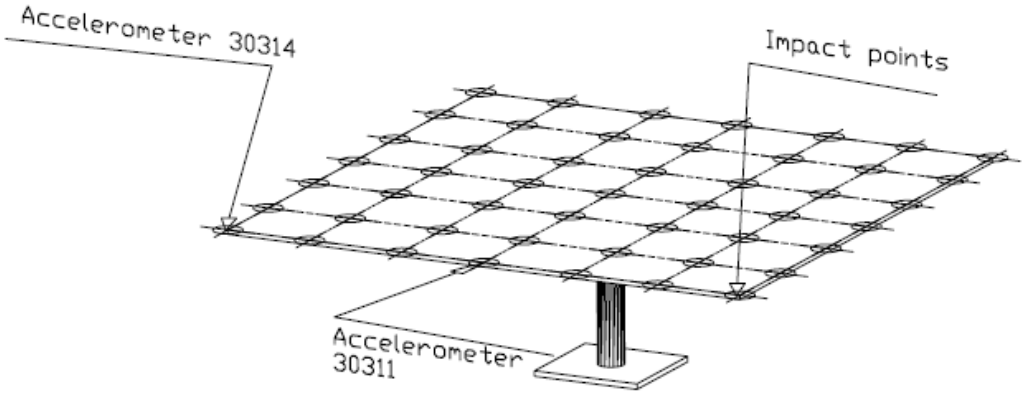

Figure 4.27. Sensor and Impact Locations of the Square Plate

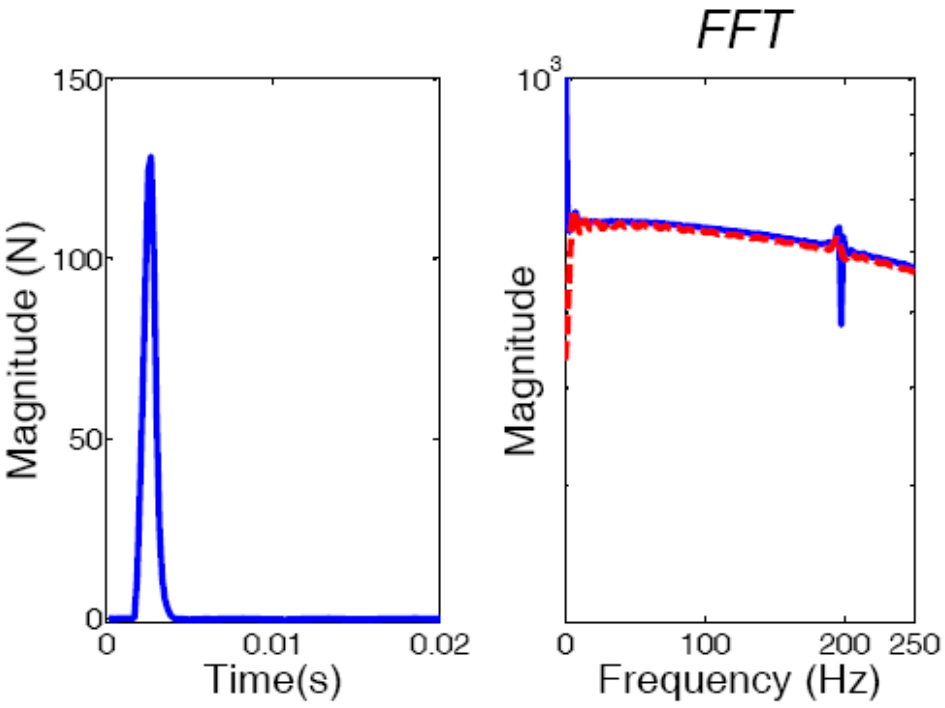

Figure 4.28. Typical Measurement Range for the Square Plate

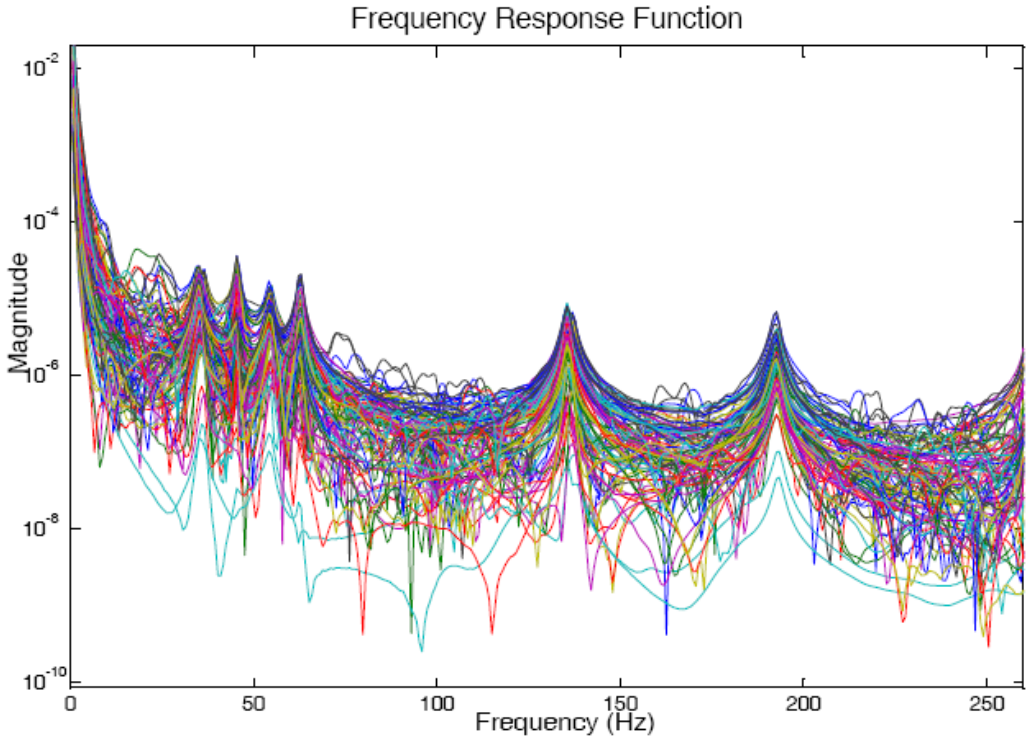

Figure 4.29. The FRFs Obtained from all Excitations

Linearity and reciprocity tests are applied to the plate in order to control suitability of the system to modal analysis basic assumptions. For the control of linearity, two reading of impulse sizes of 49 N and 79 N is compared, Figure 4.30. As it can be seen from FRF's of these excitations, Figure 4.31, there is a very good match in resonance areas of the plate. As a result, it is accepted that the linearity assumption is valid. For reciprocity check, excitation and reading is taken from two facing points, Figure 4.32. Reciprocity check is done with comparison of constructed FRFs, Figure 4.33. And again considering the resonance regions, it is accepted that the reciprocity assumption is valid.

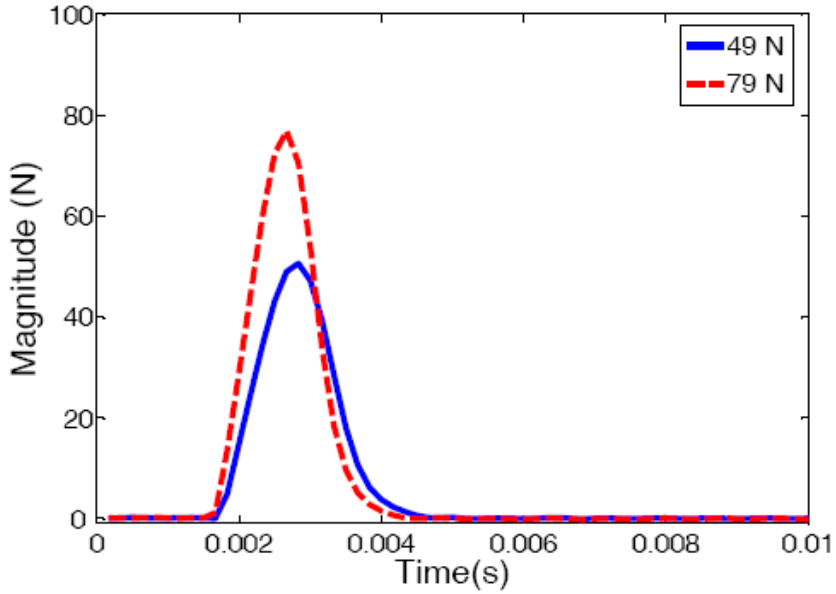

Figure 4.30. Excitations Provided for Linearity Control of Square Plate

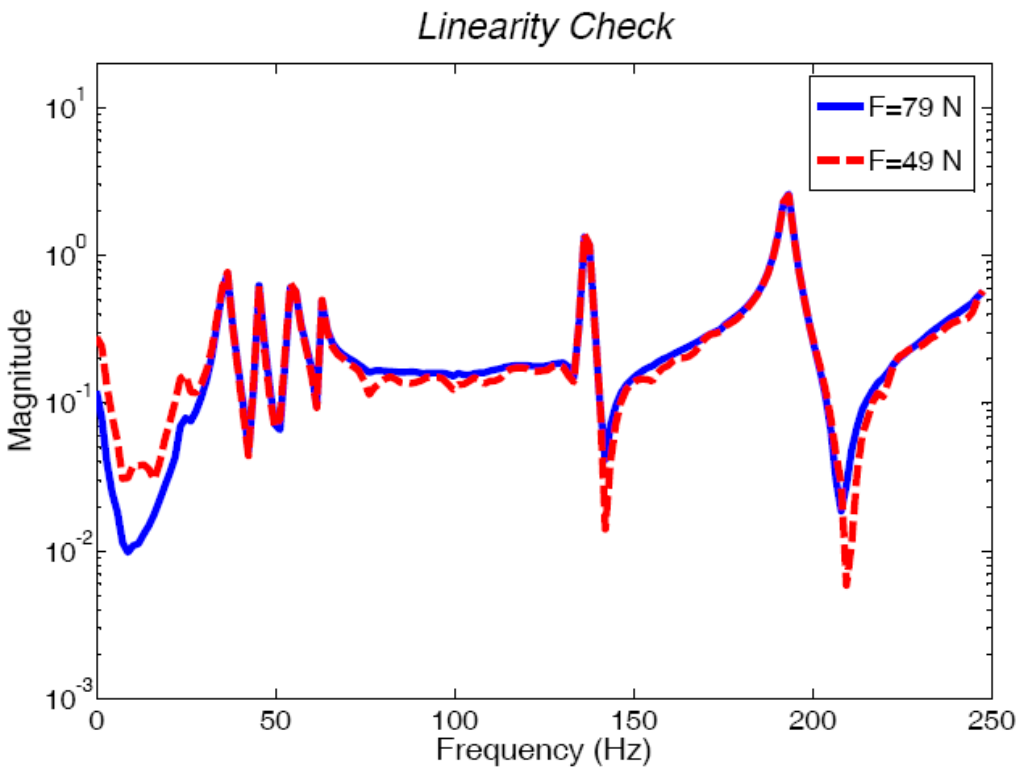

Figure 4.31. Linearity Control for Square Plate

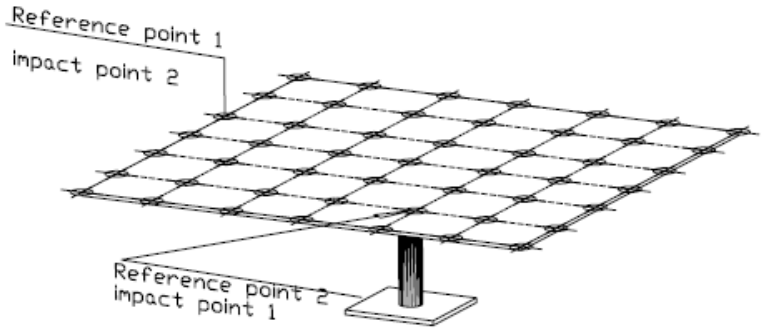

Figure 4.32. Excitation Locations for Reciprocity Control of Square Plate

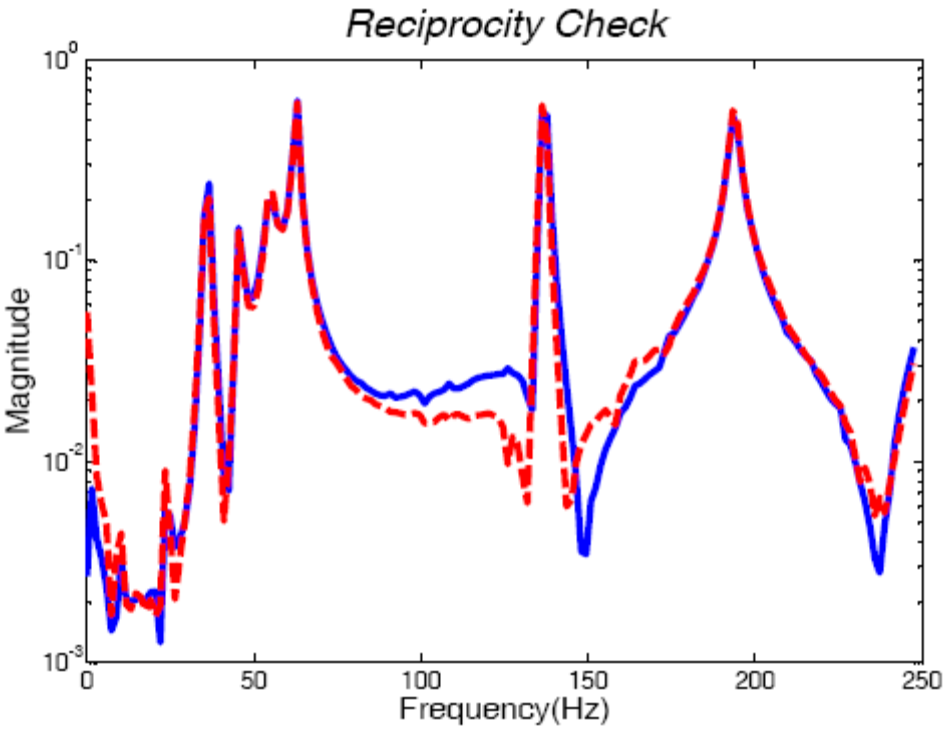

Figure 4.33. Reciprocity Control for Square Plate

Table 4.5. The Results of Frequency and Damping Values Obtained from Modal and FEM

Mode #	Modal Analysis Frequency (Hz)	Sap Model Frequency (Hz)	Frequency Difference (%)	Modal analysis Damping Constants (%)
1	34.4	34.7	1.0	1.9
2	35.1	34.7	1.2	2.4
3	54.3	45.0	17.2	0.1
4	45.4	53.1	16.9	0.6
5	62.7	77.1	23.1	-
6	136.6	139.1	1.8	0.2
7	135.5	139.1	2.6	0.4
8	192.4	182.5	5.2	0.3

The modal analysis of the system is performed with X-modal software. Natural frequencies, damping rates, shown in Figure 4.34 to Figure 4.36 and listed in Table 4.5, is obtained by using Complex Mode Indicator Function of the program. Damping rates had been corrected so that the effect of the exponential function had been eliminated (Fladung and Rost 1997). In order to obtain the dynamic parameters thru structural analysis the square plate is modeled by using 4-node shell elements and is analyzed with the SAP2000 program If the X-modal analysis results is compared with SAP2000 results, it is observed that frequency values of 3^{rd} and 4^{th} modes is displaced. Furthermore, 5^{th} mode's frequency is varied as large as 23%. Optimizations performed on finite elements model is not satisfactory to correct these differences. As a result finite elements model is left with nominal material characteristics and the idealized support conditions. The mode shapes resulted from modal and SAP analyses are presented in Figure 4.34 to. Figure 4.36.

Modal Analysis Results: **SAP Analysis Results:**

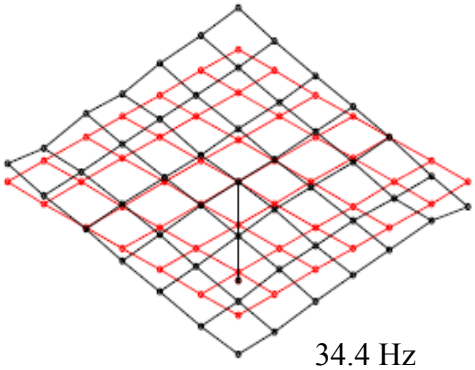

34.4 Hz

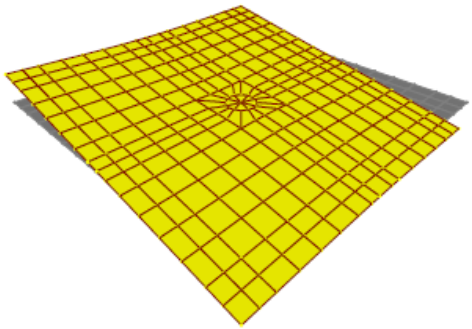

34.71 Hz

Mod 1

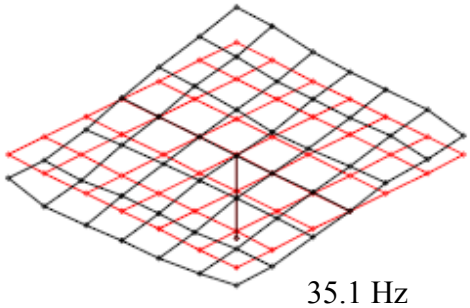

35.1 Hz

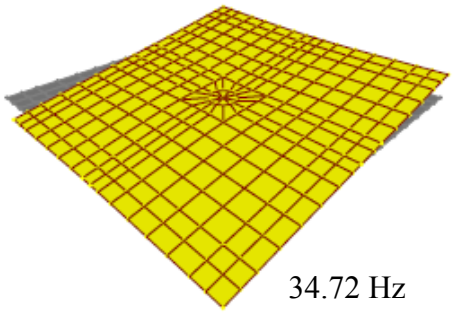

34.72 Hz

Mod 2

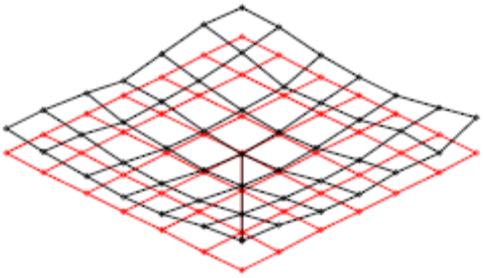

54.3 Hz

Mod 3

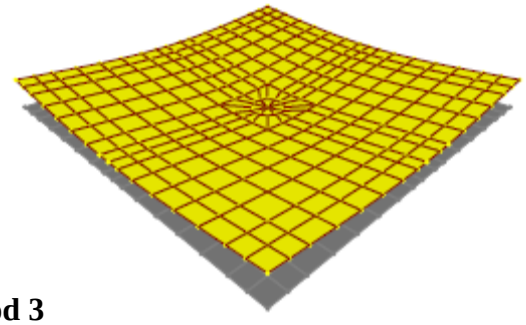

45 Hz

Figure 4.34. Comparison of Modal and FEM Analysis Results Mod 1-3

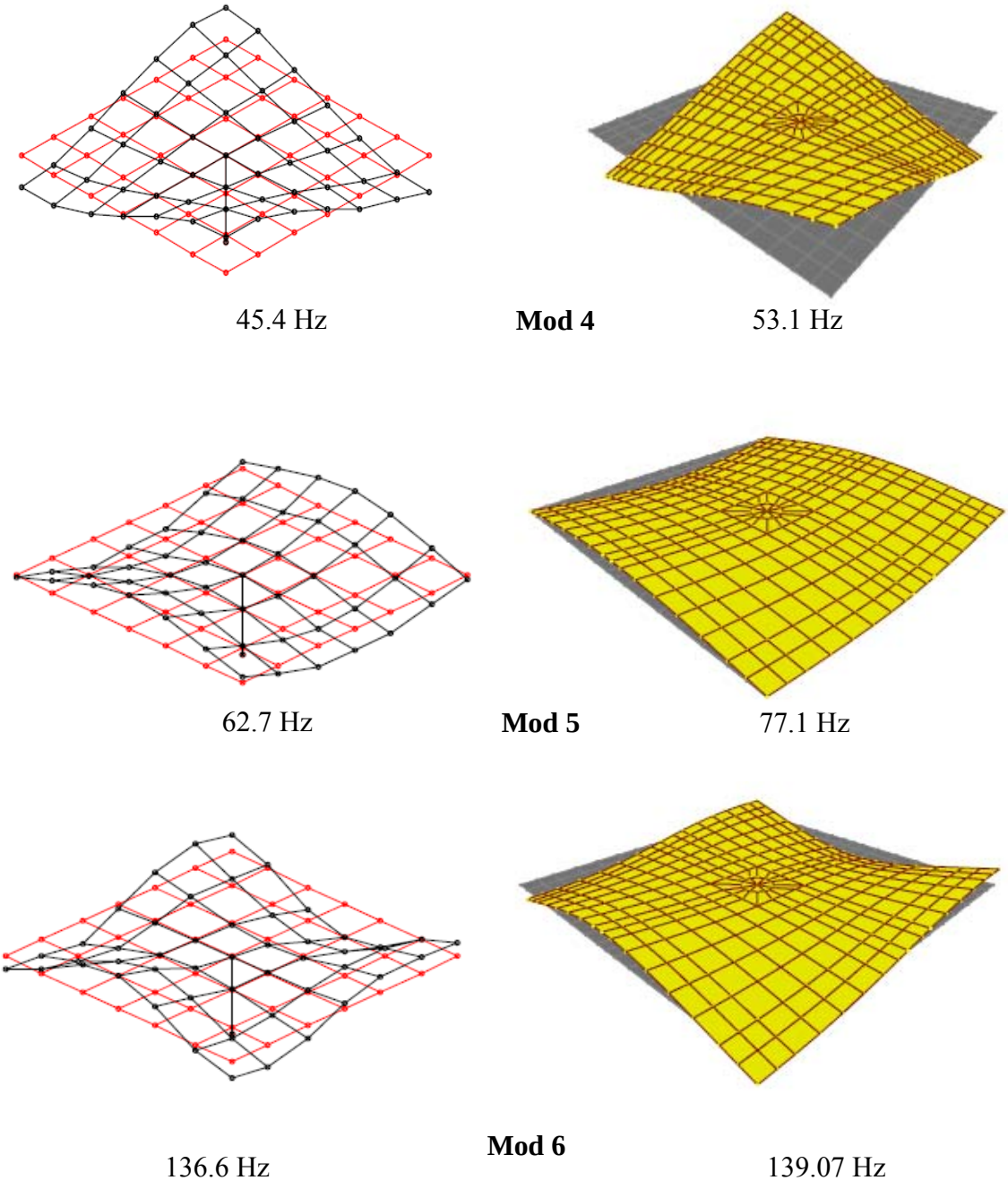

Figure 4.35. Comparison of Modal and FEM Analysis Results Mod 4-6

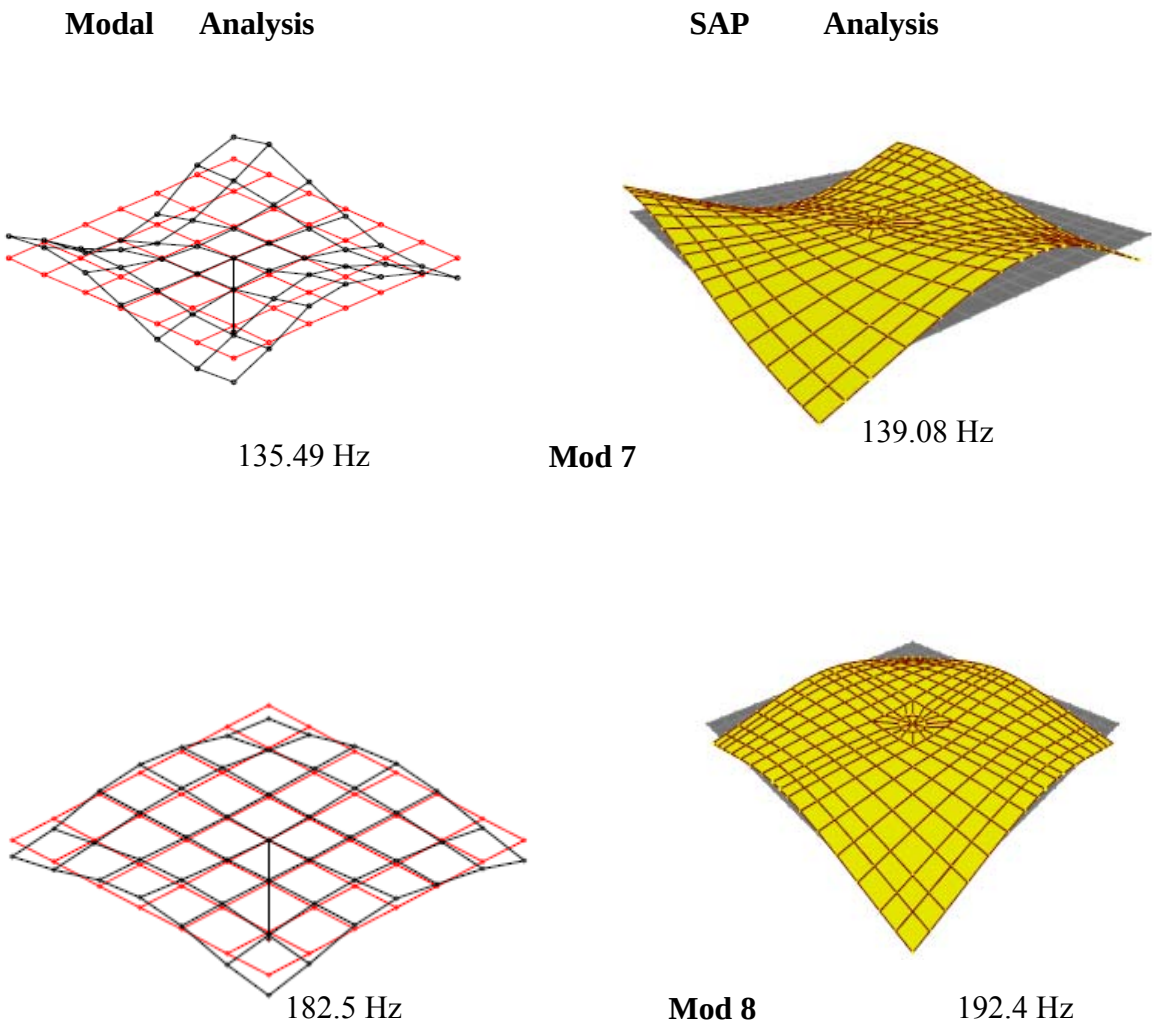

Figure 4.36. Comparison of modal and FEM analysis results Mod 7-8

4.3.4. Two Dimensional Frame

The last system studied is a two dimensional steel frame. It is a model structure and has one bay and four stories. The physical properties of 2D frame are shown in Figure 4.37 It is designed to permit the test of moment-frame behaviors. System is tested by exciting thru 16 locations and recording thru 4 locations, Figure 4.38. Modal analysis had been done by using SIMO data as multiple input multiple output (MIMO) thru reciprocity principle. Since there was no coupling observed, between directions in pre-measurements, in the

analysis only perpendicular component of the accelerometer to 2D-frame had been used. The chosen accelerometers are PCB-393B04 for moment frame case. Sensors have 1000 mV/g sensitivities, 0.05-450 Hz frequency intervals and 50 gr weight respectively. Excitation to the system had been given by super soft tip (red tip) for the moment frame. The excited frequencies with the selected hammer tips are presented in Figure 4.39 .

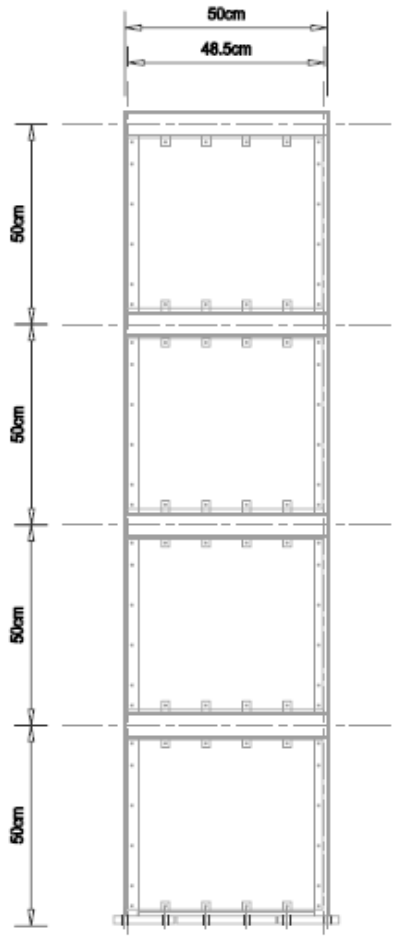

Figure 4.37. Details of 2D-frame

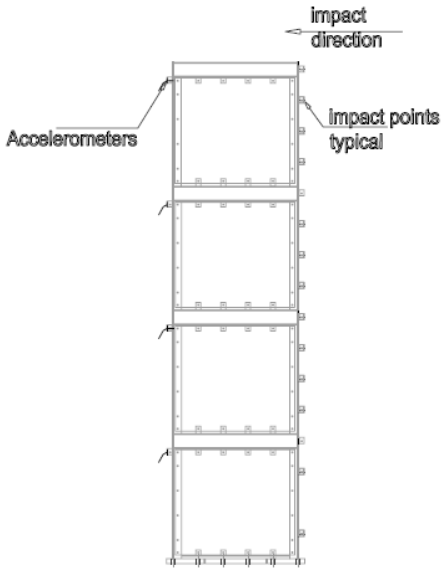

Figure 4.38. Accelerometers and impact locations for 2D-frame

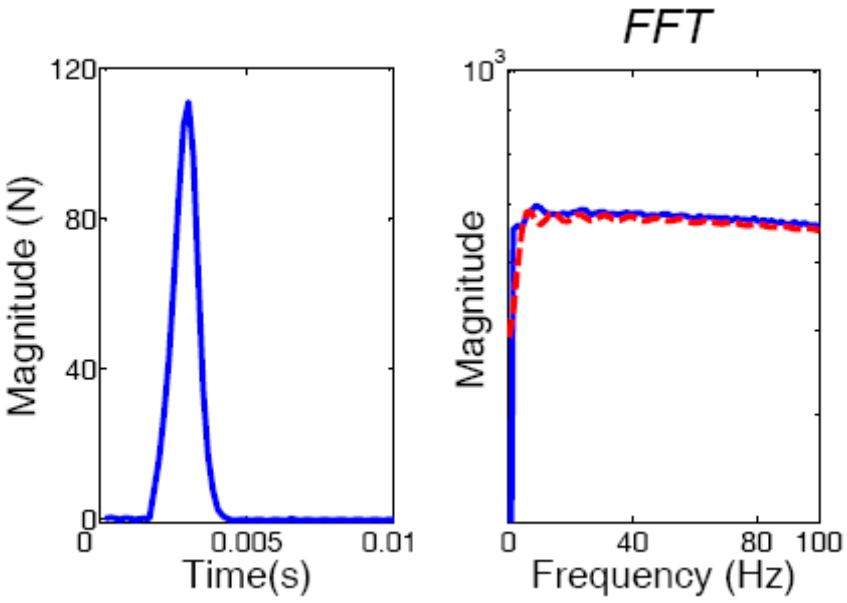

Figure 4.39. Typical Measurement range for 2D moment-frame

Figure 4.40. View of the 2D Moment-Frame

In the pre-measurements taken from the 2D-frame, it is observed that the first four frequencies for the moment frame are below 100Hz, and the 0-100 Hz frequency interval is selected as the measurement range. Data acquisition system is set to 3 seconds of record length, 6KHz sampling rate and 2.5KHz analog low pass filter.

To check the compatibility to fundamental assumptions of system modal analysis had been exposed to linearity and reciprocity tests. Different magnitude of impulses is given to the same point to check the linearity. Impulse sizes used are 65 N and 110 N, Figure 4.41. These excitations and respective frequency response functions are presented in Figure 4.42.

For reciprocity control, as shown in Figure 4.43, impulses and reactions from two facing points is recorded and FRF's formed by averaging 5 different reading sets. The results show that Maxwell reciprocity principle is valid.

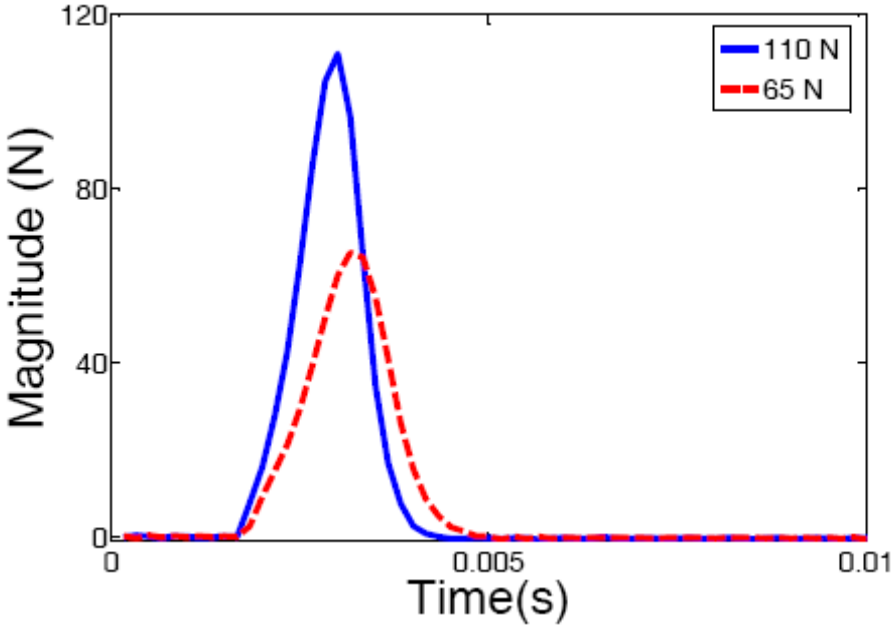

Figure 4.41. Linearity Control for Moment Frame Impact Excitation

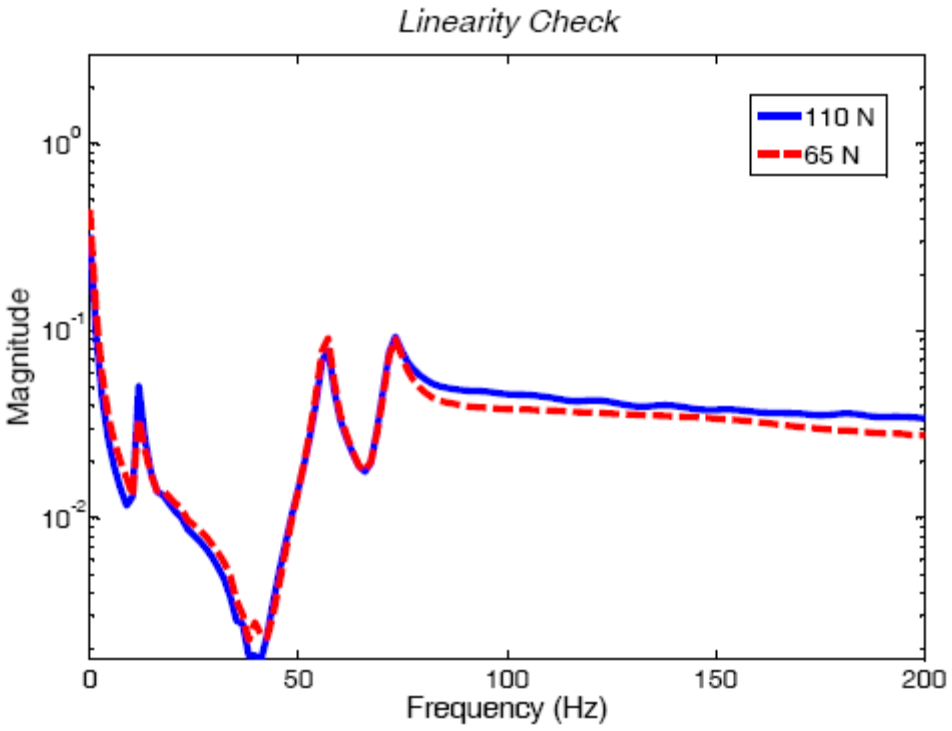

Figure 4.42. Linearity Check for Moment Frame

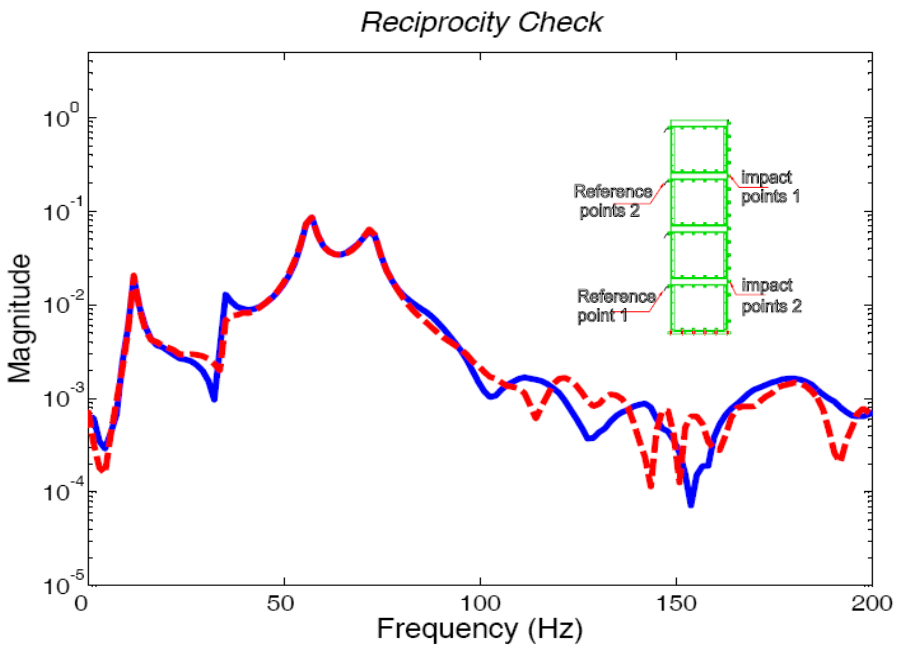

Figure 4.43. Reciprocity Control for 2D Frame

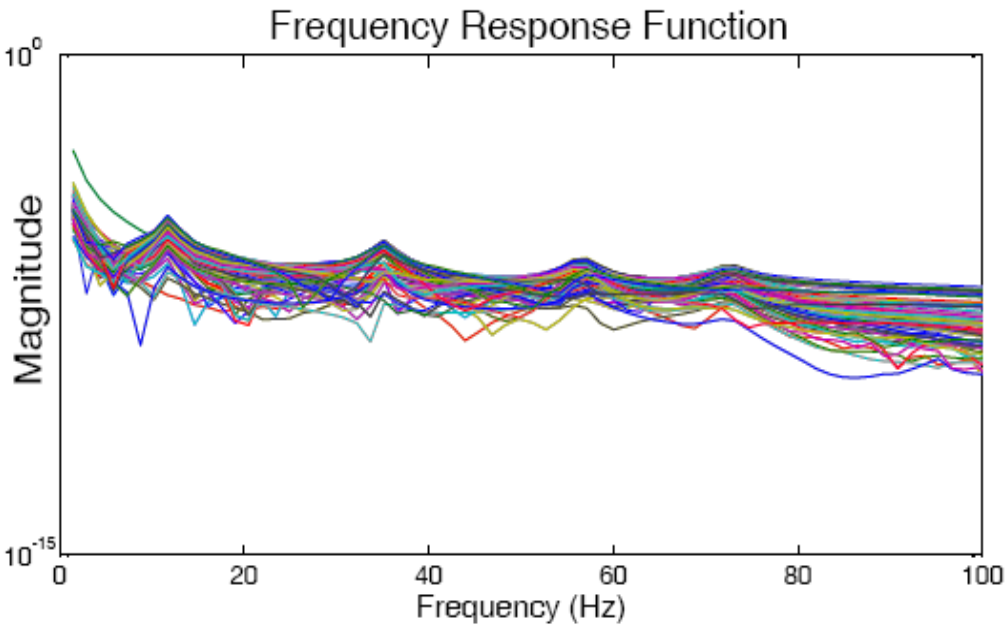

Figure 4.44. Complete View of Frequency Response Functions of Moment Frame

Defined FRFs had been applied to X-modal analysis program and the modal analysis had been performed via X-modal program. Natural frequencies, damping rates and modal shapes, shown in Figure 4.44 listed in Table 4.6, had been obtained by using Complex Mode Indicator Function of the program. Damping rates had been corrected so that the effect of the exponential function had been eliminated [Fladung and Rost, 1997]. 2D frame had also been analyzed with SAP2000 [Computers and Structures, 04], program by using shell elements having four degrees of freedom and its modal variables had been found.

Table 4.6. The Results of Frequency and Damping Values Obtained from Modal and FEM Analysis

Mode #	Modal Analysis Frequency (Hz)	Sap Model Frequency (Hz)	Frequency Difference (%)	Modal Analysis Damping Constants (%)
1	11.8	11.6	1.6	0.0
2	35.1	34.1	5.6	1.2
3	57.0	54.0	5.2	2.4
4	73.2	67.0	6.8	2.1

Moment Frame SAP Analysis Results:

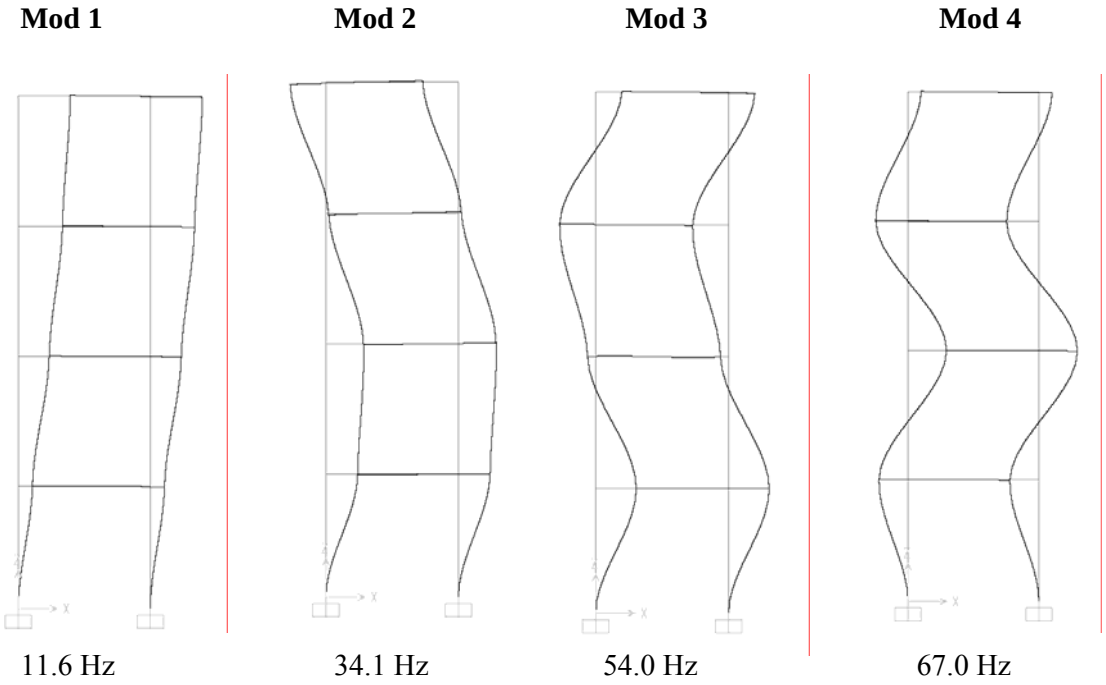

Moment Frame Modal Analysis Results:

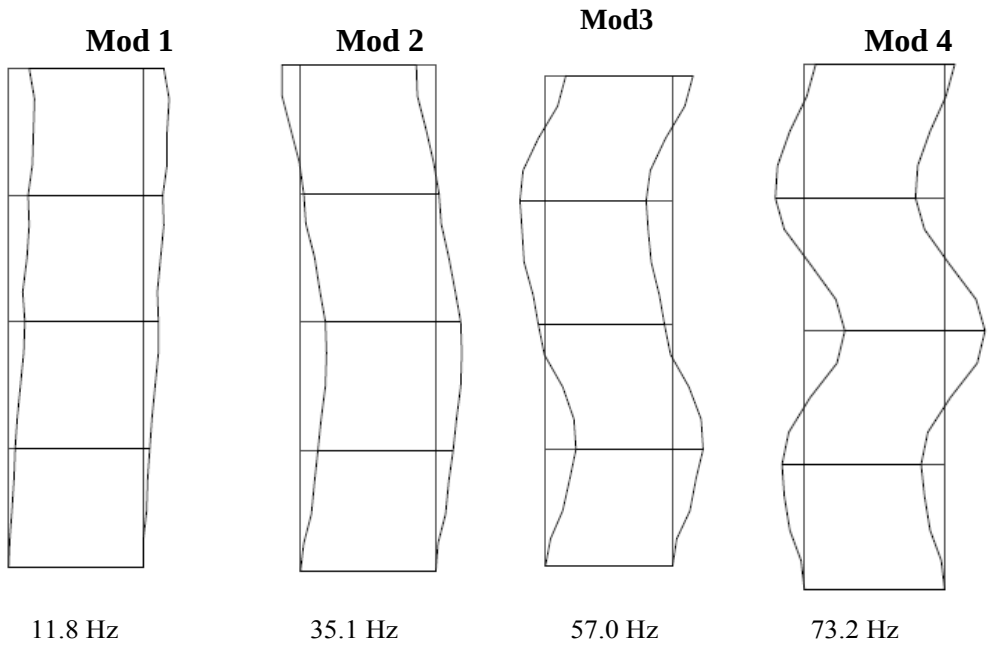

Figure 4.45. To Compare of Modal Analysis and FEM Analysis Results for Frequency and Mode Shape for Moment Frame

CHAPTER 5

SENSITIVITY OF THE FREQUENCY RESPONSE FUNCTION TO EXPERIMENTAL AND ANALYTICAL PARAMETERS

5.1. Introduction

The system information from modal experiment to modal analysis is transferred thru the FRF. Considering the importance of FRF, in this chapter the effects of some experimental and analytical parameters on FRF is studied. The experimental parameters are the hardness of the hammer tip and the materials used to attach the accelerometer to the structure under test. For this purpose, the simply supported steel beam that is discussed in chapter 4 is used as the base system. The geometry and the support information of the beam could be found in section 4.3.1.

As it is identified in chapter 4 the beam has 6 modes under 850 Hz. In this chapter measurements are designed to obtain FRFs to contain these 6 modes of the system. The modal test is performed with single triaxial accelerometer and impacts to ten different points of the beam. The basic procedure to obtain the FRF from the raw experiment data is summarized below.

Anti-Aliasing Filtering: Data from the system has whole frequency spectrum, since the received data is analog. To prevent the aliasing of high frequency signal components with needed low frequency signals after sampling, analog data should be filtered before recording them via an Anti-Aliasing analog filter. For this purpose, 2.5 kHz analog low pass filter, which we have already in data recording system, had been utilized. According to Shannon Sampling Theorem, one has to have at least (2x2.5) kHz sampling rate to record a frequency at 2.5 kHz. Because of practical limitations of filters, a little higher sampling rate is required than this theoretical limit. Therefore, in our experiments a 2.5 kHz low pass filter and 6 kHz sampling speed had been used.

As stated before, because of the present characteristics of our data recording system, data had been collected in between 0-3 kHz frequency interval. After digitization, needed 0-500 Hz interval had been obtained via Butterworth low pass filter.

Rectangular Windowing: Impact hammer gives the impulsive stimulation to the system in a very short time in reality, and it should give zero recording during the other phase of the recording. Because of the noise sources, this was not practically possible. For this reason, a rectangular windowing should be applied to hold the necessary part obtained by impact hammer's impulses.

Exponential Windowing: Since the output signals don't damp during recording completely, disturbances occur during the discrete Fourier transform. For this reason, if required exponential windowing transformation is used to damp the signals in a period to be used for the transform. Here the important point is the necessity to pass all inputs and outputs from exponential windowing, subtracting artificially added damping amount, which was added during exponential windowing, from the system's own damping value.

Averaging the Data: To reduce random noise in data, one should collect more than one data from the same physical points, and then should take averages of them. Five averages are taken typically.

Noise / Error Reduction: The most widespread used technique is the least squares technique, in noise and error reduction. This technique minimizes the size of error, and gives best guess for impulse response size. Technique has no effect on impulse response's phase (Allemang 1999). Basic difference between functions used to guess responses of impulse functions, is in prediction of the noise source in the system. These functions are called as H1, H2 and Hv algorithms. Detailed information related with these functions can be found in (Allemang 1999).

5.2. Using all hammer tips for mounting method

When choosing a mounting method, consider closely both the advantages and disadvantages of each technique. Characteristics like location, ruggedness, amplitude range, accessibility, temperature and portability are extremely critical. However, the most

important and often overlooked consideration is the effect the mounting technique has on the high-frequency performance of the accelerometer.

Adhesive mounting is often used for temporary installation. Adhesives like hot glue, gypsum, cement and wax perform well for temporary installations whereas two part epoxies and quick bonding gels (super glue) provide a more permanent installation. Two techniques are used for adhesive mounting: they are via an adhesive mounting base or direct adhesive mounting.

Adhesively mounted sensors often exhibit a reduction in high frequency range. Generally, smooth surfaces and stiff adhesives provide the best high frequency response.

Direct Adhesive mount: For restrictions of space or for convenience, most sensors can be adhesive mounted directly to the test structure Firstly, prepare a smooth, flat mounting surface. Then, place a small portion of adhesive on the underside of the sensor. Firmly, press down on the top of the assembly to displace any adhesive. The most important consideration is that excessive amounts of adhesive can make sensor removal difficult. Figure 5.1 shows that direct adhesive mounting.

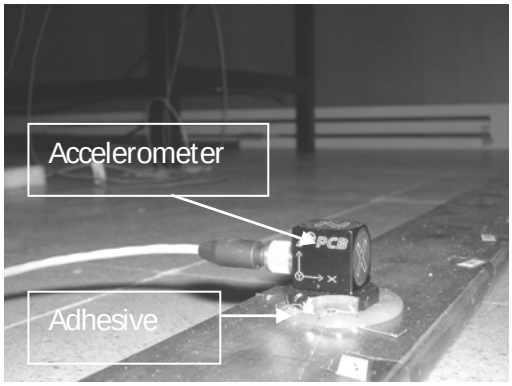

Figure 5.1. Direct Adhesive Mounting

Very often, the mounting systems which are convenient to use and allow ease of alignment with orthogonal reference axes are subject to mounting resonances which result in substantial relative motion between the transducer and the structure under test in the frequency range of interest. Therefore, the mounting system which should be used depends on the frequency range of interest and the test conditions. Test conditions are factors such

as temperature, roving or fixed transducers, and surface irregularity. A brief review of in this thesis transducer mounting methods is shown in Table 5.1.

Table 5.1. Impact Hammer Tips Used for Different Materials

(source: Allemang 1999)

Transducer Mounting Method			
Method	Frequency Range (Hz)	Main Advantages	Main Disadvantages
Hot glue	0-2000	Quick setting time, Good axis alignment	Temperature sensitive transducers (during cure)
Cement	0-5000	Mount on irregular surface Good axis alignment	Long curing time
Super Glue	0-2000	Accurate alignment if carefully machined	Difficult setup and removal from the system
Gypsum	0-2000	Good axis alignment	Long curing time

For simple beam, it is the investigation of change in Frequency Response Functions (FRF), Processed Input Data Frequency Spectrums and Impact Hammer Dimensions, by making use of different materials to attach 3 axis and various-hardness impact hammer tips. For this purpose, from hardest to softest impact hammer tips are ordered as hard tip-Medium Hardness tip-Soft tip-Super soft tip, respectively. Also, materials to attach accelerometer are: Hot Glue, Plaster, Cement and Glue. Experiments had been performed for 2 different cases: first all the hammer tips are used for all the mounting methods. Secondly, all the mounting materials are used for different kind of hammer tips.

Firstly, for the first situation of "Using all hammer tips for mounting methods", changes in FRFs, Processed Input Data Frequency Spectrums and Impact Hammer Magnitudes will be examined.

5.2.1. Hot Glue, Plaster, Cement, Glue

As seen in the experiment performed with different mounting materials for example; hot glue, cement, glue and plaster, if impact hammer has a hard tip it takes shorter time to affect as shown in Figure 5.2. In general, short term pulses affect broader frequency ranges. In general, hard hammer tips affect broader frequency ranges. Total time of tip impact is directly proportional to frequency interval. When we examine the impulse magnitudes of processed data, it is seen that the hard tip is smooth, and the softest tip has a steep decrease as shown in Figure 5.3. When the FRFs are examined, it is seen that soft tips', which are red and black ones, magnitudes are too close to each other; however the hard metal tip had lesser magnitude as shown in Figure 5.4. The graphics obtained for different hardness tips of FRF, when the accelerometer had attached with different mounting materials for a simple beam, as shown in Figure 5.4.

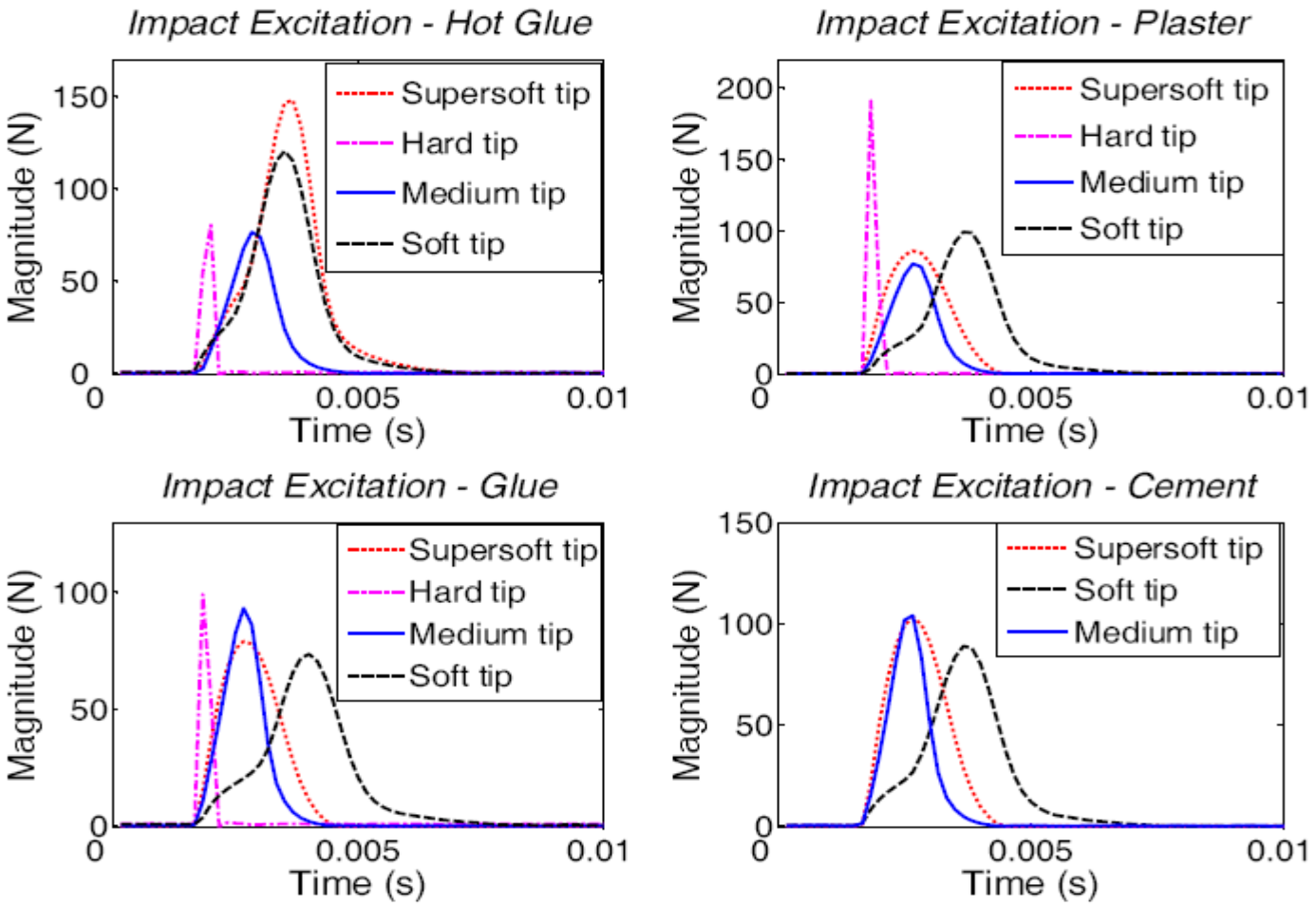

Figure 5.2. Impact Hammer Magnitudes Obtained from Different Hardness Tips for Different Mounting Materials for Simple Beam

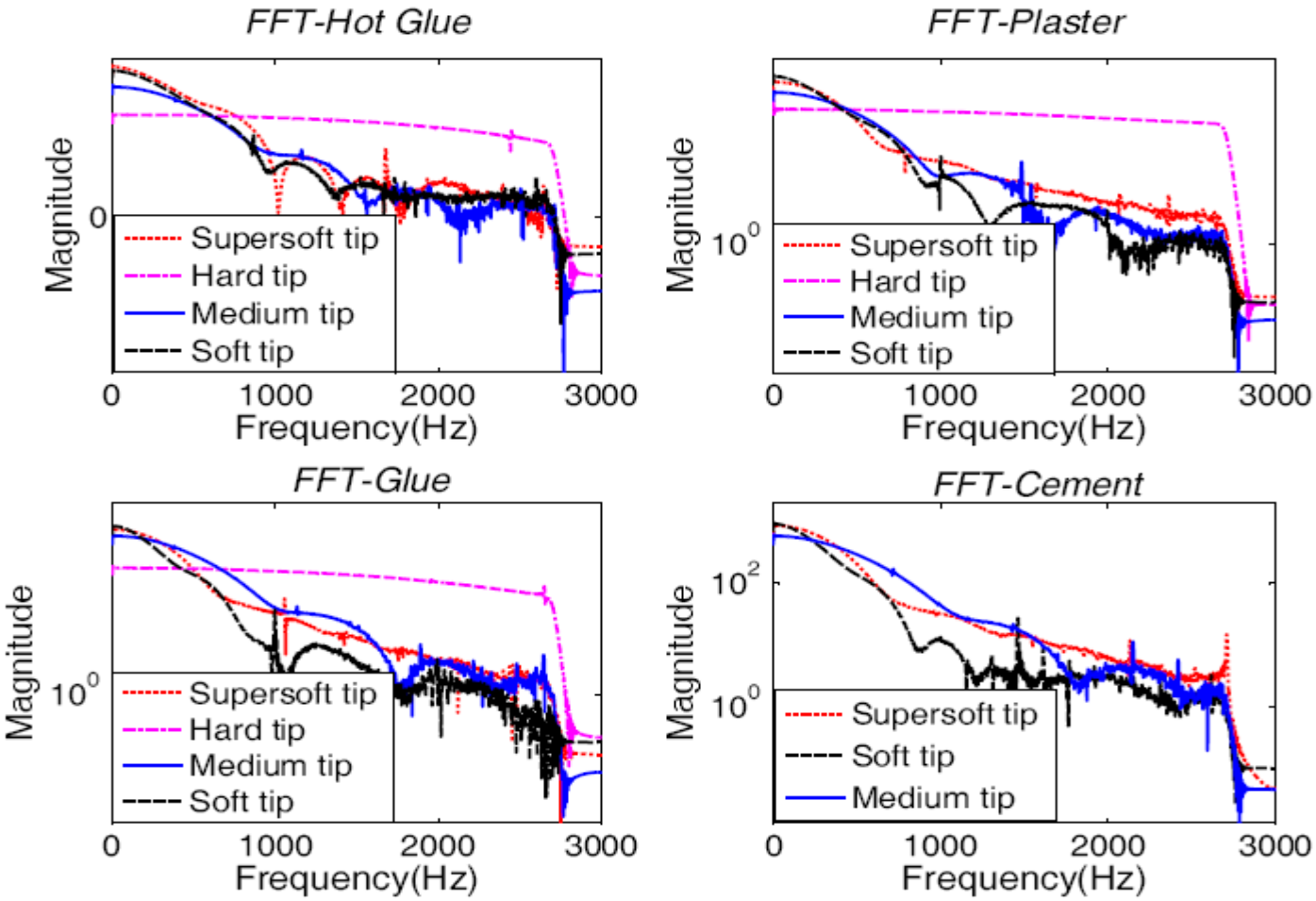

Figure 5.3 Impact Impulse Magnitudes Obtained from Different Hardness Tips for Different Mounting Materials for Simple Beam

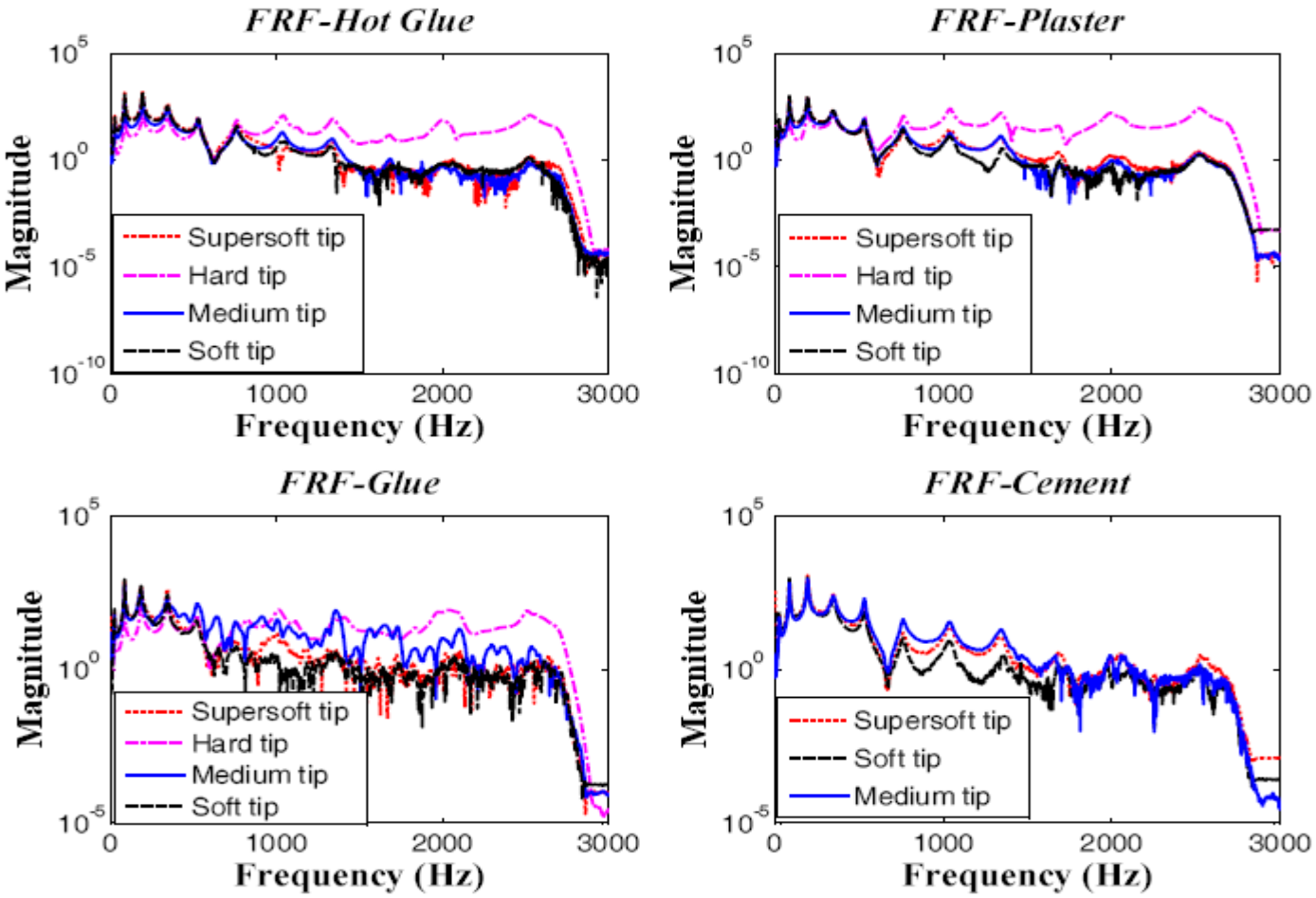

Figure 5.4. FRF Magnitudes Obtained from Different Hardness Tips for Different Mounting Materials for Simple Beam

5.3. Using different materials to stabilize the accelerometer for every impact hammer tip

The graphs obtained for different hardness tips of impact excitation, when the accelerometer had attached different mounting materials, as shown in Figure 5.5. When the total time durations are compared, super soft tip has longer time duration than the hard hammer tip. For the super soft tip, it had been observed that the time interval is the longest but the most shortest time duration is observed with using hard hammer tip .The second figure obtained by using different hardness tip of FRF, when the accelerometer had attached different mounting materials, as shown in Figure 5.6.This graphs shows that from 0 to 1000 Hz, there is no effect to use different mounting materials. In addition to this the harder hammer tip, the wider frequency range that is excited.

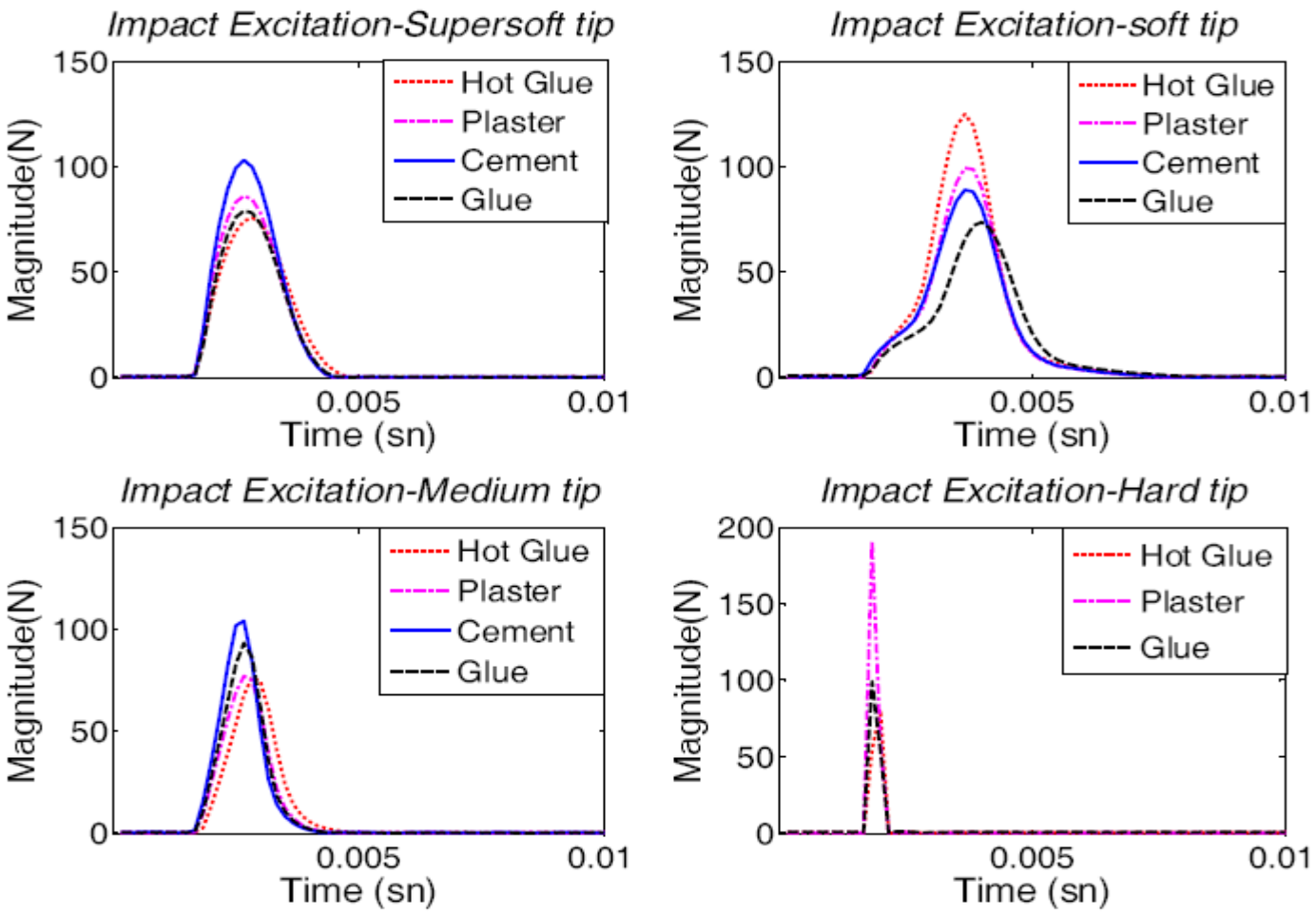

Figure 5.5. Impact Hammer Magnitudes Obtained From Different Materials for Simple Beam

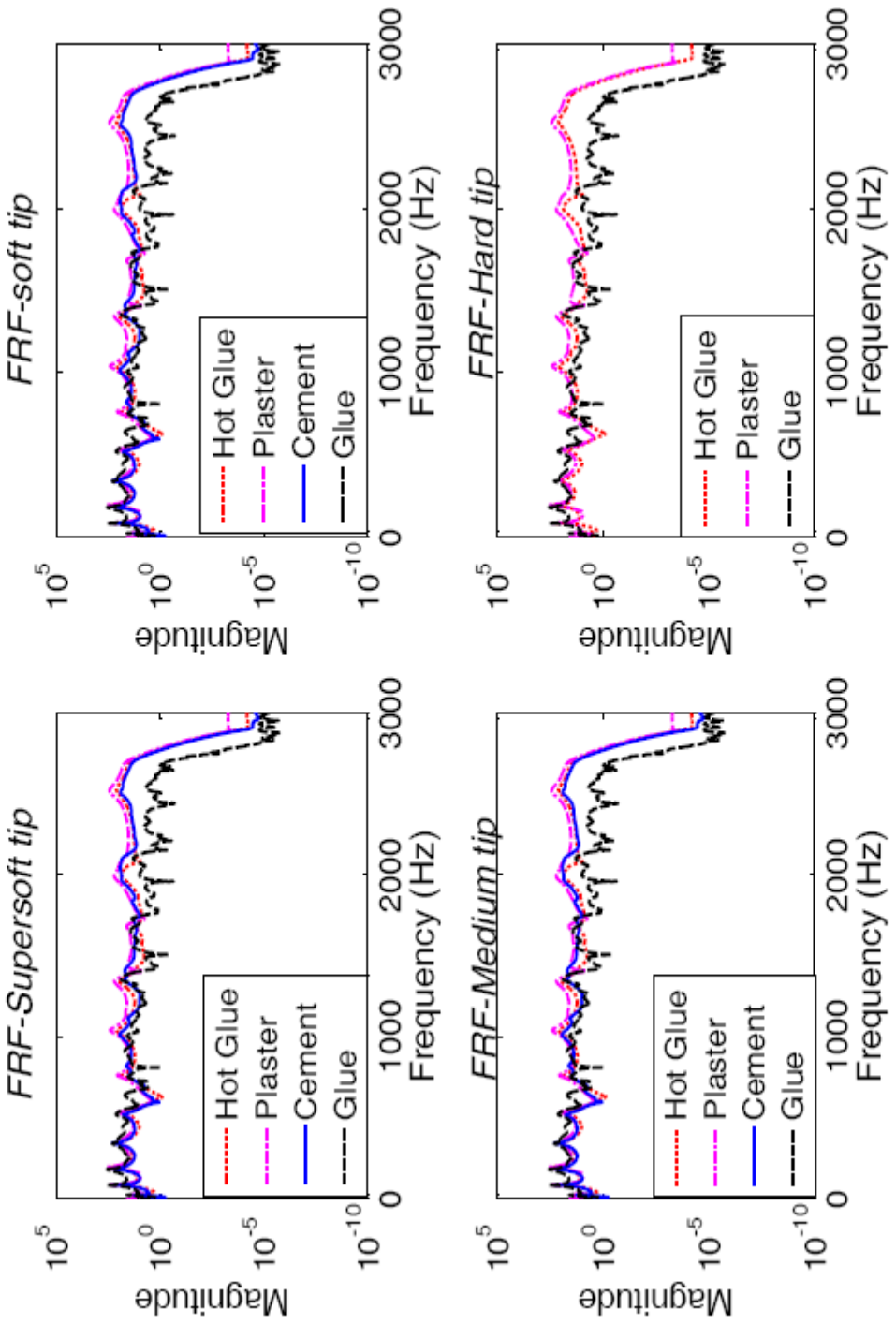

Figure 5.6. FRF Magnitudes Obtained from Different Materials for Simple Beam

5.4. Hammer tip

There are many important considerations when performing impact testing. One of the most critical items is that the selection of the hammer tip. First, the selection of the hammer tip can have a significant effect on the measurement acquired. The input excitation frequency range is controlled mainly by the hardness of the tip selected. The harder the tip, the wider the frequency range that is excited by the excitation force. The tips need to be selected such that all the modes of interest are excited by the impact force over the frequency range to be considered (Avitable 1998). If too soft a tip is selected, then all the modes will not be excited adequately in order to obtain a good measurement as seen Figure 5.7. The input power spectrum does not excite all of the frequency range shown as evidence by the roll off the power spectrum.

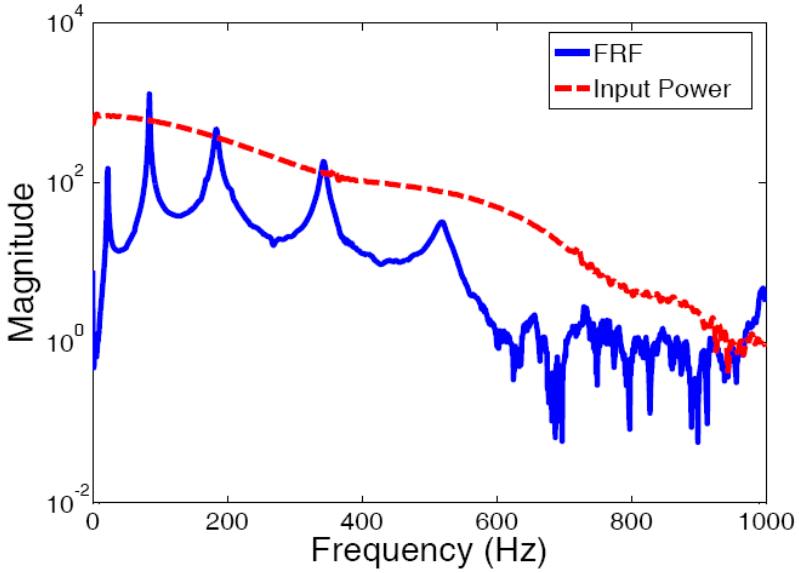

Figure 5.7. Hammer Tip not Sufficient to Excite All Modes

Typically, it is strived to have a fairly good and relatively flat input excitation forcing function. The frequency response function is measured much better. When performing impact testing, care must be exercised to select the proper tip so that all the

modes are excited well and a good frequency response measurement is obtained in Figure 5.8.

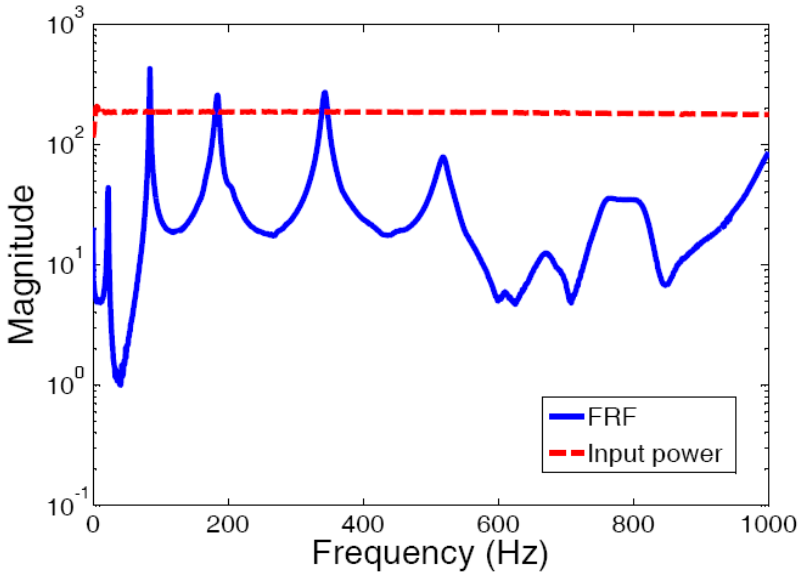

Figure 5.8. Hammer Tip Adequate to Excite All Modes

Basically, it is wanted the input spectrum to have sufficient, fairly even excitation over the frequency range of concern. If the input spectrum were to completely drop off to zero, then the structure would not be excited at that frequency which is not desirable.

First let's discuss some basics about the selection of hammer tips for an impact test. First of all, let's remember that the input force spectrum exerted on the structure is a combination of the stiffness of the hammer/tip as well as the stiffness of the structure. Basically the input power spectrum is controlled by the length of time of the impact pulse. A long pulse in the time domain, results in a short or narrow frequency spectrum. A short pulse in the time domain, results in a wide frequency spectrum.

Now let's use a very soft tip to excite a structure over a 500 Hz frequency range. As shown in Figure 5.9, it’s seen that the input power spectrum (red) has some significant roll-off of the spectrum past 300 Hz. It is also notice that the FRF (blue) does not look particularly good past 400 Hz. Also, coherence drop off significantly as shown in Figure 5.9. The problem here is that there is not enough excitation at higher frequencies to cause the structure to respond. If there is not much input, then there is not much output. Then

none of the measured output is due to the measured input and as well as the FRF is not acceptable.

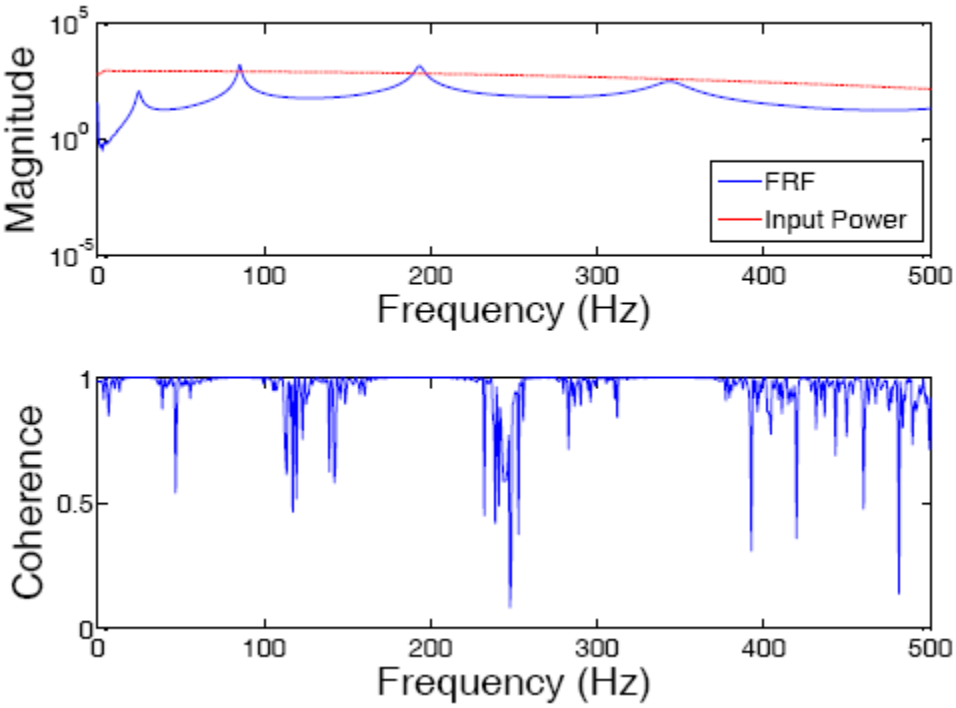

Figure 5.9. Very Soft Hammer Tip

Now let's use a soft tip to excite a structure over a 500 Hz frequency range. As shown in Figure 5.10, it's seen that the input power spectrum (red) has some significant roll-off of the spectrum past 400 Hz. It is also notice that the FRF (blue) does not look particularly good past 400 Hz. The problem here is that there is not enough excitation at higher frequencies to cause the structure to respond. If there is not much input, then there is not much output. Then none of the measured output is due to the measured input and the FRF as well as the coherence as shown in Figure 5.10 are not acceptable.

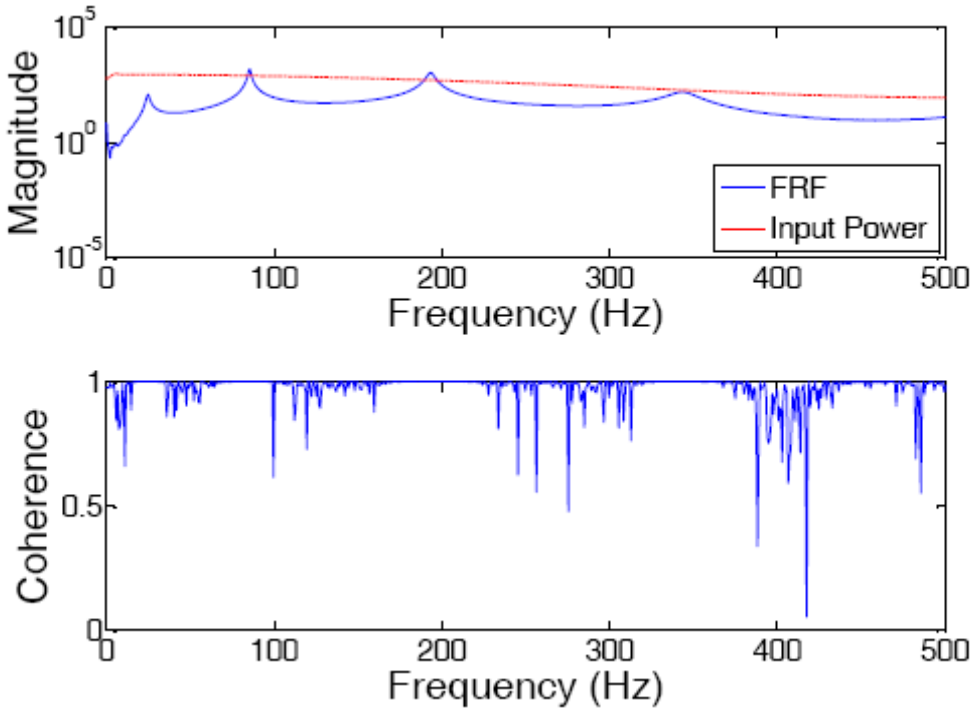

Figure 5.10. Soft Hammer Tip

Now let's use a medium hardness tip to excite a structure over 500 Hz frequency range. As shown in Figure 5.11, it’s seen that the input power spectrum (red) has some significant roll-off of the spectrum past 400 Hz. The problem here is that the input power spectrum drop off % 40 from 0 to 500 Hz. It is also notice that the FRF (blue) looks especially good at all frequencies. This is not a good measurement for coherence as shown in Figure 5.11.

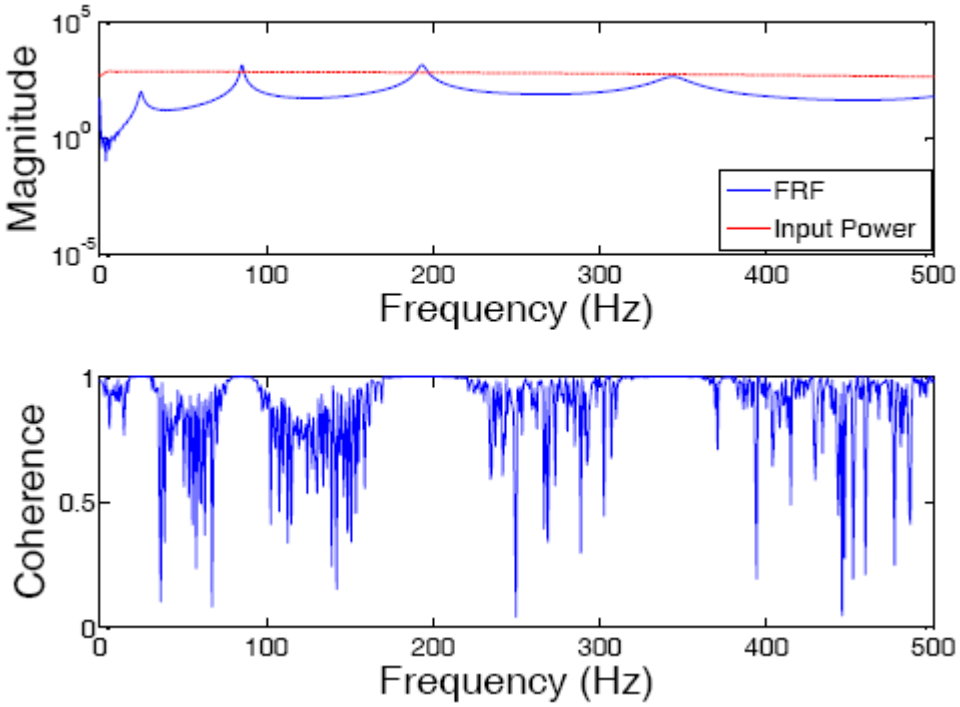

Figure 5.11. Medium Hardness Tip

Now let's use a very hard tip to excite a structure over an 500 Hz frequency range such that the input force spectrum does not drop off significantly by the end of the frequency range of interest. As shown in Figure 5.12, it is seen that the input power spectrum (red) rolls off by 3 to 5 dB by 500 Hz. It is also notice that the FRF (blue) looks especially good at all frequencies. The coherence is also good for very hard tip as shown in Figure 5.12. It is the best measurement all of them.

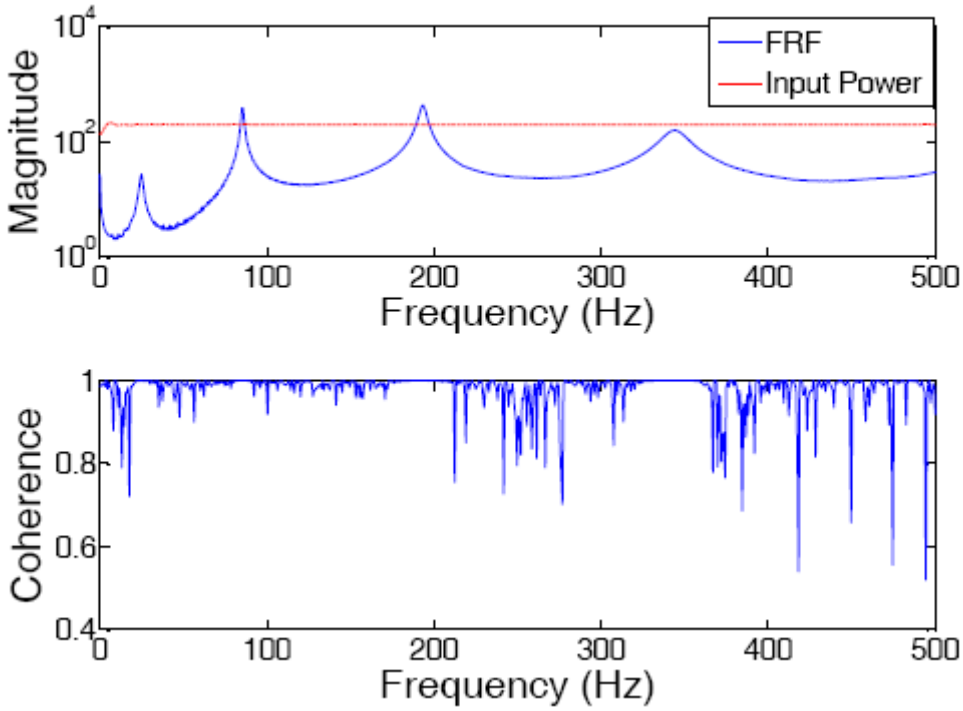

Figure 5.12. Very Hard Tip

5.5. Windowing

Two common time domain windows that are used in impact testing are the force and exponential windows. These windows are applied to the signals after they are sampled, but before the FFT is applied to them in the analyzer.

The other important aspects of impact testing relate to use of an impact window for the response transducer. Generally for lightly damped structures, the response of the structure due to impact excitation will not die down to zero by the end sample interval. When this case, the transformed data will suffer significantly from a digital signal processing effect referred to as a leakage.

In order to minimize leakage, a weighting function referred to as a window is applied to the measured data. This window is used to force the data to better satisfy the periodicity requirements of the Fourier transform process, thereby, minimizing the distortion effects of leakage as shown in Figure 5.13. For impact excitation, the most

common window used on the response transducer measurement is the exponentially decaying window.

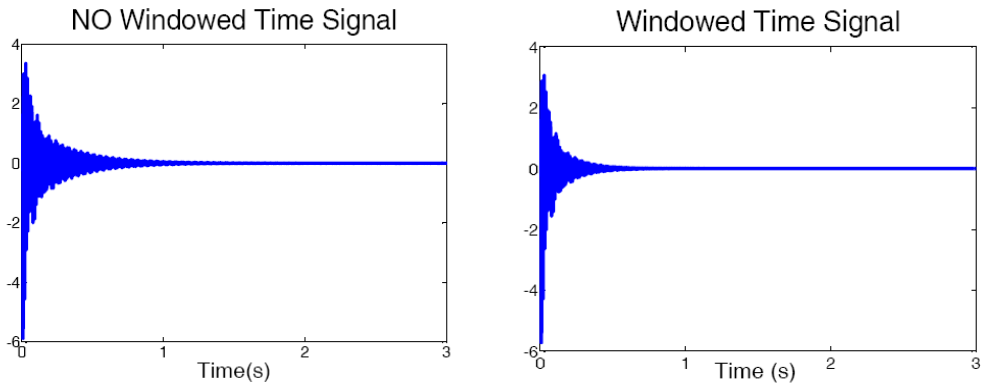

Figure 5.13. Exponential Window to Minimize Leakage Effect

Windows cause some distortion of the data themselves and should be avoided whenever possible. For impact measurements, two possible items to always consider are the selection of a narrower bandwidth for measurements and to increase the number of spectral lines resolution. Both of these signal processing parameters have the effect of increasing the amount of time required to acquire a measurement. These will both tend to reduce the needed for the use of an exponential window and should always be considered to reduce the effects of leakage.

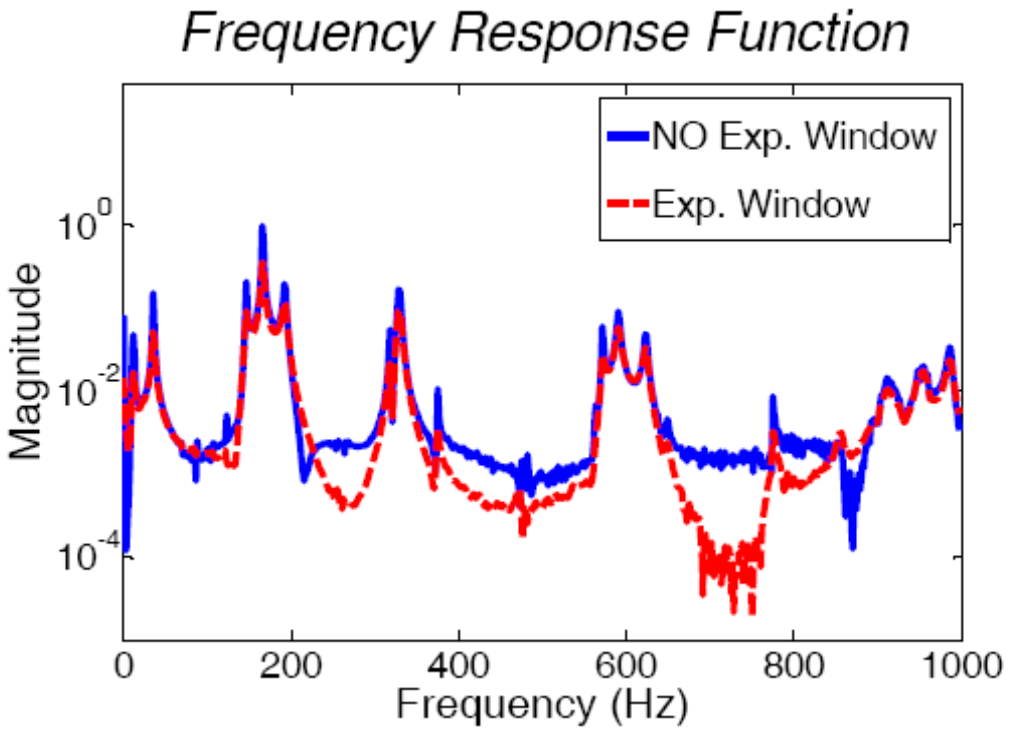

Figure 5.14. To Compare Exponential and No-Exponential Window of FRF

Without going into all the detail, windows always distort the peak amplitude as shown in Figure 5.14 measured and always give the appearance of more damping then what actually exists in the measured Figure 5.14 two very important properties that it tries to estimate from measured functions. The amplitudes are distorted as much as 66% for the first mod, 67% for the second mod, 56% for the third mod, 64% for the fourth mod, 40% for the fifth mod, 62% for the sixth mod, and 43% for the seventh mod for exponential window. The effect of these windows is best seen in the Fig. 5.24. Exponential window has a characteristic shape that identifies the amount of amplitude distortion possible, the damping effects introduced and the amount of smearing of information possible.

5.6. Averaging

There are several options which can be selected when setting an analyzer into average mode: peak hold, exponential and linear. Generally, averaging is utilized primarily as a method to reduce the error in the estimate of the frequency response functions. There is a technique for improving the signal to noise ratio of a measurement, called linear averaging. The noise is different in each time record; it will tend to average to zero. If the more averages take, the closer noise comes to zero and it continues to improve the signal to noise ratio of measurements. The linear averaging is used for this project. The comparison of with using 5and 50 samples are shown in Figure 5.15.

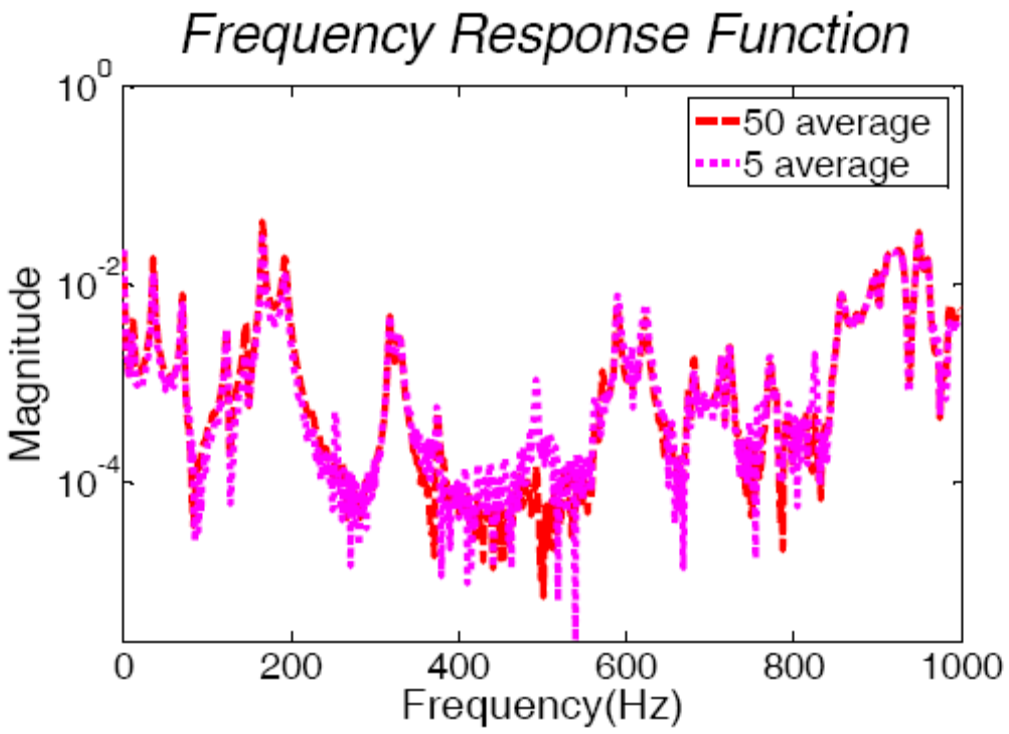

Figure 5.15. To Compare the 5&50 Average for H-Frame

5.7. Aliasing (sampling rate)

Aliasing errors are results of the inability of the Fourier transform to decide which frequencies are within the analysis band and which frequencies are outside the analysis band. In this project to compare of the aliasing errors, it is two different (6kHz and 1 kHz) sampling rate is used. It is shown in the Figure 5.16, for the first five frequency values are the same but the magnitudes of this values are different.

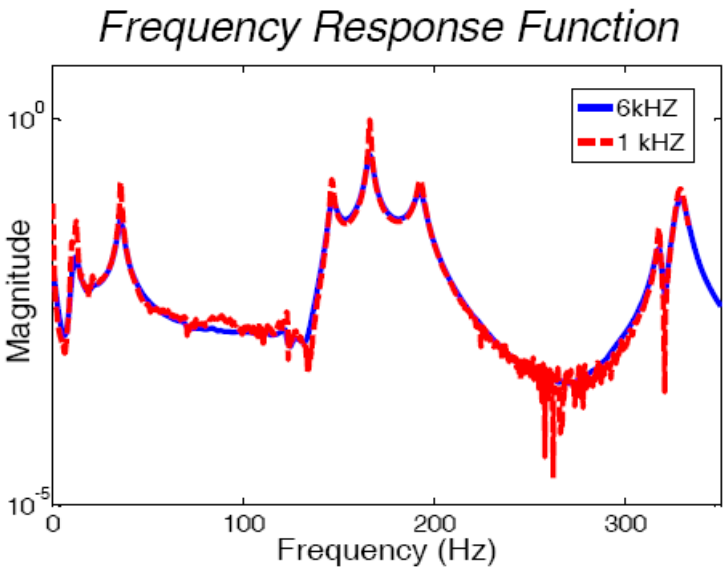

Figure 5.16. To Compare 6kHz and 1kHz Sampling Rate

The amplitudes are distorted as much as 36% for the first mod, 33% for the second mod, 57% for the third mod, 36% for the fourth mod, 27% for the fifth mod, 36% for the sixth mod, and 24% for the seventh mod for the effect of the sampling rate. The effects of these windows are best seen in the Figure 5.16.

5.8. Filtering

An ideal anti-alias filter passes all the desired input frequencies and cuts off all the undesired frequencies. A lowpass filter allows low frequencies to pass but attenuates high frequencies. In this project butterworth filter is used to cut the undesired frequencies. For that reason, for low frequencies from 0 to 350 Hz, there is no difference between the filtering case and no filtering case. The result is shown in Figure 5.17.

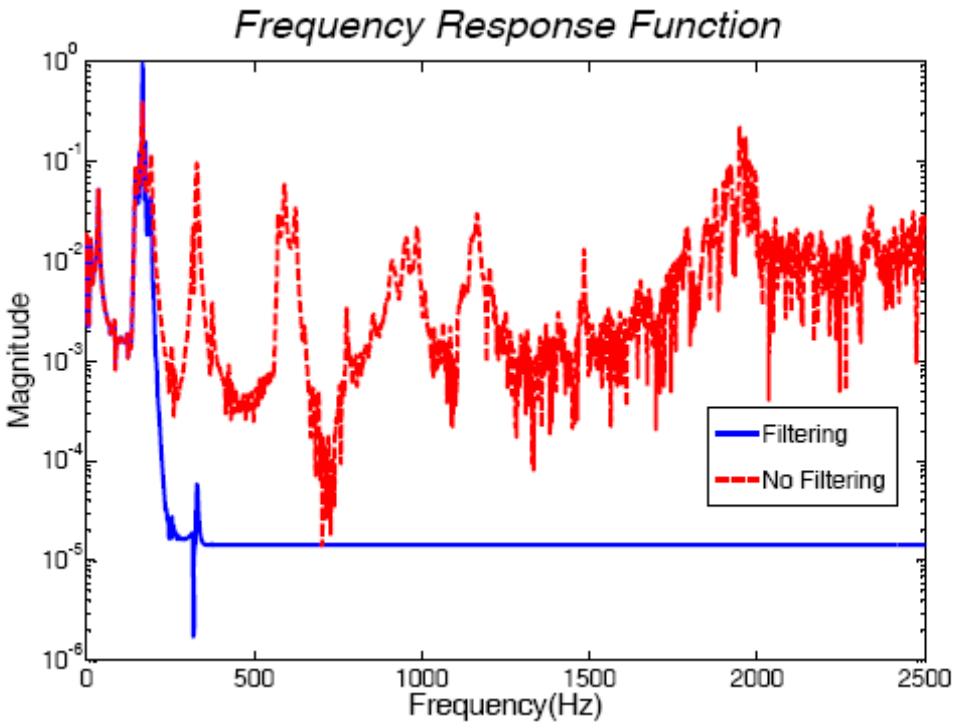

Figure 5.17. To Compare of Filtering Case

5.9. Noise Error Sources

The FRF estimate assumes that random noise and distortion are summing into the output (H1), but not the input of the structure and measurement system. The FRF estimator assumes that random noise and distortion are summing into the input (H2), but not the

output of the structure and measurement system. In this project, the two algorithms are compared and it is seen that there is no important difference between H1 and H2 algorithms for simple beam as shown in Figure 5.18. Also Figure 5.18 shows that, there is no distortion and random noise for simple beam.

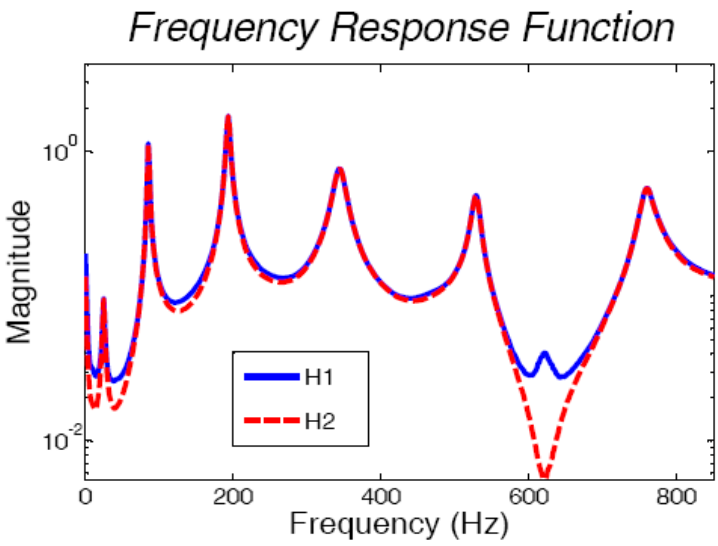

Figure 5.18. To Compare of H1 and H2 Algorithm for Simple Beam

5.10. Location of Accelerometer

If it is running modal test with using triaxial accelerometer, it will be measure one vertical and two horizontal directions. Because structures that has mode shapes that are very directional in nature. That means that the response of the structure is primarily in one direction (as shown in Figure 5.19-x direction) or no response in the other directions (as shown in Figure 5.19-Mod 1) for a given mod of the structure. Yet another mode of the structure may have response in a different direction than the first mode (for example mod 5 has three different directions).It is seen that in Fig.4.86 mode 1 of the structure has motion primarily in the Z direction and there is no motion in the other directions. However, mode 2 of the structure has primarily in the Z and Y directions with no motion in the X direction. Also it can see that mode 3 follow the same trend. Mode 4 and mod 5 have motion in three directions but for mod 4, Z direction being slightly more predominant as shown in Figure

5.19. In addition mod 6 Z and Y directions are more predominant than X direction. As a result of this, the all modes cannot be seen in every measurement.

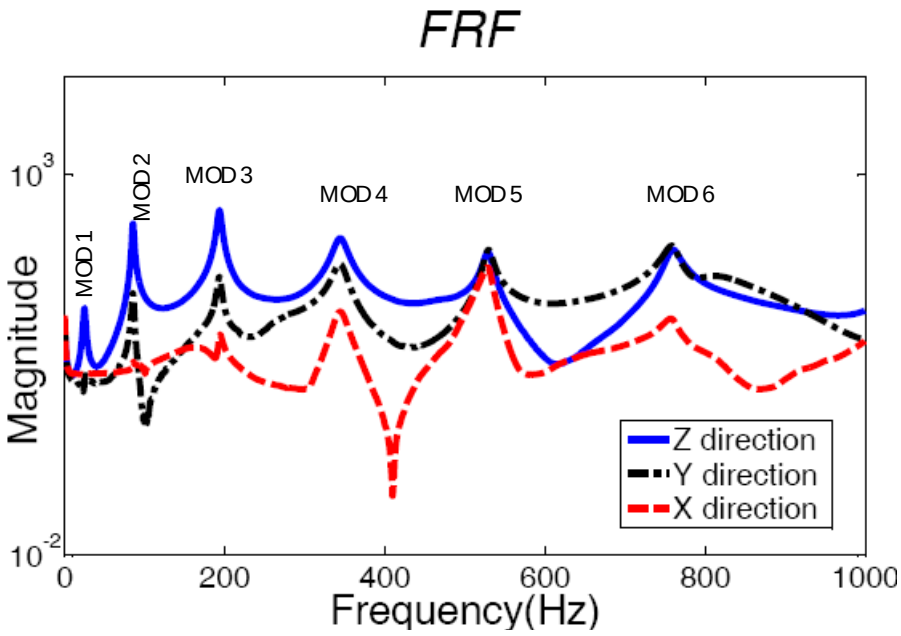

Figure 5.19. Three Different Directions for FRF Measurement

CHAPTER 6

CONCLUSION

The primary objective of this thesis is to observe the effects of various testing and analysis parameters on the synthesis of frequency response function (FRF). Dynamic parameters of the structures are obtained in order to identify the system parameters based on the measured FRF's. These parameters, which should be unique to every system, are the natural frequencies, mode shapes, and damping ratios of the system. By using several simple structural systems, the experimental and analytical parameters that are effecting the FRF are discussed. In view of the test results, the following conclusion seems to be valid:

1) Hard hammer tip had excites a broader frequency interval.
2) The main difference between the excitation given bey the hard and the soft hammer tips is the duration of the contact between the hammer and the structure. Duration is shorter with the harder tip.
3) During the experiments performed with the impact hammer, it is observed that experiment with hard tip is difficult inplement. The reason of this difficulty is the fast rebounce from the system which causes double peak excitation, which is unacceptable.
4) It is observed that the hammers contact duration is the very similiar for accelerometers that attached with different materialsfor the same hammer tip. As seen in Figure 5.15, the impact hammer magnitude graphics obtained with hot glue, plaster and glue usage for the hard tip have same impact duration although forces with different intensities are applied.
5) In experiments performed with the same impact hammer tip, peak values of Frequency Response Function for different accelerometer attachement materials had been changed. Therfore it could be said that FRFs are directly affected from used accelerometer-attaching materials (Figure 5.10).

6) As a result, in order to obtain a healty FRF the right impact hammer tip appropriate to experimental setup should be chosen. It should also be remembered that accelerometer-attaching materials have some minor effectson the FRF's obtained.

7) It is observed that even though it excited a broader spectrum band, using the harder tip is not always the best solution. The reason is the excitation of the unwanted higher modes and the lost of some input energy for this purpose.

8) There should be sufficient numbers of points to describe the mode shape for each mode with necessary precision.

9) In many impact testing situations the use of an exponential window is necessary. However, before any window is applied, it is advisable to try alternate approaches to minimize the leakage in the measurement. Increasing the number of spectral lines or halving the bandwidth is two things that should always be investigated prior to using a damping window.

REFERENCES

Allemang, Randall. 1999. *Vibrations: Experimental Modal Analysis.* Structural Dynamics Research Laboratory. Department of Mechanical, Industrial and Nuclear Engineering. University of Cincinnati.

Allemang, Randall 1999. *Vibrations: Analytical and Experimental Modal Analysis.* Structural Dynamics Research Laboratory. Department of Mechanical, Industrial and Nuclear Engineering. University of Cincinnati.

Avaitable, Pete 1998. Could you explain modal analysis for me. Society of Experimental Techniques. http://macl.caeds.eng.uml.edu/ (accessed July 10, 2006).

Avaitable, Pete 1998. Could you explain the difference between time domain ,frequency domain and modal space. Society of Experimental Techniques. http://macl.caeds.eng.uml.edu/ (accessed July 10, 2006).

Avaitable, Pete 1998. Is there any difference between a modal test with shaker excitation and impact excitation. Society of Experimental Techniques. http://macl.caeds.eng.uml.edu/ (accessed July 10, 2006).

Avaitable, Pete 1998. Which shake excitation is best? Is there any difference? Society of Experimental Techniques. http://macl.caeds.eng.uml.edu/ (accessed July 10, 2006).

Avaitable, Pete 1999. Curve fitting is so confusing me! What do all the techniques mean?. Society of Experimental Techniques. http://macl.caeds.eng.uml.edu/ (accessed July 10, 2006).

Avaitable, Pete 1999. I still Don't Understand Curve fitting… How do you get Mode Shapes from FRF? Society of Experimental Techniques. http://macl.caeds.eng.uml.edu/ (accessed July 10, 2006).

Avaitable, Pete 1999. I am still overwhelmed by all this stuff. Give me the big picture. Society of Experimental Techniques. http://macl.caeds.eng.uml.edu/ (accessed July 10, 2006).

Avaitable, Pete 1999. Are you sure you get mode shapes from one row or column of H? Society of Experimental Techniques. http://macl.caeds.eng.uml.edu/ (accessed July 10, 2006).

Avaitable, Pete 1999. I heard someone say “Pete doesn’t do windows” What is the scoop. Society of Experimental Techniques. http://macl.caeds.eng.uml.edu/ (accessed July 10, 2006).

Avaitable, Pete 2000. How many point are enough when running a modal test? Society of Experimental Techniques. http://macl.caeds.eng.uml.edu/ (accessed July 10, 2006).

Avaitable, Pete 2000. Someone told me Structural dynamic modification will never work. Society of Experimental Techniques. http://macl.caeds.eng.uml.edu/ (accessed July 10, 2006).

Avaitable, Pete 2000. Why is mass loading and data consistency so important? Society of Experimental Techniques. http://macl.caeds.eng.uml.edu/ (accessed July 10, 2006).

Avaitable, Pete 2001. I heard about SVD all the time.Could you explain it simply to me?. Society of Experimental Techniques. http://macl.caeds.eng.uml.edu/ (accessed July 10, 2006).

Avaitable, Pete 2002. Is there any real advantage to MIMO testing?, Why not just use SISO and then move the shaker. Society of Experimental Techniques. http://macl.caeds.eng.uml.edu/ (accessed July 10, 2006).

Avaitable, Pete 2003. Is it really necessary to reject a double impact? Are they really a problem? Society of Experimental Techniques. http://macl.caeds.eng.uml.edu/ (accessed July 10, 2006).

Avaitable, Pete 2004. Do I need to have an accelerometer mounted in the X, Y and Z directions to do a modal test? Society of Experimental Techniques. http://macl.caeds.eng.uml.edu/ (accessed July 10, 2006).

Avaitable, Pete 2005. When I perform impact testing, the input spectrum looks distorted – do you think my FFT analyzer has a problem? Society of Experimental Techniques. http://macl.caeds.eng.uml.edu/ (accessed July 10, 2006).

Avaitable, Pete 2005. What effect can the test set up and rigid body modes have on the higher flexible modes of interest? Society of Experimental Techniques. http://macl.caeds.eng.uml.edu/ (accessed July 10, 2006).

Avaitable, Pete 2003. I ran a modal test on a portion of a structure of concern and many modes look the same! What did I do wrong? Society of Experimental Techniques. http://macl.caeds.eng.uml.edu/ (accessed July 10, 2006).

Avaitable, Pete 2005. Sometimes my impact force is very smooth just as expected but often it looks like it is oscillating – Why is that? Society of Experimental Techniques. http://macl.caeds.eng.uml.edu/ (accessed July 10, 2006).

Avaitable, Pete 1999. Are you sure you can get mode shapes from one row or column of the H matrix? Society of Experimental Techniques. http://macl.caeds.eng.uml.edu/ (accessed July 10, 2006).

Avaitable, Pete 2001. Can the test setup have an effect on the measured modal data ? Do the setup boundary conditions and accelerometers have an effect? Society of Experimental Techniques. http://macl.caeds.eng.uml.edu/ (accessed July 10, 2006).

Avaitable, Pete 2004. Once I have set up a good measurement, is there any reason to watch the time and frequency results for every FRF? Society of Experimental Techniques. http://macl.caeds.eng.uml.edu/ (accessed July 10, 2006).

Avaitable, Pete 2005. Should the measurement bandwidth match the frequency range of interest for impact testing? Society of Experimental Techniques. http://macl.caeds.eng.uml.edu/ (accessed July 10, 2006).

Aktan A. E., Daniel N. Farhey, Arthur J. Helmicki, David L. Brown, Victor J. Hunt, Kuo-Liang, Lee, and Alper Levi 1997. Structural Identification for Condition Assessment: Experimental Arts. *Journal of Structural Engineering 1674.*

Ahlin Kjell 2006. Modal Analysis I Experimental Mechanics from http://www.bth.se/tek/mtd002.nsf/(accessed January 5, 2006).

Ahlin Kjell 2006. Modal Analysis II Experimental Mechanics from http://www.bth.se/tek/mtd002.nsf/(accessed January 5, 2006).

Bayraktar Alemdar, Türker Temel and Özcan D. Mehmet 2006. Investigation of the Added Mass Effects on the Dynamic Characteristics of Beams by Experimantal Modal Analysis *7th International Congress on Advances in Civil Engineering, 11-13.*

Champoux Y., Cotoni V., Paillard B., and Beslin O., 2003. Moment excitation of structures using two synchronized impact hammers. *Journal of sound and vibration 263 515-533.*

Çakar Orhan and Şanlıtürk Kenan Yüce. 2005. Frekans Tepki Fonksiyonlarından Transdüser Kütle Etkilerinin Kaldırılması. *İtü dergisi/d mühendislik 4(2):79-92.*

De Silva 1999.*Vibration : fundamentals and practice 1*.

Ewins D.J. 2000. *Modal Testing: Theory, Practice and Application.* Research Studies Press Ltd.

Farrar R. Charles, Doebling Scott W., Cornwell J., and Straser Erik G. 2000. *Variability of modal parameters measured on the alamaso canyon Bridge.*

Flaudung W. and Rost R. 1997, Application and Correction of the Exponential Window for Frequency Response Functions. *Mechanical Systems and Signal Processing, 11(1), 23-26.*

J.N. Juang and R.S. Pappa. 1985. An eigensystem realization algorithm for modal parameter identification and model reduction. J. Guidance, *Control and Dynamics, V. 8, No. 5, pp 620-627.*

Fladung W. and Rost R. 1996. Application and Correction of the Exponential Window for Frequency Response Function. *Mechanical System and signal Processing 11(1),23-36.*

Goldman Steve,P.E. 1999. *Vibration Spectrum Analysis.*

J. He and Z. Fu. 2001. *Modal Analysis*. Butterworth-Heinemann

Jung, H. and Ewins, D.J. 1992. On the use of simulated "experimental" data for evaluation of modal analysis methods. *Proceedings of 10th International Modal Analysis Conference 421-429.*

Labview Full Development System, NI, 2005.

Larbi N. and Lardies J. 2000. Experimental Modal analysis of a Structure excited by a random force. *Mechanical Systems and signal analysis Processing 14(2),181-192.*

[Matlab, 04] Mathlab 7.0, The Mathworks Inc. 2004

Marudachalam K. and Wicks A.L. 1991. An attempt to quantify the errors in the experimental modal analysis. *Proceedings of the 9th International Modal Analysis Conference 1522-1527.*

Mitchell, L.D. 1994. Modal test methods-quality, quantity and unobtainable. *Sound and Vibration 10-16.*

Molina F.J., Pascual R., and Golinval J.C. 2003. Description of the steelquake benchmar. *Mechanical System and Signal Processing 17(1),77-82.*

Phillips W. Allyn and Allemang Randall J. 2002. An overview of MIMO-FRF excitation/ averaging / processing techniques. *Journal of Sound and vibration 262 (2003) 651-675.*

Ren Wei-Xin and Roeck Guido De 2002. Structural Damage Identification using modal data II : Test Verification. *Journal of Structural Engineering 96-104.*

SAP2000 Structural Analysis Program, Computers and Structures Inc. 2004.

Silva M.M.Julio and Maima M.M. Nuno. 1998. Modal Analysis and Testing.*Structural GravimetricCalibration System*

UC-SDRL X-Modal II Information Sheet http://www.sdrl.uc.edu/x-modal-ii-software-project-1/x-modal2_info.pdf (accessed January 17, 2008).

Xia Yong and Hao Hong. 2000. Measurement Selection for vibration based on Structural damage identification. *Journal of sound and vibration 236(1),89-104.*

Wang Z., Lin R.M. and Lim M.K. 1997. Structural damage detection using measured FRF Data. Compute Methods Appl. *Mech. Engineering 187-197.*

Wicks, A.L. 1991. The quality of modal parameters from measured data. *Proceedings of the 9th International Modal Analysis Conference.*